RESEARCH REPORT
2007 – 2008

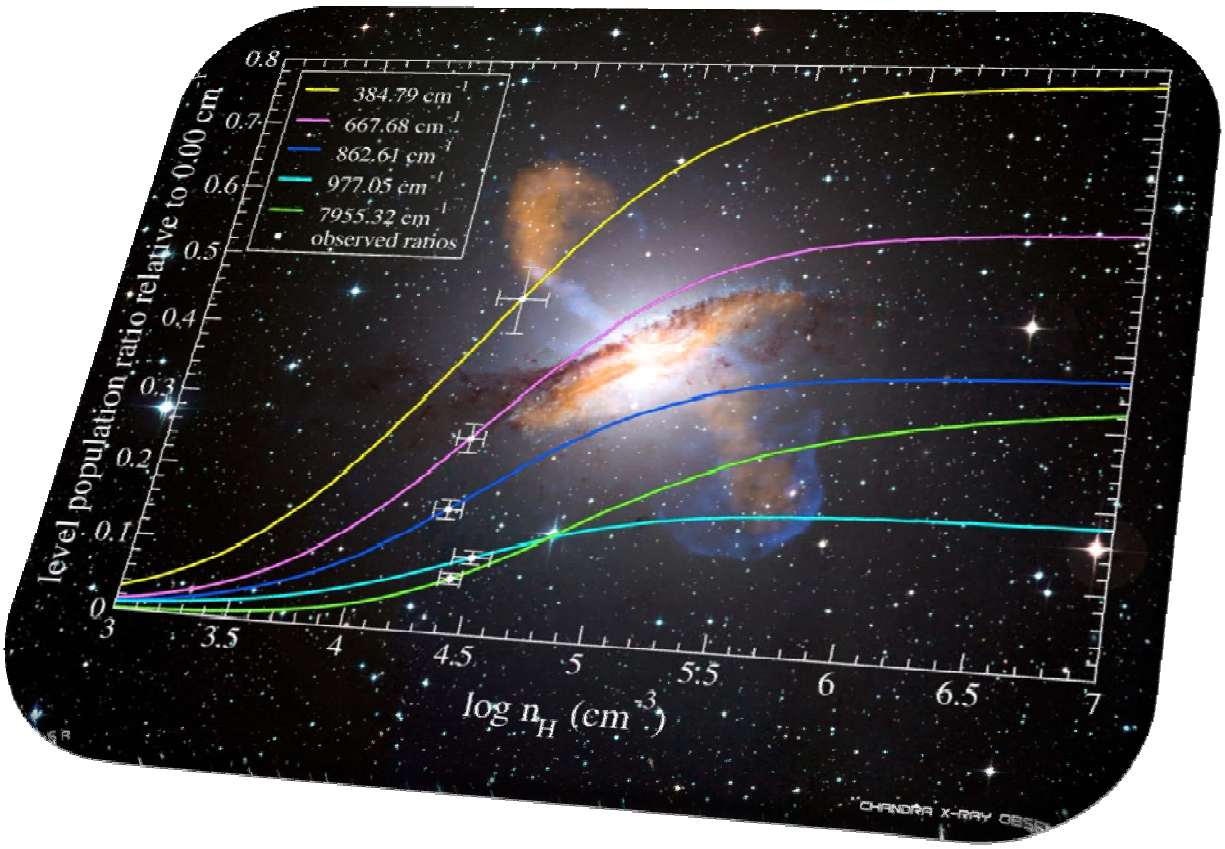

COLLEGE OF ARTS & SCIENCES

DEPARTMENT OF PHYSICS

WESTERN MICHIGAN UNIVERSITY

Department of Physics

College of Arts and Sciences

Western Michigan University

Annual Research Report

July 1st, 2007 – June 30th, 2008

Edited by

T. W. Gorczyca

CONTENTS

1 INTRODUCTION

This is the thirty-seventh in a series of annual reports that summarizes the research activities of the members of the Department of Physics at Western Michigan University. The report includes research performed in this department as well as in collaboration with the faculty of other departments at Western, faculty at other institutions, and staff members of national and international laboratories.

Special thanks to Ms. Kerry Cochran for her invaluable assistance in the preparation and presentation of this document.

Thomas W. Gorczyca
Editor

Cover Design:

This image of Centaurus A shows a spectacular new view of a supermassive black hole's power. Jets and lobes powered by the central black hole in this nearby galaxy are shown by submillimeter data (colored orange) from the Atacama Pathfinder Experiment (APEX) telescope in Chile and X-ray data (colored blue) from the Chandra X-ray Observatory. Visible light data from the Wide Field Imager on the Max-Planck/ESO 2.2 m telescope, also located in Chile, shows the dust lane in the galaxy and background stars. The X-ray jet in the upper left extends for about 13,000 light years away from the black hole. The APEX data shows that material in the jet is traveling at about half the speed of light.

This is a dramatic illustration of one of several types of outflows that emanate from active galactic nuclei. Astronomer Kirk Korista studies another type of outflow, whose gas temperature is ~10,000 K and has flow speeds of a few to 10% of the speed of light. The plot (inset) demonstrates a means by which the gas density is measured in these latter outflows. Ultraviolet absorption lines (set against the powerful UV-X-ray spectrum emitted in the vicinity of the supermassive black hole) from several resonance lines of singly-ionized iron arising from a variety of lower levels within and near the ground term are observed and their column densities (absorber per m^2) are then measured. The relative electron level populations are functions of gas density (colored curves), and these are compared to the measured values (points with error bars) indicating a consistent number density of $10^{4.4}$ cm^{-3}. The photoionization calculations that produced the predicted relations rely on a vast array of atomic data, including some of those computed by atomic theorist Thomas Gorczyca.

It has been suggested that all this activity may have begun with the merger of a small spiral galaxy and Centaurus A about 100 million years ago. Such a merger could eventually trigger both the burst of star formation and the violent activity in the nucleus of the galaxy. The tremendous energy released when a galaxy becomes "active" can have a profound influence on the subsequent evolution of the galaxy and its neighbors. The mass of the central black hole can increase, the gas reservoir for the next generation of stars can be expelled, and the space between the galaxies can be enriched with heavier elements. Centaurus A is the nearest active galaxy, about 11 million light years away.

2 FROM THE CHAIRPERSON

Welcome to this latest issue in our continuing series of Physics Department Research Reports. I hope you will find the articles and statistics of some interest. It has been a very active and successful year for Physics research at WMU. Our recent moves to emphasize nuclear astrophysics, ultrafast science, nano-capillaries and other areas of applied physics are starting to reap results, as you will see in these pages. I am especially pleased that this report shows the high quality and quantity of research production by our cadre of excellent graduate students.

This productivity is continuing despite some shrinkage in our faculty numbers, and continuing budget restrictions in Michigan and the nation. This is a tribute to the dedication and efforts of our faculty, both those who are research active and those who help with the other jobs needed to keep a department like ours healthy, as well as to the rest of the staff who support our efforts.

We have some reasons to be optimistic for the near future. Some economic stimulus funding at the Federal level will apparently be used to boost basic research, and we have proposals and projects ready to take advantage of any such funding. In addition, we are now in the process of hiring a new faculty member, who will join us in the Fall of 2009.

As always, thanks are due to all who have contributed to this report, especially to the editor and the staff who actually put it all together. We very much appreciate what you have given us in this report.

Paul V. Pancella
Chair

3 ASTRONOMY

3.1 Physical Conditions in Quasar Outflows: Very Large Telescope Observations of QSO 2359-1241

Kirk T. Korista,[1] Manuel Bautista,[2] Nahum Arav,[2] Maxwell Moe,[3] Elisa Costantini,[4] and Chris Benn[5]

[1]Western Michigan University, Kalamazoo, MI 49008
[2]Virginia Polytechnic and State University, Blacksburg, VA 24061
[3]University of Colorado, Boulder, CO 80302
[4]SRON National Institute for Space Research, Sorbonnelaan 2, CA Utrecht, Netherlands
[5]Isaac Newton Group, Observatorio del Rogue de los Muchachos, Spain

We analyze the physical conditions of the outflow seen in QSO 2359-1241 (NVSS J235953-124148), based on high-resolution spectroscopic VLT observations. This object was previously studied using Keck HIRES data. The main improvement over the HIRES results is our ability to accurately determine the number density of the outflow. For the major absorption component, the populations from five different Fe II excited levels yield a gas density $n_H = 10^{4.4}$ cm^{-3} with less than 20% scatter. We find that the Fe II absorption arises from a region with roughly constant conditions and temperature greater than 9000 K, before the ionization front where temperature and electron density drop. Further, we model the observed spectra and investigate the effects of varying gas metallicities and the spectral energy distribution of the incident ionizing radiation field. The accurately measured column densities allow us to determine the ionization parameter [$\log U_H \approx -2.4$] and total column density of the outflow [$\log N_H(\mathrm{cm}^{-2}) \approx 20.6$]. Combined with the number density finding, these are stepping stones toward determining the mass flux and kinetic luminosity of the outflow, and therefore its importance to AGN feedback processes.

Based on observations made with European Southern Observatories Telescopes at the Paranal Observatories under program 078.B-0433(A).

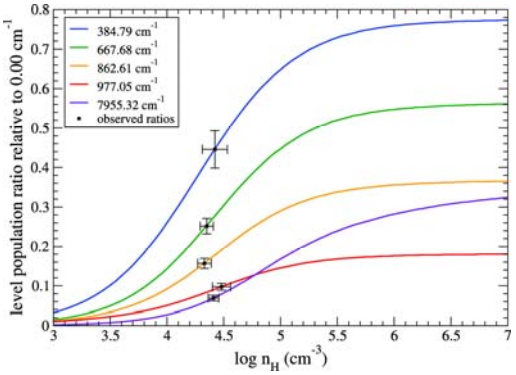

Calculated level populations of excited levels of Fe II relative to the ground level vs.

hydrogen number density in the photoionization model. The points indicate the observed column densities of each level relative to the ground level. All five independent measurements are consistent with log nH (cm-3) = 4.4 with less than 20% dispersion.

4 ATOMIC PHYSICS

4.1 Inner-Shell Double Photoionization: Coincident Energy and Angular Distributions in Xenon $4d_{5/2}$

M. Wiedenhoeft,[1] **A. A. Wills**,[1] **X. Feng**,[1] **S. Canton**,[1] J. Viefhaus,[2] **T. Gorczyca**,[1] U. Becker,[2] and **N. Berrah**[1]

[1]Western Michigan University, Kalamazoo, MI 49008
[2]Fritz-Haber-Institut der Max-Planck-Gesellschaft,14195 Berlin, Germany

Photo double-ionization (PDI), the emission of two electrons resulting from single photon absorption, has been intensively studied by many research groups over the past two decades since it is related to two important topics of modern atomic physics, namely electron correlations and the three-body Coulomb problem. Understanding the role of both effects in the PDI process can be achieved through a detailed description of the Triply Differential Cross Section (TDCS), which can only be carried out through coincidence measurements between two of the ionization fragments.

In sequential PDI, such as the $4d_{5/2}$ inner-shell ionization in xenon with subsequent $N_5O_{2,3}O_{2,3}$ Auger decay, the singly-charged intermediate 4d core hole can decay via an Auger process into a doubly-charged final state. The two outgoing electrons are correlated via the intermediate state, and further through the final states under particular experimental conditions, such as both electrons having similar kinetic energy or ejection direction. Because electrons are indistinguishable, it is necessary to describe the Auger electron as a resonance embedded in the PDI continuum. The striking theoretical prediction within this model [1] of strong interference effects in the TDCS for the case when both free electrons have the same kinetic energies has caught researchers attention and was investigated experimentally in the valence outer-shell PDI of neon and xenon.

Earlier experimental work has also shown how the spin state determines the constructive or destructive nature of the interference, which is a consequence of a general selection rule [2] already verified in direct PDI of helium. With three charged particles in the final state, PDI requires in addition a detailed delineation of Coulomb interactions in the resulting few body system, also called Post Collision Interactions (PCI). The common manifestations of PCI in non-coincident measurements are significant shifts of the atomic lines whose tails also become asymmetric. While these effects disappear in photoionization experiments when the difference in velocities between photo and Auger electron is large, they are always present if the incident particle is charged. The influence of PCI on angular distributions of the emitted electrons and the dependence of the post collision interaction on the inter electron angle were studied separately, all requiring coincidence experiments for an accurate description.

We have carried out the first kinetic energy and angular distributions for the Auger decay from xenon $4d_{5/2}$ photoionization leading to $^3P_2$ and $^1D_2$ final states of the $N_5O_{2,3}O_{2,3}$ Auger

decay. We have also shown that it is possible to describe split infinitive adequately the coincident angular distributions using a two-step model approach. Furthermore, the angular distribution data allows one to extract some information about the amplitude and phases of the emitted Auger electron and photoelectrons [1].

We have used an instrument that consists of a set of four rotating electron time-of-flight (TOF) energy analyzers, well suited to perform coincident measurements. These detectors are ideal since they can detect easily the kinetic energy of the two emitted electrons which spreads out over a wide kinetic energy range. The four TOF analyzers are placed in a plane perpendicular to the direction of the incident light which crosses an effusive gas beam. Mechanical constraints (size of the vacuum vessel) limit the length of the drift tube of the analyzers to 12.5 cm.

We measured the triply differential cross section of previously unexplored doubly charged Xe^{2+} states ($^1D_2$, $^3P_2$) by coincident measurements of the $N_5O_{2,3}O_{2,3}$ Auger electrons with the $4d_{5/2}$ photoelectron for the two final states ($^1D_2$) and ($^3P_2$) of the doubly charged ion as shown in Fig. 1. We found a very good agreement between our measurements and the theoretical models of the PCI effect given by both Kammerling et al. [3] as well as Sheinerman and Schmidt [4].

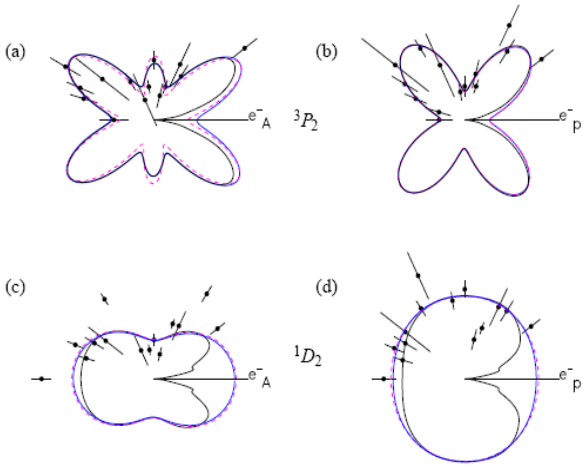

Figure 1 Polar plots of the angular distributions of the photoelectron or Auger electron. The light lines (blue in the colored version) are derived from using the best fit values for each set. The (red) dashed lines are the best common fit values for all 4 distributions used. The dark lines (black in the colored version) show the influence of the PCI effect and interchange effects. Top ($^3P_2$) final state: (a) angular distribution of the photoelectron, Auger electron ejected at 0° with respect to the photon polarization direction. (b) angular distribution of the ($^3P_2$) Auger electron. Both (a) and (b) show in general a very good agreement with the theoretical model given here. Bottom ($^1D_2$): (c) angular distribution of the photoelectron, Auger electron ejected at 0°; (d) angular distribution of the Auger electron. Again, the agreement is very good. Thus, the two-step model is applicable for inner electron angles in the range of 35° to 180° if the energy separation between the two electrons is larger than the intrinsic level width of the intermediate state. Moreover, we measured the first angular distribution pattern of the TDCS for these two final states and were able to reproduce them by a semi-empirical model which describes the transitions populating these two states in the non-relativistic dipole approximation [1].

Furthermore, the two-step model is applicable for inner electron angles in the range of 35° to 180° if the energy separation between the two electrons is larger than the intrinsic level width of the intermediate state. Moreover, we measured the first angular distribution pattern of the TDCS for these two final states and were able to reproduce them by a semi-empirical model

which describes the transitions populating these two states in the non-relativistic dipole approximation [1].

Acknowledgement:

All of the research work reported here is supported by the DoE, Office of Science, Basic Energy Sciences, Division of Chemical, Geosciences and Biological Science.

References:

[1] L.Vegh and J. H. Macek, Phys. Rev. A **50**, 4031 (1994); J. Phys. Rev. A **50**, 4036 (1994).
[2] F. Maulbetsch and J. S. Briggs, J. Phys. B **28**, 551 (1995).
[3] B. Kammerling and V. Schmidt, Phys. Rev. Lett. **67**, 1848 (1991) J. Phys. B: **26**, 261 (1993).
[4] S. A. Sheinerman and V. Schmidt, J. Phys. B **30**, 1677 (1997).

4.2 New Multi-User Movable Ion-Photon Beamline Built by WMU

R. C. Bilodeau,[1,2] **I. Dumitriu**,[1] J. D. Bozek,[2] A. Aguilar,[2] **D. Rolles**,[1,2] C. W. Walter,[3] N. D. Gibson,[3] and **N. Berrah**[1]

[1]Western Michigan University, Kalamazoo, MI 49008
[2]Advanced Light Source, Lawrence Berkeley National Laboratory, Berkeley, CA 94720
[3]Denison University, Granville, OH 43023

We (Rene Bilodeau, WMU lead person with the help of ALS staff engineers and John Bozek) have designed and built a portable ion beamline, shown in Fig. 1. This instrument has been successfully commissioned in June of 2008.

The instrument will enable us (and any ALS user) to exploit the capabilities of other ALS beamlines, below 9 eV and above 600 eV photon energies (not available on BL10.0.1 with the presently fixed instrument), including tunable circularly polarized light for the study of negative and positive ions. In addition, the instrument can be used at any other facility such as the LCLS at SLAC, Stanford University.

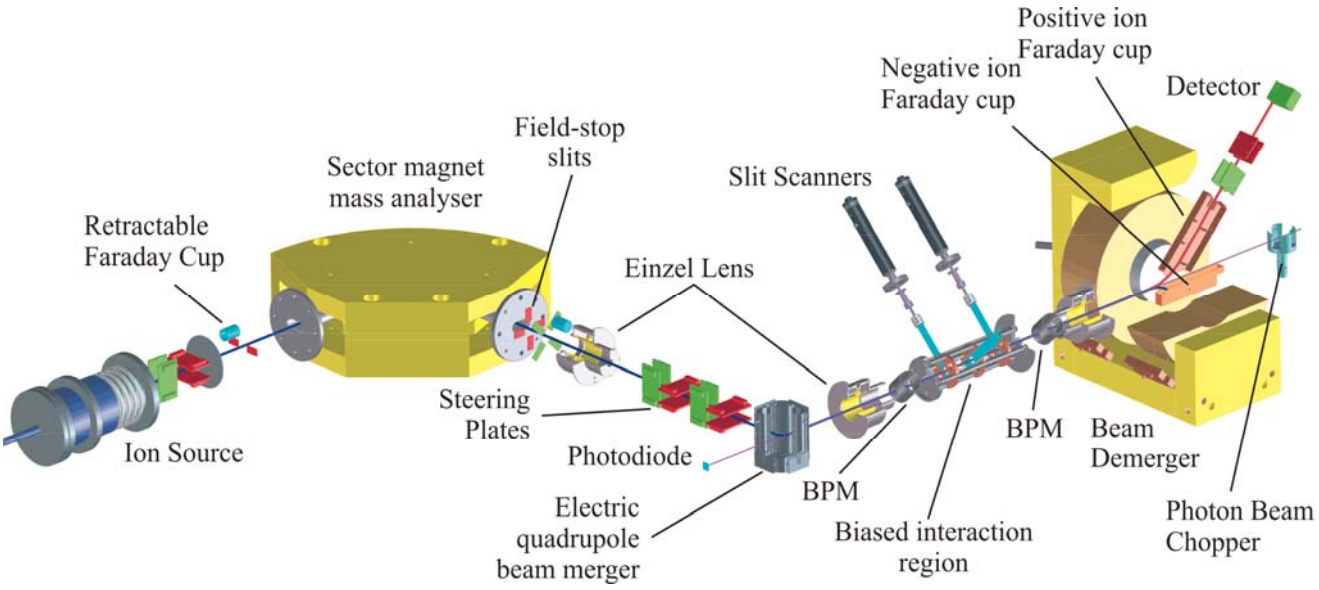

Figure 1 Schematic of the Movable Ion-Photon beamline (MIPB).

This beamline will allow ions produced by the ion source to be accelerated between 2-10 keV and mass selected by the m/q magnet. The ion beam phase space is limited by two sets of four-jaw slits in the pre-merger section of the ion beamline which act as field stops. Two sets of steering plates are located before the electrostatic merger to allow the ion beam trajectory to be tuned for optimum ion-photon overlap. The ion beam will be merged counter-propagating against the photon beam in a collinear geometry using the electrostatic quadruple

merger. The beam enters the interaction region after passing through electrostatic Einzel lenses. Two-dimensional spatial profiles of the merged ion and photon beams are monitored using 3 translating slit scanners located near the entrance, center, and exit of the 29-cm long energy-tagged interaction region as well as with rotating-wire beam profile monitors (BPMs). These allow fast feedback to facilitate the alignment of the ion and photon beams. The output from the scanners are digitized and recorded to determine the beam-overlap quality or form factor (for absolute cross section measurements). The merged path must be at an ultra-high vacuum of about $P=5x10^{-10}$ Torr insured by three 270 l/s ion pumps and an 8" titanium sublimation pump, since previous experiments were limited by high background levels due to scattering of the ion beam by residual gases. For absolute cross-section measurements, the three translating scanners each with two slits at 45° and 135° from the horizontal axis, mounted on a linear-motion feed through/stepping-motor assembly, provide two-dimensional profiles at the center of the interaction region for more accurate form-factor measurements. The 29 cm long interaction region consists of an electrically-insulated wire-mesh cylinder (for effective pumping) with 13 mm diameter apertures on each end to define the interaction region for absolute cross-section measurements. Without bias on the cylinder, the interaction region extends to 120 cm, which is useful for spectroscopy experiments. After the interaction region, the beam enters the demerging magnetic field generated by a water cooled GMW 3473-70 dipole electromagnet magnet with 15-cm diameter pole pieces mounted for vertical beam dispersion. The magnet vacuum chamber contains faraday cups for the primary ion beams (positive or negative) and a channeltron single particle detector for the product positive ions. The resulting signals are normalized to the primary ion beam current and photon intensity.

In the case of negative ions, these merged experiments are a serious challenge since even if one achieves perfect overlap between the photon and ion beams, the background counts generated by stripping collisions with residual vacuum gas can easily exceed the photodetachment signal rate by up to 4 orders of magnitude (even though the background pressure in the interaction region is $\sim 5\times10^{-10}$ Torr). In order to correct for background counts originating from collisional stripping and other background ionization, the photon beam is chopped at 1-10 Hz and the photodetachment signal is determined by subtracting the measured light-off signal from the light-on signal. The statistical error in the data is decreased by summing multiple sweeps of the photon energy of interest. The photon energies are separately calibrated using known resonance positions for neutral gases and are corrected for the Doppler shift. The photon beam is detected and recorded by a calibrated silicon photodiode, providing a measure of the photon flux.

We have produced a very strong C^- ion beam current in the past [1,2] (> 1 μA) with our Cs sputtering ion source as well as produced C_2, C_3, and C_4 anions with similar ion currents. We used our June-July 2008 beamtime to test the new MIPB as well as to fix most of the problems found during the December 2007 commissioning beamtime. As can be seen from Fig. 2, we have successfully tested the MIPB by measuring the shape resonance just above the C^- K-edge photodetachment threshold [1,2]. These raw preliminary data were collected with only approximately 15 minutes of total data collection time, while it took nearly 20 times longer to obtain data of slightly lesser statistical quality and fewer data points on beamline 10.0.1. Furthermore, we tested the photodetachment of C_2^-, as depicted in Fig. 3.

Complete photodetachment experiments in C_2^- dimmer will be conducted in June of 2009.

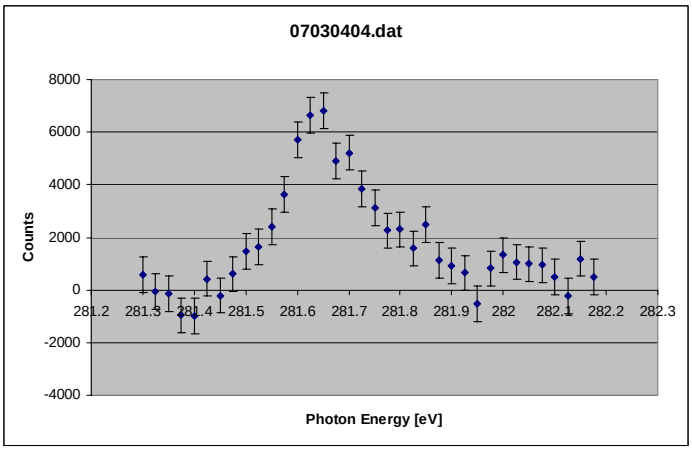

Figure 2 K-shell Photodetachement of C^- leading to C^+ via Auger decay.

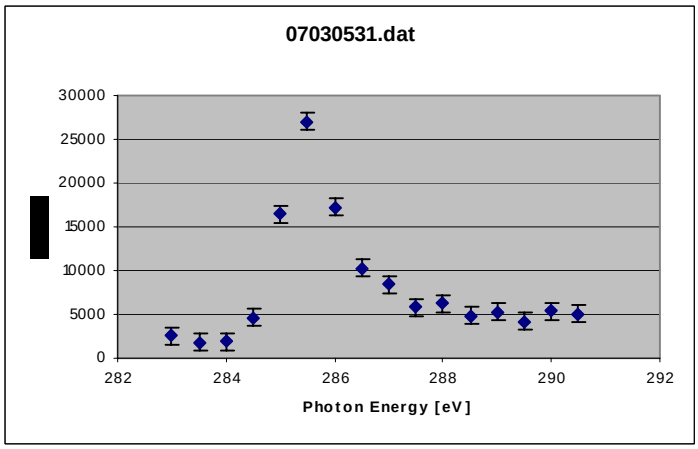

Figure 3 K-shell Photodetachement of C_2^- leading to C_2^+ via Auger decay.

Acknowledgement:

All of the research work reported here is supported by the DoE, Office of Science, Basic Energy Sciences, Division of Chemical, Geosciences and Biological Science. D. Rolles is indebted to the Alexander von Humboldt Foundation for a Feodor Lynen Fellowship.

References:

[1] N. D. Gibson, C. W. Walter, O. Zatsarinny, T. W. Gorczyca, G. D. Ackerman, J. D. Bozek, M. Martins, B. M. McLaughlin, and N. Berrah, K-shell photodetachment of C^-, Phys. Rev. A **67**, R030703 (2003)

[2] C. W. Walter, N.D. Gibson, R.C. Bilodeau, N. Berrah, J.D. Bozek, G.D. Ackerman, and A. Aguilar, Shape Resonance in K-Shell Photodetachment from C^-. Phys. Rev. A **73**, 062702 (2006).

4.3 Ultrafast Research Using the Future Linac Coherent Light Source (LCLS)

Nora Berrah,[1] **Rene Bilodeau**,[1,2] **Matthias Hoener**,[1,2] Elliot Kanter,[3] Steve Pratt,[3] Lou DiMauro,[4] and John Bozek[5]

[1]Western Michigan University, Kalamazoo, MI 49008
[2]Advanced Light Source, Lawrence Berkeley National Laboratory, Berkeley, CA 94720
[3]Argonne National Laboratory, Chemistry Division, Argonne, IL 60439
[4]Ohio State University, Columbus, OH, 43210
[5]Stanford Linear Accelerator Center, LCLS, Stanford, Menlo Park, CA 94025-7015

With the advent of a new ultrafast x-ray facility, the first of its kind in the world, we have added a new direction to our research program in the ultrafast domain. Specifically, we will study x-ray non-linear physics of atoms, molecules and clusters with intense ultrafast LCLS pulses. Lou DiMauro (OSU) and Nora Berrah (WMU) are the co-team leaders for the AMO community.

Our new program seeks to uncover the mechanisms of energy exchange among different degrees of freedom in systems ranging from diatomic molecules to large clusters such as the fullerenes. Specifically, this program will address fundamental questions concerning the ionization and fragmentation of molecules by intense, short pulses of x-rays from the LCLS. The study of short-time molecular dynamics that will be enabled by the LCLS is expected to provide new insight into fundamental aspects of molecular physics and chemistry.

We proposed to utilize the unprecedented LCLS peak power to study nonlinear and strong-field effects by carrying out excitation and ionization measurements of small molecules. Specifically, we will measure the relaxation mechanisms and Coulomb explosion subsequent to *inner-shell* ionization. Moreover, we plan to use the LCLS photon beam focused to a spot diameter of 1μm using KB mirrors to investigate *multiple*- and *multi*-photon-ionization processes, as well as the production of molecules with multiple core holes. We also plan to identify sequential/non-sequential many-photon multiple ionization. The understanding of such excitation and decay mechanisms will provide new information into the ionization and fragmentation dynamics of molecules, and into the correlated motion of the electrons remaining in the targets. In particular, fragmentation channels producing multiple heavy-particle fragments, subsequent to multiple ionization, will be measured using the AMO instrument ion detector simultaneously with electrons of all kinetic energies detected in five time-of-flight spectrometers.

The interaction of high-intensity x-rays with matter is somewhat different than the interaction of high-intensity infrared or optical photons with matter because the electron ponderomotive potential defined as $U_p = e^2F^2 / 4m\omega^2$ (quiver energy) is in general much weaker in the former case due to the much higher frequency of the x-rays. Unlike the case of lower frequency photons, x-rays couple strongly to inner-shell electrons, so we will observe new processes with the LCLS, including multiphoton processes involving core electrons, and sequential and

non-sequential ionization of inner-shell electrons. The LCLS will also enable the study of *multiphoton* ionization in the x-ray regime, that is, sub threshold ionization involving the use of *multiple photons* to ionize a *single electron* from a molecule.

Our proposed research will provide important information on damage mechanisms that will be important for the single bio-molecule imaging program. The damage mechanism for a single bio-molecule in a focused x-ray laser beam such as the LCLS is unknown. However, AMO physics can investigate the effect of nonlinear damage mechanisms, the effect of coherence and also find ways to diminish the radiation damage by varying the properties of the LCLS beam, such as shortening the duration of the LCLS pulse [1].

Acknowledgement:

All of the research work reported here is supported by the DoE, Office of Science, Basic Energy Sciences, Division of Chemical, Geosciences and Biological Science. M. Hoener is indebted to the Alexander von Humboldt Foundation for a Feodor Lynen Fellowship.

References:

[1] L. F. DiMauro, J. Arthur, N. Berrah, J. Bozek, J. N. Galayda and J. Hastings, Progress report on the LCLS XFEL at SLAC, J. Phys.: Conf. Ser. **88**, 012058 (2007).

4.4 Dielectronic Recombination of Al-Like Sulfur

Sh. A. Abdel-Naby,[1] **D. Nikolić**,[1] **T. W. Gorczyca**,[1] N. R. Badnell,[2] and D. W. Savin[3]

[1]Western Michigan University, Kalamazoo, MI 49008
[2]University of Strathclyde, Glasgow G4 0NG, United Kingdom
[3]Columbia University, New York, NY 10027

There has been much interest in measuring the oxygen-to-sulfur ratio in Jupiter's plasma torus [1]. Calculations for total DR rate coefficients for all sulfur ions were done with an application to magnetic fusion plasma in mind, in which a single-configuration approximation to calculate energies and transition rates was employed. Also, a cutoff on the number of states was applied [2]. DR rate coefficients for S^{q+} (q=1-5) ions have been calculated in the low density limit over the temperature range $T = 3\times10^4 - 10^6$ K that is applicable to the Io plasma torus [3]. Cross sections and rate coefficients for S^{3+} have been done using single-configuration and non-relativistic Hartree-Fock wave functions [4]. Photoionization cross sections and electron-ion recombination rate coefficients for S^{3+} were calculated in the close coupling approximation using the R-matrix method [5]. Other DR calculations were done for S^{3+} [6, 7]. All of these previous calculations for S^{3+} were performed only within a non-relativistic LS-coupling approximation and at higher temperatures more suitable for collisionally-ionized plasmas but not at the lower temperatures appropriate for photoionized plasmas. Our calculations include both LS coupling and intermediate coupling (IC) using a multi-configuration Breit-Pauli (MCBP) approximation.

We have used the AUTOSTRUCTURE code to calculate energy levels and radiative and autoionization rates in LS- and IC-couplings, with non-relativistic radial functions [8, 9]. The autoionization rates are calculated in the isolated resonance approximation using distorted waves. This enables the generation of final-state level-resolved and total DR rate coefficients in the independent-processes approximation, i.e., we neglect interference between the radiative recombination (RR) and DR processes [10]. In our calculation, n values were included up to 55 and a quantum-defect approximation for high-level values of n up to 1000 was used, while ℓ values were included up to 13.

The DR rate coefficient, as a function of temperature, from an initial ground or metastable state v to a final state i is given by:

$$\alpha_{iv}^{z+1}(T) = \left(\frac{4\pi a_0^2 I_H}{k_B T}\right)^{3/2} \sum_j \frac{g_j}{2g_v} \exp\left(-\frac{E_c}{k_B T}\right) \frac{\sum_\ell A_{a\,j\to v,E_{c\ell}} A_{rj\to i}}{\sum_h A_{r\,j\to h} + \sum_{m,\ell} A_{a\,j\to m,E_{c\ell}}}, \qquad (1)$$

where g_j is the statistical weight of the (N+1)-electron doubly-excited resonance state j, g_v is the statistical weight of the N-electron target state, and the autoionization rates, A_a, and radiative rates, A_r, are in inverse seconds. E_c is the energy of the continuum electron with angular momentum ℓ, which is fixed by the position of the resonance, I_H is the ionization potential energy of the hydrogen atom, k_B is the Boltzmann constant, and $(4\pi a_0^2)^{3/2}$ =

6.6011×10^{-24} cm^3. For $\Delta n = 0$ core-excitation, the resonance energies are empirically adjusted so that the series limits match the $3\rightarrow3$ excitation energies obtained from the NIST database [11].

A study of the DR cross section for S^{3+} in LS- and IC-coupling schemes reveals that the dominant capture channel is via n = 3 target core excitations. One can see from Fig. 1 that, at higher energies, the strongest contribution to the DR cross section, and therefore to the DR rate coefficient, comes from the $3p \rightarrow 3d$ excitation. Also, the calculated DR cross section for S^{3+} using IC-coupling is lower than the corresponding LS-coupling result. This is in contrast to the general IC vs LS trend [13, 14], where IC-coupling effects increase the number of resonances, and the resulting cross section, by roughly 50%. But this is for the case of a pure ground state such as Li-like ions ($1s^2 2^s\ 2S_{1/2}$). In our case, the ground state has a fine-structure splitting ($3s^2 3p\ ^2P_{1/2,\ 3/2}$) of around 0.118 eV.

The present *reduction* in the IC DR cross section is manifested in the DR rate coefficient, particularly in higher electron temperatures (see Fig. 2). At lower energies, the reason that the rate coefficient is higher using IC-coupling is due to additional contributions from the $3s^2 3p[^2P_{3/2}]n\ell$ core-excited resonances that are forbidden in LS-coupling, and more additional core-excited autoionizing states are open. The RR calculations are also shown in Fig.2.

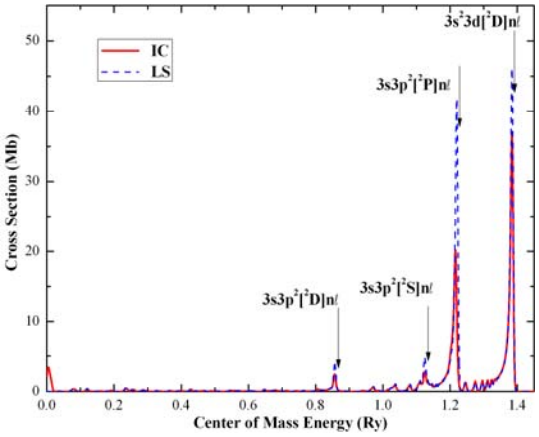

Figure 1 DR cross section of S^{3+} using both LS and IC coupling schemes, convoluted with a FWHM Gaussian of 0.1 eV for illustrative purposes, indicating that the dominant contribution to the Maxwellian-averaged rate coefficient comes from both $3s3p^2n\ell$ and $3s^2 3dn\ell$ Rydberg series.

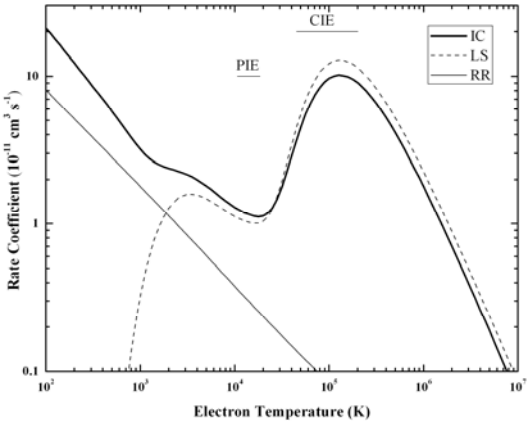

Figure 2 DR IC, DR LS, and RR rate coefficients of S^{3+} using both LS coupling and IC schemes. PIE and CIE denote typical temperatures of photoionized and collisionally-ionized plasmas, respectively [16].

Accurate resonance energies are particularly important for the calculations of low-temperature DR rate coefficients. The radial wave functions are obtained by using the Slater-type-orbital model potential [12]. The 3s, 3p, and 3d radial scaling parameters, $\lambda_{n\ell}$, were determined by minimizing the equally-weighted sum of energies of the 40 lowest terms.

In an attempt to understand the suppression of the DR cross section in IC-coupling, calculations were carried out for the 3s → 3p excitation ($e^- + 3s^2 3p\ [^2P_{1/2}] \rightarrow 3s3p^2\ [^2P_{1/2,\ 3/2}]n\ell$). The resulting DR cross sections for both $3s3p^2\ [^2P_{1/2},\ ^2P_{3/2}]n\ell$ series are convoluted with a full-width at half-maximum (FWHM) Gaussian of 1.2 meV (see Fig. 3). Both series begin to autoionize at principle quantum number $n = 31$. Also, the same calculations for the 3p → 3d excitation ($e^- + 3s^2 3p\ [^2P_{1/2}] \rightarrow 3s^2 3d\ [^2D_{3/2,\ 5/2}]n\ell$) were studied, and the resulting DR cross sections are plotted in Fig. 4. Again, the DR cross section drop occurs abruptly at $n = 31$. Thus, the reason for the reduction in the IC cross section is that the $3s3p^2 n\ell$ and $3s^2 3d n\ell$ series autoionize to additional continua for $n \geq 31$, decreasing the resultant radiative branching ratio in Eq. 1 [15]. In Fig. 5, we present comparisons between our calculated LS-coupling and IC results and other available data for S^{3+} [3, 5-7].

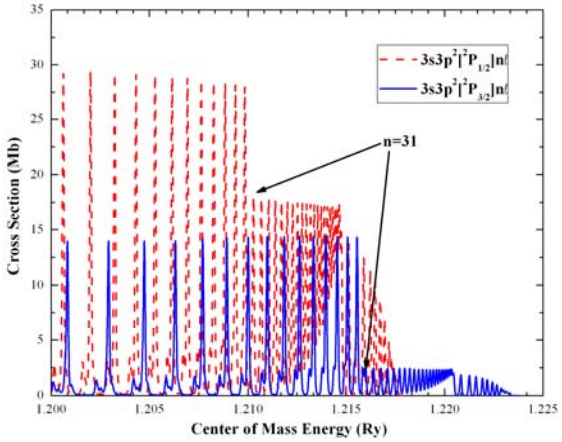

Figure 3 DR cross section for S^{3+} in IC-coupling for the collision $e^- + 3s^2 3p[^2P_{1/2}] \rightarrow 3s3p^2[^2P_{1/2},^2P_{3/2}]n\ell$, convoluted with a FWHM Gaussian of 1.2 meV. A sudden drop in the cross section occurs for both series at n = 31.

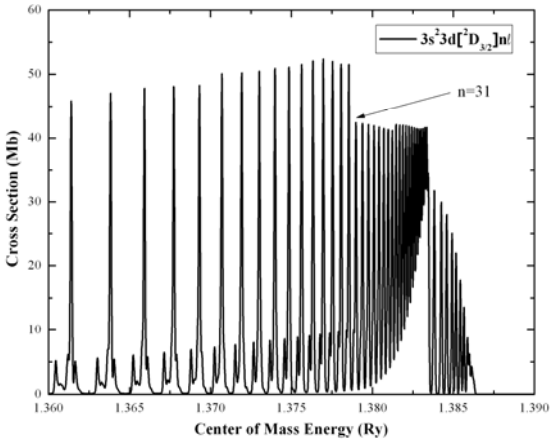

Figure 4 Same as Fig. 3 but for the collision $e^- + 3s^2 3p[^2P_{1/2}] \rightarrow 3s^2 3d[^2D_{3/2}]n\ell$.

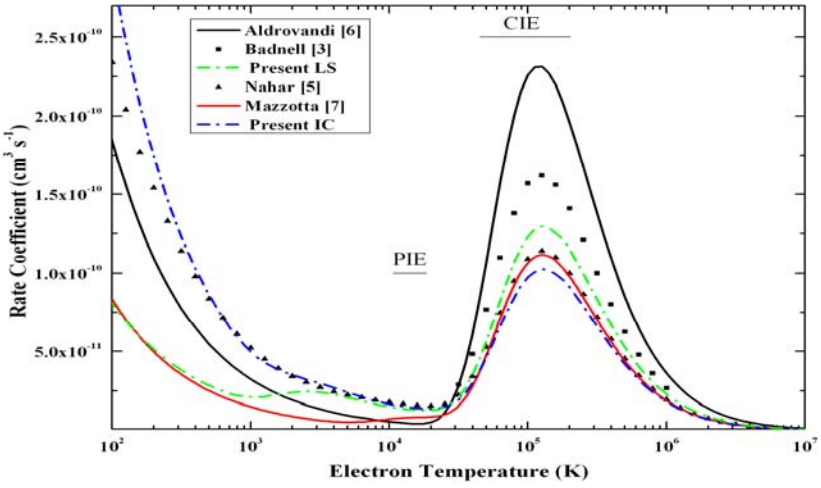

Figure 5 Comparisons between present and previously existing DR + RR rate coefficients for S^{3+} [3, 5-7].

Our present investigation into the DR process of Al-like S^{3+} has revealed that a sufficiently large atomic configuration basis leads to fairly accurate energies and transition rates for the target levels, and should yield reliable DR cross sections. With the inclusion of IC-coupling effects, additional radiatively-decayed states can autoionize, thereby decreasing the DR cross section. This occurs near the Rydberg limits and reduces the high-temperature rate coefficient that is more important for collisionally-ionized plasmas. On the other hand, IC effects open up additional core-excited autoionizing states, thereby increasing the low-energy DR cross section. This leads to a substantial increase in the low-temperature rate coefficient that is important for photoionized plasmas. These findings are a reminder that, as usually is the case, relativistic (i.e., spin-orbit) effects can have a profound effects even for low ionization. Despite the relative weakness of spin-orbit effects, which scale as z^4 and are expected to be least important for low ionization stages such as the present case of S^{3+}, even small energy shifts create additional autoionizing levels that greatly affect the resulting rate coefficient.

Acknowledgments:

This work was supported in part by NASA APRA and SHP SR&T programs.

References:

[1] D. E. Shemansky, J. Geophys. Res. **92**, 6141 (1988).
[2] V. L. Jacobs, J. Davis, J. E. Rogerson, and M. Blaha, Astrophys. J **230**, 627 (1979).
[3] N. R. Badnell, Astrophys. J. **379**, 375 (1991).
[4] A. Al-Mulhem and I. Nasser, Phys. Rev. A **46**, 2945 (1992).
[5] S. N. Nahar, Astrophys. J. Suppl. Ser. **126**, 537 (2000).
[6] S. M. V. Aldrovandi and P. Pequignot, A&A **25**, 137 (1973).
[7] P. Mazotta, G. Mazzitelli, S. Colafrancesco, and N. Vittorio, Astron. Astrophys. Suppl. Ser. **133**, 403 (1998).
[8] N. R. Badnell, J. Phys. B **19**, 3827 (1987).
[9] N. R. Badnell, J. Phys. B **30**, 1 (1997).
[10] M. S. Pindzola, N. R. Badnell, and D. C. Griffin, Phys. Rev. A **46**, 5725 (1992).
[11] http://physics.nist.gov/asd3.
[12] A. Burgess, H. E. Mason, and J. A. Tully, Astron. Astrophys. **217**, 319 (1989).
[13] E. J. Trefftz, in *in Physics of The One and Two Electron Atoms*, edited by F. Bopp and H. Klein-Poppen, North-Holand, Amsterdam, 1969, pp. 839.
[14] D. C. Griffin, M. S. Pindzola, and C. Bottcher, Phys. Rev. A **31**, 568 (1985).
[15] M. Blaha, Astrophys. Letters **10**, 179 (1972).
[16] P. Bryans, E. Landi, and D. W. Savin, Astrophys. J, **in press**, [arXiv:0805.3302] (2008).

4.5 Electron Capture by Ne^{6+} Ions from H_2O and CO_2

A. Hasan,[2] O. Abu-Haija,[3] **A. Kayani,**[1] and **E. Y. Kamber**[1]

[1]Western Michigan University, Kalamazoo, MI 49008
[2] American University of Sharjah, Sharjah, UAE
[3] Tafila Technical University, Tafila, Jordan

Using translational energy-gain spectroscopy technique [1], we have measured the energy-gain spectra and absolute total cross sections for single- and double-electron capture in collisions of Ne^{6+} recoil ions with H_2O and CO_2 at laboratory impact energies between 250 and 3000 eV. The translational energy-gain spectra show that only a few final states were selectively populated depending on the target and collision energy. In all collision systems studied here, the dominant reaction channels are due to non-dissociative single-electron capture into excited states of the projectile product. The final state populations were discussed on the basis of the reaction windows, which are calculated using the single-crossing Landau-Zener model [2] and the extended version of the classical over-the-barrier model [3].

Preliminary measurements of total cross sections for single-electron capture by Ne^{6+} ions from H_2O and CO_2 are shown in Fig. 1 together with the predictions of the multi-channel Landau-Zener model [2] and the classical over-the-barrier (COB) model [3]

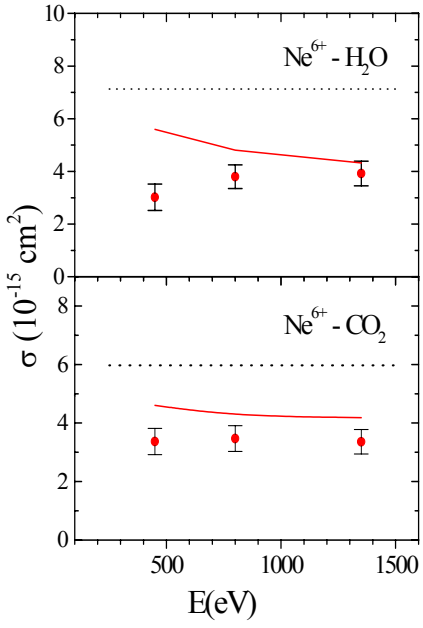

Figure 1 Total cross sections for single-electron capture by Ne^{6+} ions from H_2O and CO_2. •, present work; dotted curves; COB model; solid lines, MCLZ calculations.

For Ne^{6+} + H_2O collisions, the total cross sections increase with increasing impact energy, a pattern that is well documented for such collisions at low energies [4]. This can be understood by the reaction window, which broadens with increasing energies and therefore increases the

probability of capture channels with large Q-values. The energy dependence of cross sections is in direct contradiction with the MCLZ calculation which decreases with increasing energy, and the COB model over predicted the total cross section for capture by at least a factor of two. For Ne^{6+} - CO_2 collisions, the total cross sections show no significant dependence on `the collision energy. Our data are lower than those of the MCLZ model and about a factor of two smaller than the COB model predictions.

References:

[1] S. Yaltkaya, E. Y. Kamber, and S. M. Ferguson, Phys. Rev. A **48**, 382 (1993).
[2] R. E. Olson and A. Salop, Phys. Rev. A **14**, 579 (1976).
[3] A. Niehaus, J. Phys B. **19**, 2925 (1986).
[4] H. Winter, Phys. Scr. **T3**, 159 (1983).

4.6 Differential Cross Sections for Single-Electron Capture by Low-Energy O_2^{2+} Ions with Ne and O_2

E. Y. Kamber

Western Michigan University, Kalamazoo, MI 49008

A large variety of molecular ions have been identified in cold astrophysical environments and in planetary atmospheres. Molecular oxygen ions are of particular interest due to their potential influence on the properties of the ionosphere and their involvement in many atmospheric phenomena. Furthermore, electron capture involving multiply charged molecular ions has been proposed as a mechanism for generating ions in the earth's upper atmosphere [1,2].

In the present work, a differential energy-gain spectrometer [3], capable of measuring simultaneously the scattering angle and the energy-gain of projectile products in ion-atom collisions, has been used for the study of state-selective non-dissociative single-electron capture in collisions of O_2^{2+} recoil ions with Ne and O_2 at an impact energy 100 eV and scattering angles between 0^o and 6^o. Unfortunately, the peak of doubly charged molecular ion O_2^{2+} coincides with the atomic ion O^+ peak in mass spectrum at m/q =16. No attempt was made to estimate the fraction of O_2^{2+} in the O^+ beam. However, we were able to easily separate the O_2^+ products resulting from electron capture by using an electrostatic analyzer (ESA) voltage which was double that required to transmit the elastically scattered ion beam. Following the nomenclature described by Kamber et al. [4], the observed reaction channels are denoted in the following fashion: the designations I, II, and III represent, respectively, the ground, first, and second electronically excited states of O_2^{2+}; α, β, γ, represent the ground and subsequent electronically excited states of O_2^+ ion; X, represents the ground state of the target product.

Figure 1 shows the translational energy-gain spectra obtained for single-electron capture by 100 eV O_2^{2+} ions from Ne at different scattering angles. At 0^o scattering angle, the energy-gain spectrum indicates that the dominant reaction channel is due to non-dissociative single-electron capture into the ground state ($X\ ^2\Pi_g$) of the product O_2^+ from the ground state incident O_2^{2+} ($X\ ^1\Sigma_g^+$) ions with contributions due to capture from the low-lying metastable state ($A\ ^3\Sigma_u$) of the O_2^{2+} into the ($A\ ^2\Pi_u$) state of O_2^+. There are smaller contributions due to capture into the a $^4\Pi_u$, A $^2\Pi_u$, and b $^4\Sigma_g^-$ states from the metastable states W $^3\Delta_u$, B $^3\Pi_g$, and B' $^3\Sigma_g^-$ of the O_2^{2+} ions via reaction channels IIβX, IIIγX, IIIβX, VδX, IVγX, IVβX, and VβX. A comparison with the measurements of Pederson [5] at 100 eV, and Hamdan and Brenton [6] at 6 keV shows good agreement with the present measurements.

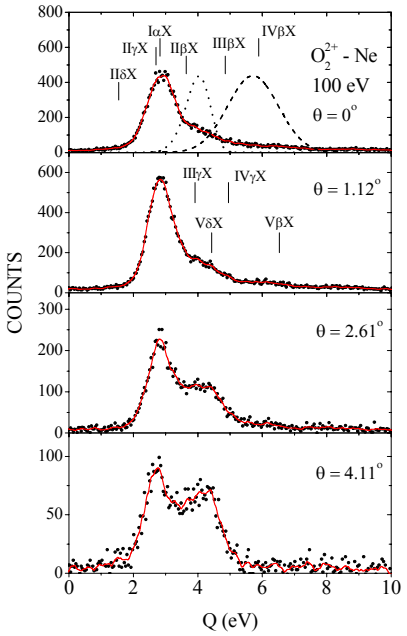

Figure 1 Translational energy-gain spectra for single-electron capture by 100 eV O_2^{2+} ions from Ne at different projectile laboratory scattering angles. Also shown are reaction windows calculated on the basis of a single-crossing LZ model (dotted curve) and the ECOB model (dashed curve). Smooth lines are drawn to guide the eye.

As the scattering angle is increased, capture into the X $^2\Pi_g$ state (the IαX channel) remains dominant but contributions from reaction channels IIβX, IIIγX, and VδX, respectively, due to capture from the metastable states W $^3\Delta_u$ and B' $^3\Sigma_g^-$ of the O_2^{2+} ions into the a $^4\Pi_u$, A $^2\Pi_u$, and b $^4\Sigma_g$ states of O_2^+, increase with increasing the scattering angles. This indicates that the angular distribution for the IαX channel is more strongly peaked in the forward direction than for the reaction channels IIβX, IIIγX, and VδX. Figure 1 also shows our calculated reaction windows for 100 eV O_2^{2+} - Ne collisions, using both a single-crossing Landau-Zener (LZ) model [7] and the extended version of the classical over-the-barrier (ECOB) model [8]. Calculated peak values have been normalized to our observed peak values in the energy spectrum. The reaction based on a single-crossing LZ model does not describe the position of the dominant reaction channel, while the reaction window based on the ECOB model maximizes at about 6 eV and underestimates the contribution of the IαX channel.

Figure 2 shows the translational energy-gain spectra for single-electron capture by 100 eV O_2^{2+} ions from O_2 at different projectile laboratory scattering angles. The observed spectra clearly indicate that non-dissociative single-electron capture into the O_2^+ (c $^4\Sigma_u$) state from the low-lying metastable state (A $^3\Sigma_u$) of the O_2^{2+} is the predominant channel, although

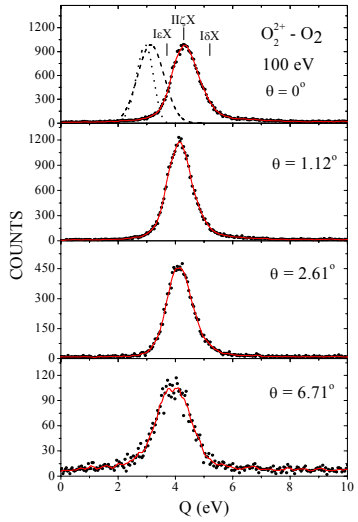

Figure 2 Translational energy-gain spectra for single-electron capture by 100 eV O22+ ions from O2 at different projectile laboratory scattering angles. Also shown are reaction windows calculated on the basis of a single-crossing LZ model (dotted curve) and the ECOB model (dashed curve). Smooth lines are drawn to guide the eye.

capture by the ground state (X $^1\Sigma_1$) of O_2^{2+} ions into b $^4\Sigma_g$, and B $^2\Sigma_g$ states are also significant. As the scattering angle is increased, a relative shift of about 0.45 eV in the energy gain of the IIζX channel is observed going from scattering angle of 0º to 6.71º. This is attributed to the energy given to the target and is in accordance with energy and momentum conservation rules. The reaction windows favor Q values smaller than those observed and are positioned near the IεX channel.

The experimental total differential cross sections (dσ/dΩ) for single-electron capture by 100 eV O_2^{2+} ions from Ne and O_2 are shown in Figure 3. The general features of the distributions are qualitatively explained in terms of semi-classical model based on Coulomb potential curves which have been described in detail by Andersson et al. [9]. The traditional two-state model has been used to estimate the critical angle θ_c, which corresponds to capture at an impact parameter equal to the crossing radius, by assuming that capture occurs at a localized curve crossing between the potential energy curves for entrance and exit channels. For small angles, $\theta_c = Q/2E$, where Q is the exoergicity of the collision and E is the collision energy. This angle separates the events scattered at smaller angles due to capture on the way-out of the collision and events scattered at larger angles due to capture on the way-into the collision.

For O_2^{2+} - O_2 collisions, the distribution is peaked in the forward direction inside the critical angle $\theta_c = 1.32º$, which corresponds to the IIζX capture channel. This distribution represents contributions from electron capture that takes place on the way-out of the collisions. For O_2^{2+} - Ne collisions, the measurements show that the projectile products which correlate with capture into the (X $^2\Pi_g$) state are distributed forward inside the critical angle $\theta_c = 0.8º$, indicating that capture takes place on the way-out of the collision.

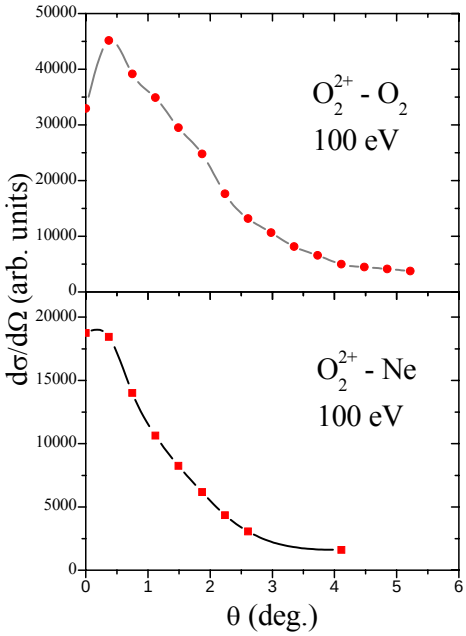

Figure 3 Experimental differential cross sections for single-electron capture by O_2^{2+} ions from Ne and O_2. Spline lines are drawn to guide the eye.

References:

[1] D. Mathur, Phys Rep **225,** 193 (1993).
[2] S. S. Prasad and D. R. Furman, J GeoPhys **80**, 1360 (1975).
[3] S. Yaltkaya, E. Y. Kamber and S. M. Ferguson, Phys Rev A **48**, 382 (1993).
[4] E. Y. Kamber, D. Mathur and J. B. Hasted, J Phys B **16**, 3025 (1982).
[5] J. O. P. Pedersen, M. S. Thesis, 1986 University of Aarhus, Aarhus, Denmark.
[6] M. Hamdan and A. G. Brenton, Chem Phys Lett **164**, 413 (1989).
[7] R. E. Olson and A. Salop, Phys Rev A **14**, 579 (1976).
[8] A. Niehaus, J Phys B **19**, 2925 (1986).
[9] L. R. Andersson, H. Danared and A. Barany, Nucl Instrum and Meth B **23**, 54 (1987).

4.7 State-Selective Electron Capture by O^{3+} Ions from Atomic and Molecular Targets

E. Y. Kamber,[1] **O. Abu-Haija**,[1,2] and **J. A. Wardwell**[1]

[1]Western Michigan University, Kalamazoo, MI 49008
[2]Tafila Technical University, Tafila, Jordan

State-selective electron capture processes in low-energy collisions of O^{3+} recoil ions with He, Ar, D_2, O_2, H_2O and CO_2 at impact energies between 0.3 and 1.2 keV and scattering angles between 0º and 6º have been studied using a differential energy-gain spectrometer [1], capable of measuring simultaneously the energy-gain and the scattering angle of projectile products in ion-atom/molecule collisions, The energy-gain spectra showed that the dominant reaction channels were due to capture into excited states of the projectile product O^{2+}. In this work, no clear evidence of the processes involving long-lived metastable state O^{3+} ($2s\ 2p^2\ ^4P$) was observed. The energy-gain spectra were interpreted qualitatively in terms of the reaction windows, which are calculated using the single-crossing Landau-Zener (LZ) model and the extended version of the classical over-the-barrier (ECOB) model.

The experimental total differential cross sections ($d\sigma/d\theta$) for single-electron capture by 300 eV O^{3+} ions from He, D_2 and H_2O are shown in Figure 1. The differential cross sections were determined using the translational energy-gain technique, by calculating the area under the peaks in the energy-gain spectra at different projectile laboratory scattering angles using a curve fitting program. The general features of the distributions are qualitatively explained in terms of semi-classical model based on Coulomb potential curves, which have been described in detail by Andersson et al. [2]. The traditional two-state model has been used to estimate the critical angle θ_c, which corresponds to capture at an impact parameter equal to the crossing radius, by assuming that capture occurs at a localized curve crossing between the potential energy curves for entrance and exit channels. For small angles, $\theta_c = Q/2E$, where Q is the exoergicity of the collision and E is the collision energy. This angle separates the events scattered at smaller angles due to capture on the way out of the collision and events scattered at larger angles due to capture on the way into the collision. The critical angle for each dominant channel is indicated by an arrow in Fig. 1.

For 300 eV O^{3+} - He collisions, the distribution contains a broad peak lying slightly outside the critical angle $\theta_c = 1.21º$ for capture into the excited state $2s2p^3\ ^3P$ of the O^{2+} ion. This distribution represents contributions from electron capture that takes place on the way into the collisions. For 300 eV O^{3+} - D_2 collisions, the spectrum shows a smooth rise to a broad maximum around 2º outside $\theta_c = 0.61º$, assuming that electron capture occurs into 2p 3s of the O^{2+} ion. The distribution is due to capture on the way into the collision. For 300 eV O^{3+} - H_2O collisions, the distribution contains a peak slightly greater than $\theta_c = 0.59º$, which corresponds to the 2p 3p capture channel, indicating that capture takes place on the way into the collision.

The measured total cross sections for single-electron capture by O^{3+} ions from He, D_2, H_2O and CO_2 are shown in Fig. 2 together with other available measurements and calculations.

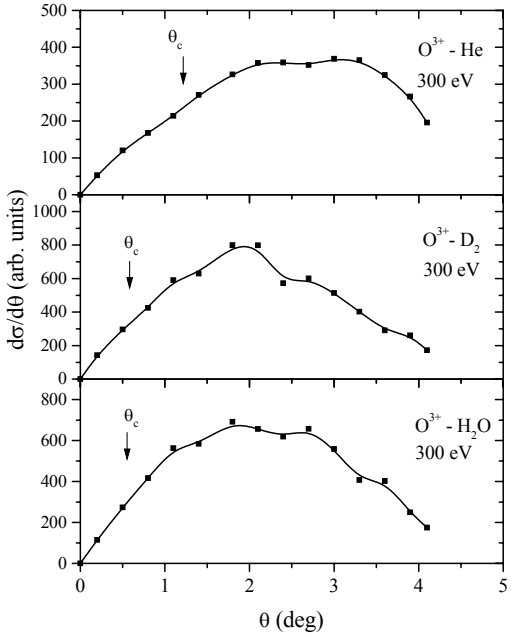

Figure 1 Experimental differential cross sections ($d\sigma/d\theta$) for single-electron capture by 300 eV O^{3+} ions from He, D_2, and H_2O. Spline lines are drawn to guide the eye.

For O^{3+} - He collisions, the total cross sections show no significant dependence on the collision energy. Our data are in reasonably good agreement with the experimental results of Bangsgaard et al. [3] and Ishii et al. [4]. The data presented in this study, however, are considerably higher than the recommended cross sections of Janev et al. [5] and found to be 60% higher than the multi-channel Landau-Zener calculations [6], based on the Taulberg expression for the coupling matrix H_{12} [7]. The measured cross sections are about a factor of 2 smaller than the classical over-the-barrier (COB) model [8] prediction of 10.737×10^{-16} cm^2 assuming the capture probability A = 0.5. An average value for A of 0.253 is found experimentally, by dividing the measured total cross section by the classical cross section (πR_c^2). This small value of A is probably due to the population of core excited states. The responsible coupling matrix element (H_{12}), which couples the incoming channel with the outgoing reaction channels leading to these core excited states, is small and thus will yield measured cross sections smaller than πR_c^2.

For O^{3+} + D_2 collisions, the total cross sections slowly decrease with increasing collision energies. Our data are in good agreement with the measurements of Phaneuf et al. [9], and the recommended cross sections of Janev et al. [5] for O^{3+} + H_2 collisions, but are a factor of 2 higher than the results of Beijers et al. [10]. The present measurements are in good agreement with the COB model prediction of 27.24×10^{-16} cm^2 with A = 0.5, and MCLZ calculations at low energies ($\leq$ 900 eV) and show similar behavior (cross sections slowly decrease with increasing collision energies). Recently Wang et al. [11] performed a nearly complete *ab initio* study of single-electron capture in collisions of ground state O^{3+} ($2s^2(^1S)2p\ ^3P$) ions with molecular hydrogen using a fully quantum-mechanical, molecular-orbital (QMO) coupled-channel method, adopting the so-called infinite order sudden approximation (IOSA), the vibrational sudden approximation (VSA), and the electronic approximation (EA). The data presented here is considerably lower than those of EA calculations by a factor of 1.35, and found to be on average 1.42 and 3.33, respectively, higher than VSA and IOSA predictions.

For O^{3+} + H_2O and CO_2 collisions, the total cross sections increase with increasing impact energy, a pattern that is well documented for such collisions at low energies [7,12]. This can be understood by the reaction window, which broadens with increasing energies and therefore increase the probability of capture channels with large Q-values. For O^{3+} + H_2O collisions, the energy dependence of cross sections is in direct contradiction with the MCLZ calculation which decreases with increasing energy, and the COB model over predicted the total cross section for capture by at least of a factor of 1.2. For O^{3+} + CO_2 collisions, The MCLZ results are at least a factor of 2 smaller than the experimental results and show the same energy dependence, whereas, the prediction of the COB model lie about 30 – 40% below the experimental results.

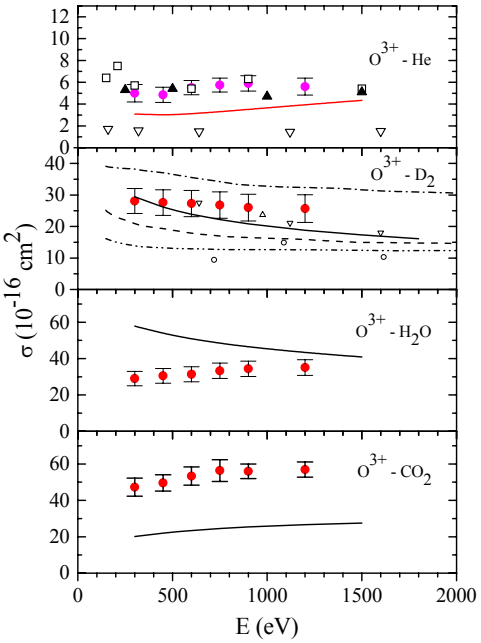

Figure 2 Total cross sections for single-electron capture by O^{3+} ions from He, D_2, H_2O and CO_2. •, present work; □, Ishii et al. [4]; ▲, Bangsgaard et al. [3]; ▽, Janev et al. [5]; Δ, Phaneuf et al. [9]: ○, Beijers et al. [3]; dotted curves; COB model; dash-dot, EA – Wang et al. [11]; dash-dot-dot, IOSA – Wang et al. [11]; dash, VSA – Wang et al. [11]; solid lines, MCLZ calculations.

References:

[1] S. Yaltkaya, E. Y. Kamber, and S. M. Ferguson, Phys. Rev. A **48**, 382 (1993).
[2] L. R. Andersson, H. Donard, and A. Barany, Nucl. Instrum and Meth. B **23**, 54(1987).
[3] J. P. Bangsgaard, P. Hvelplund, J. O. P. Pedersen, L. R. Andersson, and A. Barany, Physica Scripta **T28**, 91 (1989).
[4] K. Ishii, A. Itoh, and K. Okuno, Phys. Rev. A **70**, 042716 (2004).
[5] R. K. Janev, R. A. Phaneuf, and H. T. Hunter, At. Data Nucl. Data Tables **40**, 249 (1983).
[6] R. E. Olson R E and A. Salop, Phys. Rev. A **14**, 579 (1976).
[7] K. Taulbjerg, J. Phys. B **19**, L367 (1986).
[8] A. Niehaus, J. Phys B. **19**, 2925 (1986).
[9] R. A. Phaneuf, I. Alvarez, F. W. Meyer, and D. H. Crandall, Phys. Rev. A **26**, 1892 (1982).
[10] J. P. M. Beijers, R. Hoekstra, and R. Morgensterm, J. Phys. B **29**, 1397 (1996).
[11] J. G. Wang, P. C. Stancil, A. R. Turner, and D. L. Cooper, Phys. Rev. A **69**, 62702 (2004).
[12] H. Winter, Phys. Scr. **T3**, 159 (1983).

4.8 Suppression of Primary Electron Interferences in the Ionization of N_2 by 1 – 5 MeV Protons

J. L. Baran,[1] **S. Das**,[1] F. Járai-Szabó,[2] K. Póra,[2] L. Nagy,[2] and **J. A. Tanis**[1]

[1]Western Michigan University, Kalamazoo, MI 49008
[2]Faculty of Physics, Babes-Bolyai University, 400084 Cluj, Romania

It is well known that electrons have both particle and wavelike properties similar to photons. A manifestation of this duality has recently been shown to occur in the ejection of electrons from H_2 impacted by fast ions [1]. Whereas electron ejection from an atom gives rise to a single outgoing ionization "wave", corresponding ejection from H_2 occurs simultaneously from both atomic centers, resulting in coherent ionization waves that can interfere. This phenomenon of interference associated with electron ejection from molecules is analogous to Young's two-slit experiment with the atomic centers acting as "slits", and was considered already more than forty years ago in the photoionization of molecules [2,3]. Prior to recognition of this Young-type interference involving simultaneous emission from two atomic centers, Kronig [4] attributed oscillatory structures in the K-shell ionization spectra of heteronuclear molecules to intramolecular scattering. In the latter case, the ionization wave originating at one nucleus is scattered from the adjacent nucleus causing subsequent interference between the original and scattered waves. This phenomenon is related to the well-known EXAFS (extended x-ray absorption fine structure) technique [5,6] used in solid-state physics to study the structure of materials. Hence, while atomic ionization is generally well understood [7,8], more subtle effects arising from coherent electron emission distinguish molecular ionization from its atomic counterpart and consequently reveal the wavelike aspects of the ejected electrons.

In the present work, interferences associated with electron ejection are investigated for N_2 impacted by 1 – 5 MeV H^+ ions (see Ref. [9] for details). For diatomic molecules such as N_2 ionization can occur from several molecular orbitals, as opposed to the single K-shell orbital in H_2. However, the probability for ionization of the valence L-shell orbitals in N_2 is about three orders of magnitude larger than for the K-shell orbitals [7,8], which are not expected to contribute significantly to any interference effects. To compare the experimentally observed oscillatory structures with the expected Young-type interference structures, theoretical calculations were performed for the ionization of N_2 obtaining molecular to atomic cross section ratios using a formulation similar to that developed by two of the present authors for H_2 [10]. The main difference is that N_2 has several molecular orbitals giving different interference patterns.

From measurements conducted at Western Michigan University using the 6-MV tandem Van de Graaff accelerator, experimental molecular N_2 cross sections were divided by the theoretical atomic N cross sections, giving the ratios shown in Fig. 1. The cross section ratios, normalized to about unity for convenience, show clear evidence of oscillatory behavior with no significant dependence on the electron observation angle or collision velocity, in contrast to earlier results for Kr^{33+} [1,11] and H^+ [12] + H_2 for which there was a strong dependence of

the primary interference structures on the observation angle and a smaller but definite dependence on the collision velocity. Thus, the observed oscillatory structures for N_2 suggest an origin other than primary Young-type interferences, and are suggestive of previously observed secondary interferences that have been attributed to interference of the primary ejected electron wave with the secondary wave that results from scattering at the other atomic center [13].

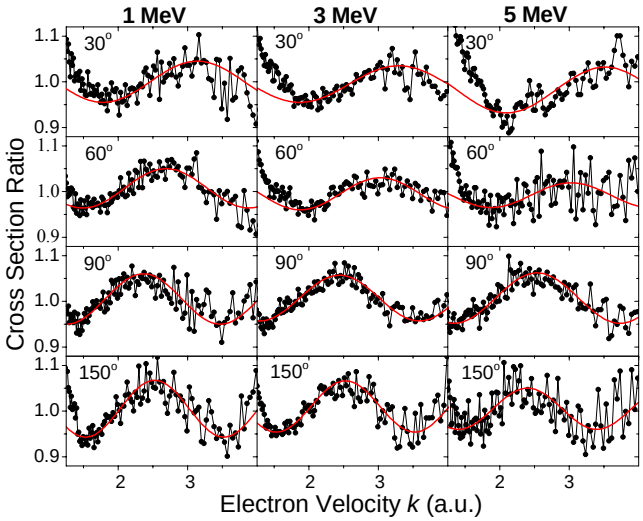

Figure 1 Ratios of measured molecular N_2 to theoretical atomic N cross sections. Results shown are for 1, 3 and 5 MeV H^+ ions at the indicated observation angles. The smooth curves are the results of fitting Eq. 1 to the ratios.

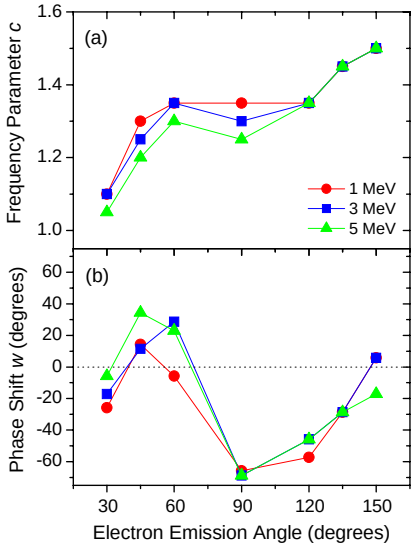

Figure 2 Frequency parameters c and phase shifts w obtained by fitting Eq. 1 to the data of Fig. 1 for all measured angles at projectile energies of 1, 3 and 5 MeV.

To quantitatively characterize the oscillatory structures and frequencies for N_2, the normalized cross section ratios of Fig. 1 were parameterized according to the function

$$f(k) = A\left[1 + \sin(kcd - w)\right] + B\,, \qquad (1)$$

where k is the electron momentum (velocity), d is the internuclear separation, c is a fitting parameter representing the oscillation frequency, w allows for a phase shift, and A and B are normalization constants. Allowance for a phase shift was also utilized in Refs. [12,13] to describe the secondary interference structures attributed to intramolecular scattering.

The values obtained for c and w from the fitting are shown in Figs. 2a and 2b, respectively. The frequency parameter c (Fig. 2a) shows only a small dependence on the electron observation angle (note the suppressed ordinate) and the collision velocity in sharp contrast to results for the primary interferences in H_2 [11,12]. On the other hand, the second-order oscillations for these same collisions gave values for c in the range ~ 2.5-3 that were nearly independent of the observation angle. Regarding the phase shift w, Fig. 2b shows this parameter to have a maximum around 45° and a minimum at 90°, with little dependence on the collision velocity. The presence of this shift can be seen already by careful examination of the cross section ratios in Fig. 1. On the contrary, the second-order oscillations in $Kr^{33+} + H_2$ [13] and $H^+ + H_2$ [12] exhibited a constant phase shift of $w \sim \pi$. The exact reason for the

angular dependence of this phase shift is presently unknown, but is likely contained in the amplitude factors governing the secondary interferences (see Ref. [13]).

If the observed oscillatory structures in Fig. 1 are indeed secondary interferences, then the underlying mechanism for their production must be understood. It might be argued that secondary interference occurs when an L-shell electron undergoes large momentum transfer in a relatively "hard" binary encounter, causing the electron to scatter off the adjacent nucleus, leading to interference between the initial L-shell ionizing event and the subsequent secondary scattering event. Such scattering is similar to that resulting from the core ionization of heteronuclear molecules discussed by Kronig [4], and also to that observed in EXAFS studies [5,6], for which oscillations occur in the energy region just above the threshold for core ionization.

The present results can also be compared to those for photoionization of N_2. In the case of K-shell photoionization [14], the localized nature of the K electrons suppresses Young-type interferences because the ejected electron is not coherently emitted from both centers. On the other hand, ionization of the valence electrons produces modulations in the resulting cross sections that have been attributed to Young-type interference [2,3]. The fact that there are several L orbitals delocalized over the molecule might be the reason that primary Young-type interferences are strongly suppressed for ionization of N_2 by fast ions.

Similar measurements for other diatomic molecules such as O_2 shed additional light on the observed oscillatory structures (see next report). The differences in the structures observed for H_2 and heavier molecules such as N_2 further highlight the unique character of molecular ionization compared to atomic ionization.

Three of the authors (F. J-Sz., K.P. and L.N.) were supported by the Romanian National Plan for Research (PN II) under contract No. ID-539.

References:

[1] N. Stolterfoht *et al*., Phys. Rev. Lett. **87**, 023201 (2001).
[2] J. A. R. Samson and R. B. Cairns, J. Opt. Soc. Am. **55**, 1035 (1965).
[3] H. D. Cohen and U. Fano, Phys Rev. **150**, 30 (1966).
[4] R. de L. Kronig, Z. Physik **75**, 468 (1932); H. S. W. Massey and E. H. S. Burhop, *Electronic and Ionic Phenomena* (Clarendon Press, Oxford, England 1952), p. 201.
[5] B. K. Teo, *EXAFS: Basic Principles and Data Analysis* (Springer, Berlin, 1986).
[6] D. C. Koningsberger, R. Prins, *X-ray Absorption, Principles, techniques of EXAFS, SEXAFS and XANES* (John Wiley & Sons, New York, 1988).
[7] M. E. Rudd, Y. K. Kim, D. H. Madison and T. J. Gay, Rev. Mod. Phys. **64**, 441 (1992).
[8] N. Stolterfoht, R. D. Dubois and R. D. Rivarola, *Electron Emission in Heavy Ion–Atom Collisions*, Springer Series on Atoms and Plasmas, (Springer, Heidelberg, 1997).
[9] J. L. Baran *et al.*, Phys. Rev. A **78**, 012710 (2008).
[10] L. Nagy, L. Kocbach, K. Póra, and J. P. Hansen, J. Phys. B **35**, L453 (2002).
[11] N. Stolterfoht *et al*., Phys. Rev. A **67**, 030702(R) (2003).
[12] S. Hossain, A. L. Landers, N. Stolterfoht, and J. A. Tanis, Phys. Rev. A **72**, 010701(R) (2005).
[13] N. Stolterfoht *et al*, Phys. Rev. A **69**, 012701 (2004).
[14] D. Rolles *et al*., Nature **437**, 711 (2005).

4.9 Interferences in Electron Emission from O_2 by 30 MeV $O^{5,8+}$ Impact

M. Winkworth,[1] P. D. Fainstein,[2] M. E. Galassi,[3] **J. Baran**,[1] **B. S. Dassanayake**,[1] **S. Das**,[1] **T. Elkafrawy**,[1] **D. Cassidy**,[1] **A. Kayani**,[1] and **J. A. Tanis**[1]

[1]Western Michigan University, Kalamazoo, MI 49008
[2]CNEA, Centro Atómico Bariloche, Bariloche, Argentina
[3]Instituto de Física de Rosario (CONICET-UNR), Rosario, Argentina

As discussed in the preceding report, investigations of electron interferences for 1-5-MeV H^+ + N_2 exhibit mainly secondary oscillations resulting from intramolecular scattering [1]. Strong suppression of the primary Young-type interferences is attributed to cancellation of the contributions from the symmetric and anti-symmetric L orbitals of N_2. The present work extends the experimental studies for N_2 to 30 MeV $O^{5,8+}$ impact with O_2 (see Ref. [2] for details).

The 30 MeV $O^{5,8+}$ ion beams were obtained from the tandem Van de Graaff accelerator at Western Michigan University. After collimation, the ion beam was directed into the scattering chamber onto an O_2 target supplied by a gas jet with a flow rate set to maintain single collision conditions. The energy spectra of electrons emitted from the target were measured with a parallel-plate analyzer equipped with a channel electron multiplier for angles of 30º, 60˚, 90º, 120º, and 150º with respect to the incident beam and ejected electron energies of 15 - 400 eV.

The measured molecular cross sections were divided by theoretical molecular O_2 cross sections calculated using one-center wave functions following the methods developed in [3]. The resulting ratios, shown in Fig. 1, exhibit oscillations that do not change significantly with observation angle, a behavior expected for primary Young-type oscillations [4,5]. To quantify the oscillatory structures, the ratios were fit to the phase shifted sinusoidal function [6]:

$$f(k) = \mathrm{A}[\sin(kcd - w)] + \mathrm{B} \qquad (1)$$

where k is the electron velocity (in a.u.), d is the internuclear distance (2.28 a.u.), c is an adjustable frequency parameter, w is an adjustable phase shift, and the constants A and B represent the interfering and non-interfering cross-section fractions, respectively.

The frequency parameter c shown in Fig. 2 for 30-MeV $O^{5,8+}$ + O_2 is indeed found to be nearly constant for all angles and both incident charge states, a behavior similar to that observed for 1-5 MeV H^+ + N_2 collisions [1], and the phase parameter w also follows a pattern similar to that reported for H^+ + N_2 with an apparent minimum near 90˚. The independence of c on the electron observation angle is suggestive of secondary interferences as found previously for ~ 60 MeV/u Kr^{34+} + H_2 [6] and 1-5 MeV/u H^+ + H_2 collisions [5]. Furthermore, no obvious evidence for primary interferences is seen as was the case for H^+ + N_2 [1]. On the contrary, the oscillation interval of $\Delta k \sim 4$ a.u. for O_2 has a value two times larger than the $\Delta k \sim 2$ a.u. found for N_2. The reason for this difference in Δk for O_2 and N_2 is not known and is presently being explored.

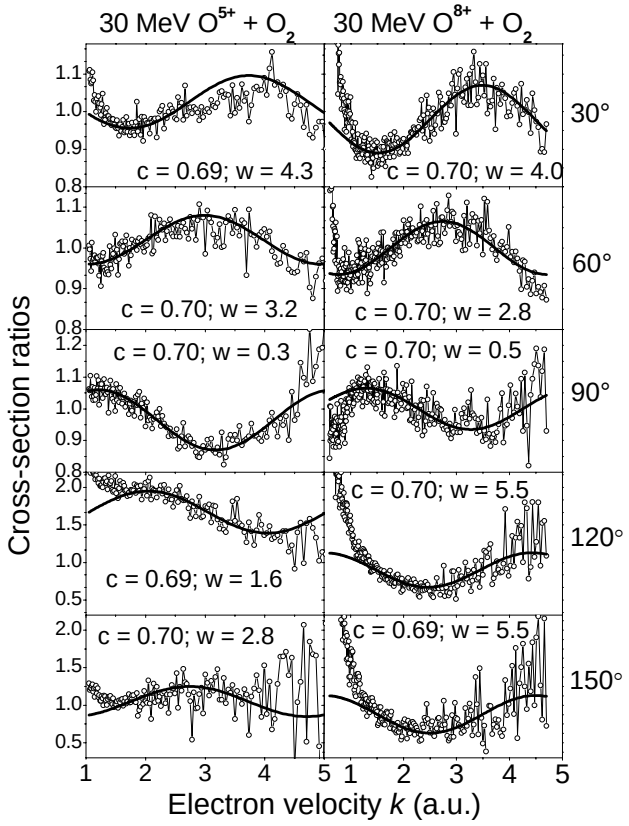

Figure 1 Experimental-to-theoretical cross section ratios for 30 MeV $O^{5,8+}$ + O_2 at the indicated observation angles. The smooth curves are the results of fitting the phase-shifted sinusoidal function given by Eq. 1 to the ratios.

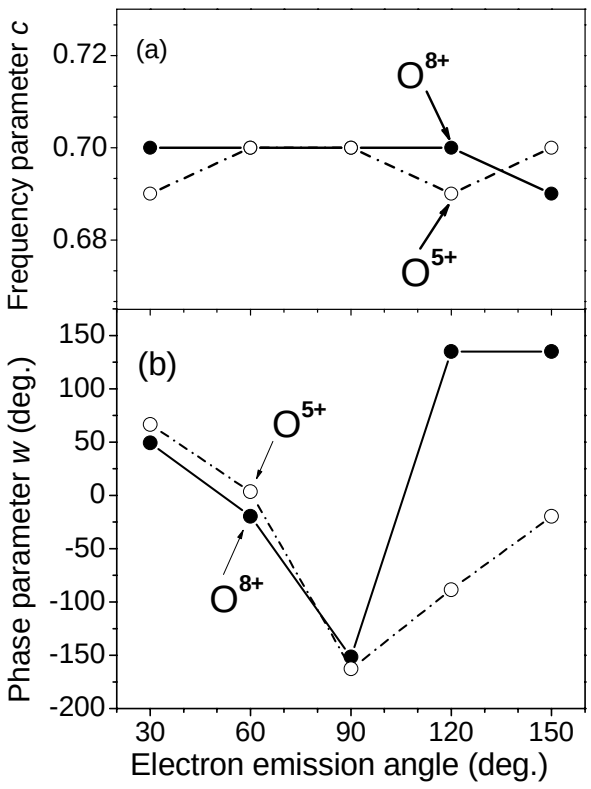

Figure 2 Frequency *c* and phase shift *w* parameters determined from fitting Eq. 1 to the cross section ratios of Fig. 1.

References:

[1] J. L. Baran et al., Phys. Rev. A **78**, 012710 (2008).
[2] M. Winkworth, P. D. Fainstein, M. E. Galassi, J. Baran, B. S. Dassanayake, S. Das, A. Kayani and J. A. Tanis, Interferences in Electron Emission from O2 by 30 MeV O5,8+ Impact, Nucl. Instrum. Meth. Phys. Res. B (2008), in press.
[3] M. E. Galassi, R. D. Rivarola, M. Beuve, G. H. Olivera, P. D. Fainstein, Phys. Rev. A **62**, 022701 (2000).
[4] N. Stolterfoht et al., Phys. Rev. A **67**, 030702(R) (2003).
[5] S. Hossain, A. L. Landers, N. Stolterfoht, J. A. Tanis, Phys. Rev. A **72**, 010701(R) (2005).
[6] N. Stolterfoht, B. Sulik, B. Skogvall, J. Y. Chesnel, F. Fremont, D. Hennecart, A. Cassimi, L. Adoui, S. Hossain, J. A. Tanis, Phys. Rev. A **69**, 012701 (2004).

4.10 Nonstatistical Enhancement of the 1s2s2p ^{4}p State in Electron Transfer in 0.5-1.0 MeV/u $C^{4,5+}$ + He and Ne Collisions

Diane Strohschein,[1] D. Röhrbein,[2] T. Kirchner,[2] S. Fritzsche,[3,4] **J. Baran**,[1] **J. A. Tanis**[1]

[1]Western Michigan University, Kalamazoo, MI 49008
[2]Institut für Theoretische Physik, Technische Universität Clausthal, D-38768 Clausthal-Zellerfeld, Germany
[3]Gesellschaft für Schwerionenforschung (GSI), D-64291 Darmstadt, Germany
[4]Max-Planck-Institut für Kernphysik, D-69029 Heidelberg, Germany

Nonstatistical enhancements for formation of the metastable 1s2s2p ^{4}P state compared to the similarly configured 1s2s2p $^2P_-$ and 1s2s2p $^2P_+$ states were observed following single electron transfer to C^{4+}(1s2s ^{3}S) and double electron transfer to C^{5+}(1s) ions, respectively. In our previous work, similar enhancements were observed in the population of the ^{4}P metastable state resulting from electron transfer in ~1 MeV/u $F^{7,8+}$ + He and Ne collisions [1]. The enhancements were attributed to a dynamical Pauli exchange mechanism involving projectile and target electrons having the same spin alignment [1].

More recently, it was suggested that, in addition to the Pauli exchange mechanism, cascading following electron transfer to (1s2s ^{3}S)nl ^{4}L states with $n \geq 3$ can lead to ^{4}P enhancement [2]. In such a scenario, capture to an nl ^{4}L state is followed by successive prompt radiative transitions with $\Delta l = 1$ until the captured electron reaches the 1s2s2p ^{4}P from which it cannot decay radiatively, and which has a long Auger lifetime as well.

To further understand the observed enhancement of the ^{4}P state, new investigations of Auger emission spectra in collisions of 0.5-1 MeV/u $C^{4,5+}$ with He and Ne targets were undertaken [3]. Experimental ratios of the resulting ^{4}P intensities to the sum of the $^2P_-$ and $^2P_+$ intensities, i.e., $R = {}^4P/({}^2P_- + {}^2P_+)$, for the collision systems studied give values three to four times larger than the expected value of two based solely on spin statistics [4] for single transfer to C^{4+}(1s2s ^{3}S) and double transfer to C^{5+}(1s). Detailed theoretical calculations of the effect of electron cascading on the measured value of R indicate that cascade feeding due to capture into $n \geq 3$ levels does indeed play an important role, but explains only about half of the observed enhancement as shown in Fig. 1. Consequently, Pauli exchange during electron transfer of similarly aligned target and projectile electrons, as originally proposed in Ref. [1], is still deemed to be a viable mechanism for selectively populating the ^{4}P state. Nevertheless, quantitative calculations are needed to better assess its significance.

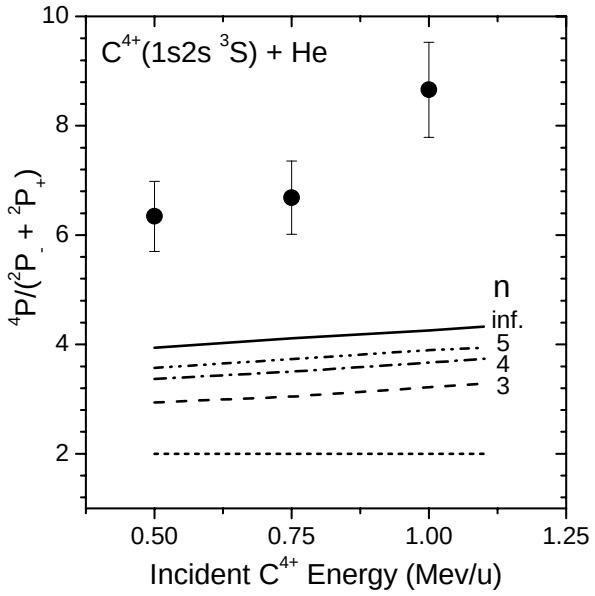

Figure 1 Calculated and measured ratios of the 1s2s2p ^{4}P intensities to the sum of the 1s2s2p ^{2}P$_-$ and 1s2s2p ^{2}P$_+$ intensities as a function of the incident projectile energy for single transfer in C^{4+}(1s2s ^{3}S) + He collisions. Dashed line: calculation including cascades from all relevant states up to n=3, dash-dotted line: calculation including cascades from all relevant states up to n=4, dash-dot-dot line: calculation including cascades from all relevant states up to n=5, full line: extrapolation to n→∞ (see text). The observed ^{4}P intensities were corrected for contributions from the C^{4+}(1s^2) ground state and for lifetime effects (see text). The horizontal short dashed line at $^4P/(^2P_- + {}^2P_+) = 2$ represents the value expected from spin statistics.

References:

[1] J. A. Tanis *et al*, Phys. Rev. Lett. **92**, 133201 (2004).

[2] T. J. M. Zouros, private communication.

[3] D. Strohschein, D. Röhrbein, T. Kirchner, S. Fritzsche, J. Baran, and J.A. Tanis, Phys. Rev. A **77**, 022706 (2008).

[4] E. P. Benis, T. J. M. Zouros, T. W. Gorczyca, A. D. Gonzales, and P. Richard, Phys. Rev. A **69**, 052718 (2004); and Phys. Rev. A **73**, 029901(E) (2006).

4.11 Guiding of Electrons through Insulating PET Nanocapillaries

B. S. Dassanayake,[1] **S. Das**,[1] N. Stolterfoht,[2] and **J. A. Tanis**[1]

[1]Western Michigan University, Kalamazoo, MI 49008
[2]Hahn-Meitner-Institut Berlin GmbH, D-14109 Berlin, Germany

The interaction of highly-charged ions (HCI) with surfaces has been the subject of extensive research both experimentally and theoretically not only because of its potential application in the field of nanotechnology but also from the point of view of fundamental understanding [1,2]. In recent years attention has centered on the transmission of HCI through nanocapillaries with the reported *guiding* of slow positive ions (3 keV Ne^{7+}) through insulating nanocapillary foils of polyethylene terephthalate (PET) by Stolterfoht *et al.* [3]. Surprisingly, ion transmission with negligible energy loss or charge change was observed for foil tilt angles up to 20^0 with respect to the incident beam direction, indicating only distant encounters with the capillary walls. These observations have been attributed to a self-organizing charge-up of the walls of the capillaries [3] that, after a characteristic charging time, deflects the traversing ions causing them to be "guided" through the sample along the capillary axis. In subsequent work by these authors additional properties of slow ion guiding in PET foils were investigated [4].

Experimental and theoretical works by other investigators have been conducted for slow (~1-10 keV) positive ions [5,6,7,8,9], including in addition to PET nanocapillary samples of SiO_2 [6], alumina [8] and tapered glass [9]. In all cases, the surfaces of the insulating nanocapillary foils were coated with a thin conducting layer, e.g., gold, to prevent charging of the sample during the measurements. More recently, guiding for 200-350 eV electrons in Al_2O_3 nanocapillary foils has been reported [10].

In this work, the transmission and guiding of 500 and 1000 eV electrons through insulating PET nanocapillaries of diameter 200 nm and aspect ratio 50 have been investigated [11]. The experiment was performed at Western Michigan University. The sample was mounted in a goniometer that allowed precise two-dimensional positioning with respect to the incident beam. The electron beam was produced from a simple filament source and collimated to a diameter of ~1.5 mm. The transmitted electrons were energy analyzed with a parallel-plate spectrometer located a few centimetres behind the sample and counted with a channel electron multiplier (CEM).

Fig. 1 shows the angular distributions of the transmitted electrons for 500 and 1000 eV. The transmitted intensity was normalized to the incident beam current on the sample and all data were taken after the guiding had reached its equilibrium (~ 15 minutes). From Fig. 1 we observe that electron guiding depends strongly on the foil tilt angle ψ and the incident electron energy. Specifically, the transmitted intensity decreases exponentially with tilt angle and with incident electron energy (for 500 eV guiding was observed up to $\psi = 11^0$, whereas for 1000 eV only up to $\psi = 7^0$). Furthermore, a plot of the centroids of the angular distributions of the

observation angles vs. foil tilt angles, displayed in Fig. 2, shows a linear relationship, agreeing with results observed for HCIs.

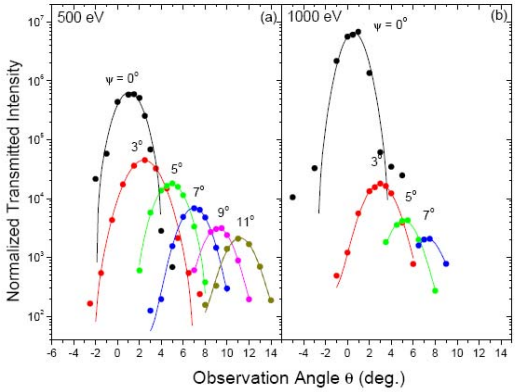

Figure 1 Angular distributions of the integrated normalized transmitted electron intensities as a function of observation angle θ for the indicated foil tilt angles ψ for (a) 500 eV and (b) 1000 eV incident electrons.

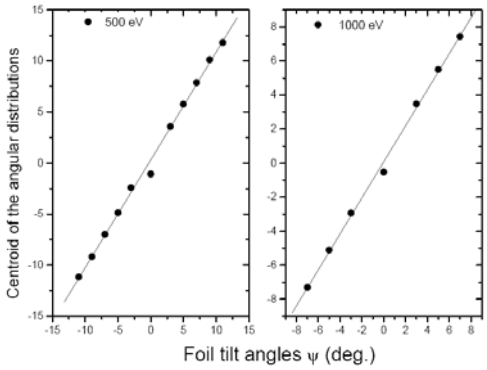

Figure 2 Plot of the centroids θ_{cent} of the angular distributions vs. foil tilt angle ψ for 500 and 1000 eV electrons incident on PET. The linear dependence demonstrates guiding.

These results show that electron transmission and guiding depend strongly on the capillary foil tilt angle as well as the incident electron energy. It is seen that the transmission intensity at zero degree tilt angle increases with increasing energy, while the relative transmission intensity decreases with increasing tilt angle. The observation angle and the tilt angle show a linear relationship, demonstrating that electrons are guided through nanocapillaries in a manner similar to positive ions. These studies are ongoing to determine additional properties of electron guiding in insulating capillaries.

References:

[1] A. Arnau *et al.,* Surf. Sci. Rep. **27**, 113 (1997), and references therein.
[2] Y. Yamazaki, Phys. Scrip. T **73**, 293 (1997).
[3] N. Stolterfoht, J.-H. Bremer, V. Hoffmann, R. Hellhammer, D. Fink, A. Petrov, and B. Sulik, Phys. Rev. Lett. **88**, 133201 (2002).
[4] See, N. Stolterfoht, R. Hellhammer, J. Bundesmann, and D. Fink, Phys. Rev. A **77**, 032905 (2008); and references therein.
[5] Gy. Vikor, R. T. Rajendra Kumar, Z. D. Pesic, N. Stolterfoht, and R. Schuch, Nucl. Instrum. Methods Phys. Res. B **233**, 218 (2005).
[6] M. B. Sahana, P. Skog, Gy. Vikor, R. T. Rajendra Kumar, and R. Schuch, Phys. Rev. A **73**, 040901(R) (2006).
[7] K. Schiessl, W. Palfinger, K. Tókési, H. Nowotny, C. Lemmel, and J. Burgdörfer, Phys. Rev. A **72**, 062902 (2005).
[8] S. Mátéfi-Tempfli *et al*., Nanotechnology **17**, 3915 (2006).
[9] T. Ikeda, T. M. Kojima, Y. Iwai, Y. Kanai, T. Kambara, T. Nebiki, T. Narusawa, and Y. Yamazaki, Jour. Phys.: Conf. Series **58**, 68 (2007).
[10] A. R. Milosavljević, Gy. Víkor, Z. D. Pešić, P. Kolarž, D. Šević, B. P. Marinković, S. Mátéfi-Tempfli, M. Mátéfi-Tempfli, and L. Piraux, Phys. Rev. A **75**, 030901(R) (2007).
[11] S. Das, B. S. Dassanayake, M. Winkworth, J.L. Baran, N. Stolterfoht, and J.A. Tanis, Phys. Rev. A **76**, 042716 (2007).

4.12 Dissociative and Non-Dissociative Charge-Changing Processes in 1.0-2.0 MeV/u O^{5+} + O_2 Collisions

D. P. Cassidy, **E. Y. Kamber**, **A. Kayani**, and **J. A. Tanis**

Western Michigan University, Kalamazoo, MI 49008

Interactions of molecular oxygen in collisions with charged particles are relevant to many fields of study including astrophysics, atmospheric physics, and the life sciences. These interactions are especially relevant to the life sciences as both atomic and molecular oxygen are abundant in most living matter, as well as being one of the essential components of many organic molecules. The generation of ion-radiation induced reactive oxygen and how it affects surrounding cellular tissue is a primary example [1]. Within the field of atomic physics results for the ionization of molecular oxygen by fast ions are important for analyzing the fragmentation of H_2O and other molecules. Similar work has been the subject of recent attention for protons, neutral hydrogen, and carbon projectiles [2,3] colliding with H_2O. In an effort to gain additional understanding of such interactions, dissociative and non-dissociative products of O_2 associated with single electron capture, single electron loss, and direct ionization have been measured for 1.0, 1.5, and 2.0 MeV/u O^{5+} + O_2 collisions.

These measurements were conducted at Western Michigan University using the tandem Van de Graaff accelerator. Time-of-flight techniques were used to detect coincidences between target ion fragments and individual outgoing projectile charge-state components. A collimated O^{5+} beam interacted with O_2 contained within a differentially pumped target gas cell, in which the pressure was kept below 2.0 mTorr. In all cases, spectra were measured for several target pressures to check for single-collision conditions. Recoiling target ions were extracted by an electric field transverse to the beam direction and detected with a set of coupled microchannel plates. Following interaction with the target gas, the projectile beam was magnetically analyzed and the individual charge-changed components were counted with silicon surface-barrier detectors. To ensure the validity of the data, spectra for He and Ne were collected and the ratios for multiple ionization were compared with previously measured values [4,5], as well as the measured yields for total single electron capture and loss [4,6]. These latter yields also provided the calibration factor to determine absolute cross sections for the O_2 data.

Fig. 1 shows the target ion products associated with projectile electron capture in 1.0 – 2.0 MeV/u O^{5+} + O_2 collisions compared with the corresponding spectrum for 2 MeV/u O^{5+} + Ne. Both non-dissociative molecular and dissociative atomic products are formed with charge states up to 4+. In the figure the total integrated beam current is the same for each spectrum, indicating a strong decrease in the relative cross sections as a function of projectile energy. The spectra for projectile electron loss and direct ionization (not shown) gave similar results. From these spectra, absolute cross sections can be determined, as well as the relative yields for dissociative and non-dissociative ionization of O_2, to obtain information on the mechanisms for the molecular fragmentation of O_2. Additional measurements for incident oxygen charge states 6, 7, and 8+ are planned to determine the charge-state dependence of the various processes.

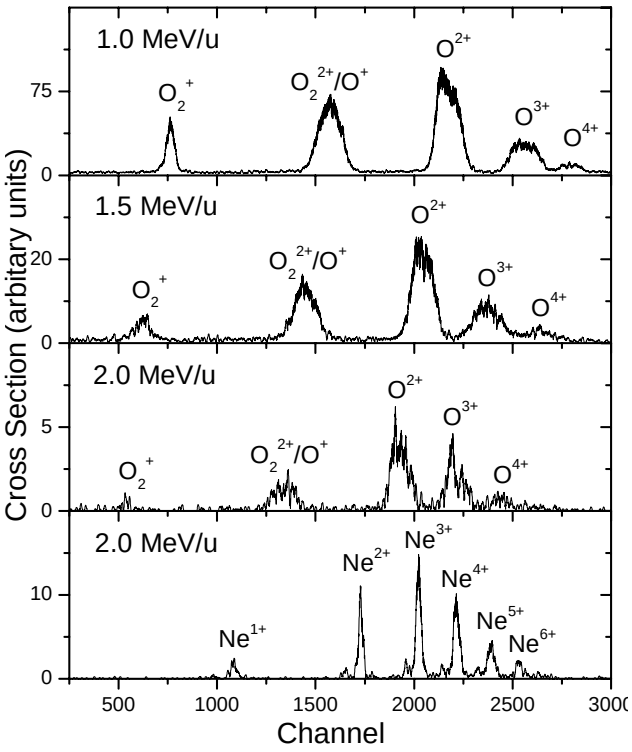

Figure 1 Target ion fragments associated with projectile electron capture for 1.0, 1.5, and 2.0 MeV/u O5+ + O2 collisions compared with the corresponding spectrum for 2.0 MeV/u 05+ + Ne.

References:

[1] J. K. Leach, G. Van Tuyle, P.-S. Lin, R. Schmidt-Ullrich, and R. B. Mikkelsen, Cancer Res. **61**, 3894 (2001).

[2] H. Luna *et al*., Phys. Rev. A **75,** 042711 (2007).

[3] E. C. Montenegro, M.B. Shah, H. Luna, S.W.J. Scully, A.L.F. de Barros, J.A. Wyer, J. Lecointre, Phys. Rev. Lett. **99**, 213201 (2007).

[4] R. Price, M.A. thesis, Western Michigan University, 1988, unpublished.

[5] R. J. Maurer, C. Can, R. L. Watson, Nucl. Instrum. Meth. A **262**, 99 (1987).

[6] S. A. Boman, E. M. Bernstein, and J. A. Tanis, Phys. Rev. A **39**, 4423 (1989).

4.13 Zero-Degree Electron and Ion Spectrometer for the Shanghai EBIT

J. A. Tanis,[1] R. Hutton,[2] B, Wei,[2] X. Wang,[2] D. Lu,[2] and S. Lin,[2] and Y. Zou[2]

[1]Western Michigan University, Kalamazoo, MI 49008
[2]Applied Ion Beam Physics Laboratory, Fudan University, Shanghai, China

A tandem parallel-plate electrostatic energy analyzer has been constructed for use at the Shanghai electron-beam-ion trap (EBIT) [1]. The spectrometer is similar to the one used at Western Michigan University and is designed for use at zero degrees, i.e., for electron or ion emission along the beam direction. It is of the same type as that used successfully by Stolterfoht and co-workers for studies of high-resolution electron spectroscopy for many years [2]. At WMU, the spectrometer has been used for making high-resolution Auger measurements [3,4] and forward-going continuum (i.e., cusp) electron measurements [5].

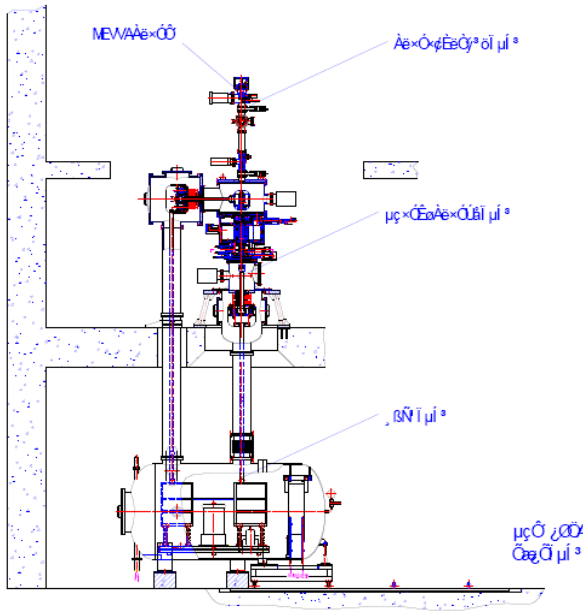

Figure 1 Schematic of the Shanghai EBIT.

To date, the EBIT facility in Shanghai has been used for spectroscopic and dynamical measurements of collisions taking place inside the trap region [6]. A schematic of the EBIT is shown in Fig. 1. Work is presently underway to extract ions from the EBIT, and it is anticipated that this capability will be accomplished within the next year. Following vertical extraction the ions will be deflected electrostatically into a horizontal plane and a magnetic analyzer will be used to select beams of the desired species and charge state and direct them into the experimental beamline. The extracted beam will be used for spectroscopic and dynamical studies of collisions between the slow highly-charged ions and atomic or molecular targets. Beam intensities are expected to be about 10^5 ions per pulse.

A major component in the extracted beam studies is a recoil-ion momentum spectrometer and its associated supersonic “cold” target, constituting a so-called COLTRIMS apparatus [7]. This instrumentation permits detailed investigations of collision dynamics by simultaneously recording the momenta of the recoiling target ions and electrons. Construction of this instrument is nearly complete.

To further enhance the capabilities of the beamline and to enable an even wider range of investigations, the zero-degree spectrometer will be installed immediately following and in close proximity to the COLTRIMS apparatus. A schematic of the spectrometer is shown in Fig. 2. With this spectrometer, two principal areas of investigation are presently envisioned:

(1) high-resolution Auger emission from highly-charged high-Z ions [3,4], and (2) transmission and guiding of ions through insulating nanocapillary foils [8].

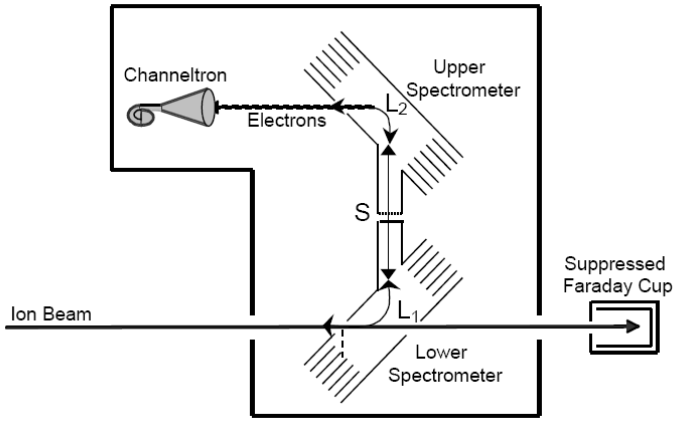

Figure 2 Schematic of the zero-degree electron spectrometer to be used at the Shanghai EBIT.

Following the zero-degree spectrometer an electrostatic state analyzer will be installed so that the outgoing projectile charges states may be determined. This latter capability will enable the detection of specific outgoing projectile charge states in coincidence with forward ejected electrons detected in the spectrometer, or in coincidence with recoiling target ions or electrons observed in the COLTRIMS apparatus. Moreover, electrons detected in the spectrometer can be recorded in coincidence with these same recoiling target products. The combined capabilities of the COLTRIMS apparatus and the zero-degree spectrometer will constitute a powerful and unique facility not presently duplicated elsewhere.

References:

[1] See M. He et al., J. Phys.: Conf. Ser. **58**, 419 (2007).
[2] See N. Stolterfoht. Physics Reports 146 (1987).
[3] D. Strohschein, D. Röhrbein, T. Kirchner, S. Fritzsche, J. Baran, and J. A. Tanis, Phys. Rev. A **77**, 022706 (2008).
[4] A. S. Alnaser, A. L. Landers, and J. A. Tanis, Phys. Rev. Lett. **94**, 023201 (2005).
[5] M. Zhu and et al., Nucl. Instrum. Meth. Phys. Res. B **98**, 351 (1995).
[6] R. Hutton, Proceedings of the 14th International Conference on the Physics of Highly Charged Ions, Tokyo, Japan, September 2008; to be published in Nucl. Instrum. Meth. Phys. Res. B (2009).
[7] J. Ullrich, R. Moshammer, R. Dörner, O. Jagutzki, V. Mergel, H.. Schmidt-Böcking and L. Spielberger, J. Phys. B **30**, 2917 (1997).
[8] N. Stolterfoht, J.-H. Bremer, V. Hoffmann, R. Hellhammer, D. Fink, A. Petrov, and B. Sulik, Phys. Rev. Lett. **88**, 133201 (2002).

5 CONDENSED MATTER PHYSICS

5.1 Entanglement Perturbation Theory for the Quantum Ground States in Two Dimensions

S. G. Chung[1] and K. Ueda[2]

[1]Western Michigan University, Kalamazoo, MI 49008
[2]Institute for Solid State Physics, the University of Tokyo, Japan

To calculate the partition functions and to solve the Schrödinger equations for macroscopic quantum systems are undoubtedly the most fundamental problems in theoretical physics. It would not be an exaggeration to say that the history of the development of quantum theory is primarily that of a pursuit of a variety of methods for this problem. Methods are roughly categorized into two, a variety of mean field theories and otherwise. The essence of mean field theories is to make truncations of correlations [1]. The merit of mean field theories lies in an essential simplification of calculations. When the systems of interest are very complex with many local degrees of freedom, such as involving electrons of orbital degeneracy and phonons, mean field methods are currently the only methods available. The penalty is, nevertheless, conceptually huge: if we don't know the importance of those neglected correlations, we are not sure how good the results of mean field approximations are. This is precisely the starting point and motivation of non-mean field theories. Here we currently have roughly three methods. First are rigorous methods such as Bethe Ansatz [2-8]. In spite of its remarkable success over the last several decades, a major drawback of rigorous methods is that they are mostly limited to 2D classical or 1D quantum systems of rather special structures. Second are numerical simulations such as exact diagonalization and Monte Carlo [9]. With an ever-increasing computer power and a steady supply of various ingenious ideas in algorithm, they provide a solid starting point often with a superb accuracy, but the finite size problem continues to be a serious issue. The negative sign problem is yet another serious problem in Monte Carlo. Third is the method of NRG (numerical renormalization group), initiated by Wilson [10], developed further first by White's DMRG (density matrix RG) [11] and most recently by Vidal's ER (entanglement renormalization) [12]. However, the inability of DMRG for two dimensions is now clear and one still needs to see how much that inability of DMRG can be improved by ER. Indeed, a deep question remains, namely how far one can go with the very idea of the Hilbert space truncation.

In recent papers, one, two and three of us (SGC) started a novel many-body method to calculate partition functions for dimensional macroscopic classical systems and the ground states of macroscopic quantum systems in one dimension [13,14]. We call this method EPT (entanglement perturbation theory). The key point of EPT is that it does not truncate the Hilbert space (no RG), and it does not have the finite size problem. Of particular interest among many possible extensions and applications of the EPT is how the EPT handles the fermion anticommutation algebra leading to infinite range correlations among fermions. Let us call this problem simply the sign problem in a wider sense [15]. No existing non-mean-field methods can handle this sign problem satisfactorily.

We here formulate the EPT for the quantum ground states in two dimensions. Our preliminary calculations on the 2D Heisenberg antiferromagnet and the Hubbard model show that EPT is computationally feasible [16]. A fortunate situation for EPT is that, due to the fact that it is based on the local basis, the free electron gas is most challenging but of course soluble by hand. Moreover, the fermion sign problem can still be handled by EPT: An essential difference from spins and bosons is that we need to calculate the excited states of an 1D infinite object but with an essential simplification that only the excited states with the same translational symmetry as the ground state need to be calculated, making the EPT calculation highly executable. We thus recognize the following issues for EPT: (1) to establish a stable and converging numerical procedure, and (2) to treat 2D fermions on a rigorous footing. It is also known that Monte Carlo encounters a negative sign problem not only in fermions but also in spins on a frustrated lattice such as Kagomé. EPT is free from this difficulty, and the quantum spin liquid issue offers an excellent testing ground for EPT.

References:

[1] Y. Kakehashi, Advances in Physics **53**, 497 (2006).
[2] L. Onsager, Phys. Rev. **65**, 117 (1944).
[3] C. N. Yang, Phys. Rev. **85**, 809 (1952).
[4] B. M. McCoy and T.T.Wu, *The Two Dimensional Ising Model* (Harvard University Press, Cambridge, Mass, 1973).
[5] R. J. Baxter, *Exactly Solved Models in Statistical Mechanics* (Academic Press, London, 1989).
[6] N. Andrei and K. Furuya and J. H. Lowenstein, Rev. Mod. Phys. **331, (**1983).
[7] S. G. Chung and Y. Oono and Y. C. Chang, Phys. Rev. Lett. **51**, 241 (1983).
[8] E. H. Lieb and F. Y. Wu, Phys. Rev. Lett. **25**, 1445 (1968).
[9] B. Sutherland, Beautiful models: 70 years of exactly solved quantum many-body problems, (World Scientific, New Jersey, 2004).
[10] M. Suzuki, Quantum Monte Carlo methods in condensed matter physics (World Scientific, Hong Kong, 1993)
[11] K. G. Wilson, Rev. Mod. Phys. **47**, 773 (1975).
[12] S. R. White, Phys. Rev. B **48**, 10345 (1993).
[13] G. Vidal, Phys. Rev. Lett. **99**, 220405 (2007).
[14] S. G. Chung, Phys. Lett. A **359**, 707 (2006).
[15] S. G. Chung, Phys. Lett. A **361**, 396 (2007).
[16] S. G. Chung and K. Ueda, Phys. Lett. A **372**, 4845 (2008).

5.2 High Temperature Thermal Stability and Oxidation Resistance of Magnetron-Sputtered Homogeneous CrAlON Coatings on 430 Steel

A. Kayani,[1] **K. J. Wickey**,[1] **M. I. Nandasiri**,[1] **A. Moore**,[1] **E. Garratt**,[1] R. J. Smith,[2] T. L. Buchanan,[2] W. Priyantha,[2] M. Kopczyk,[2] P. E. Gannon,[2] and V. I. Gorokhovsky[3]

[1]Western Michigan University, Kalamazoo, MI 49008
[2]Montana State University, Bozeman, MT 59717
[3]Arcomac Surface Engineering, LLC, Bozeman, MT 59715

Current energy crises and fuel prices have made Solid oxide fuel cells (SOFC) increasingly attractive as a way of converting chemical energy into electrical energy by means of the electrochemical combination of hydrogen and oxygen via an ion-conducting solid oxide electrolyte. The operational requirements of high ionic conductivity and good catalytic performance in the fuel cell must be balanced against the practical requirements of low cost and high-temperature corrosion resistance for components in the fuel cell stack [1]. Of particular interest in our work is the bipolar plate serving as the current collector or interconnect between adjacent cells of the SOFC stack. The interconnect must not only retain low electrical resistivity throughout the operating lifetime of the fuel cell, but must also have good surface stability, necessitating that thermal expansion and other physical properties be compatible with the materials in the stack [2]. Doped $LaCrO_3$ plates have worked well for cells operating at 1000^{o}C, but suffer from high cost as well as difficulties in fabrication. A thorough evaluation of several heat-resistant alloys with a variety of compositions led to the conclusion that it would be difficult for most traditional alloys to meet the material requirements of long-term operation above 700^{o}C [2]. Alloys of bcc, ferritic stainless steels appear to have thermal expansion coefficients that are well matched to other components in the stack, but do not possess the high electrical conductivity needed for required operation. The authors conclude that for improved oxidation resistance and electrical conductivity, either new alloys need to be developed, or surface engineering of existing alloys is required [3]. The present work falls into the latter category of surface engineering, namely, the use of coatings to improve oxidation resistance while maintaining acceptably low resistivity values. Related research on surface engineering includes the use of conducting oxide coatings and thermal nitridation [4].

Chromium nitride is a good oxidation resistant material with anti-corrosive properties. Its uses include applications in metal forming and plastic molding [5,6]. It is presently known that exposing CrN to oxygen at elevated temperatures leads eventually to loss of nitrogen and the formation of Cr_2O_3 [7] a semiconductor with sufficient low resistivity for use in interconnect applications at an operating temperature of 800^{o}C [8]. In our study, using an RF and DC magnetron sputtering technique, we deposited coatings of varying Cr/Al ratios onto a 430 stainless-steel plate sample substrate. For this particular study balanced magnetron heads were used to deposit CrAlN coatings. For analysis of sample elemental composition and oxidation resistance, Rutherford backscattering spectrometry (RBS) and Non-Rutherford scattering were used. The films were annealed at 800^{o}C in air for up to 25 hrs, and subsequently analyzed.

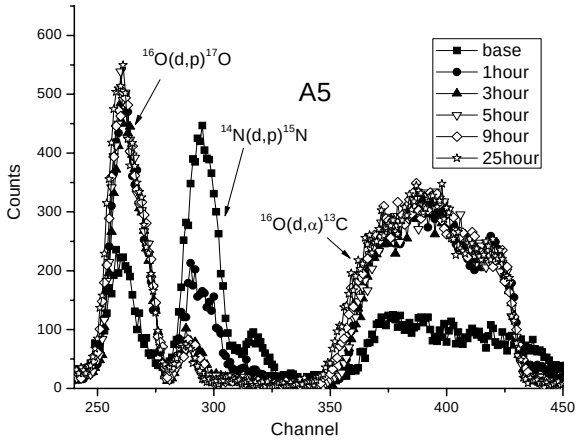

Figure 1 Overlapped spectra of sample A5, taken after each oxidation period, with 1.1 MeV D+ beam at 170 degree scattering angle. Reactions shown are protons from the 16O(d,p)17O, 14N(d,p)15N and alpha from 16O(d,α)13C

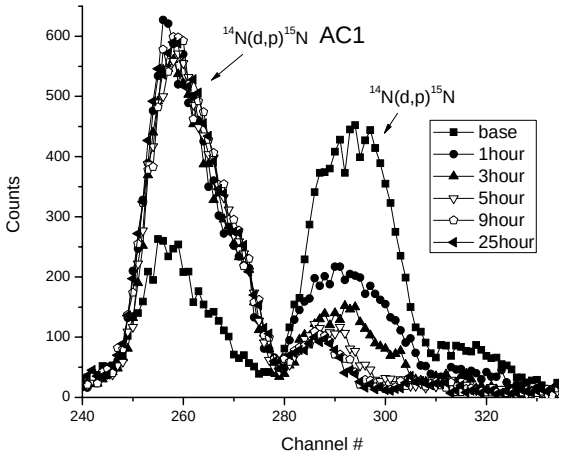

Figure 2 Overlapped spectra of sample AC1, taken after each oxidation period, with 1.1 MeV D+ beam at 170 degree scattering angle. Reactions shown are protons from the 16O(d,p)17O and 14N(d,p)15N.

After the each oxidation period, samples were removed from the tube furnace and were placed in a vacuum chamber for ion beam analysis (IBA) measurements. For the present measurements a beam of 1.1 MeV deuterium ions (D^+) and 3.0 MeV protons (p^+) were incident on the samples at an angle of 0^o from the surface normal. Reaction products were detected at a scattering angle of 170^o. Proton beam was used mainly to determine the Cr and Al concentration, whereas, deuterium beam was used to measure the oxygen and nitrogen concentrations. Nuclear reaction analysis (NRA) using D^+ can be quite useful in this case because the spectral peaks originating from O and N typically sit on a very low or zero-background signal [9]. Using the SIMNRA program, the set of target composition profile parameters was adjusted until a single set of parameters could be used to accurately simulate both the proton and deuteron spectra of the as deposited samples [10]. The spectra obtained using D^+ are shown in the figures 1, 2, 3 and 4, which are the overlapped spectra of the

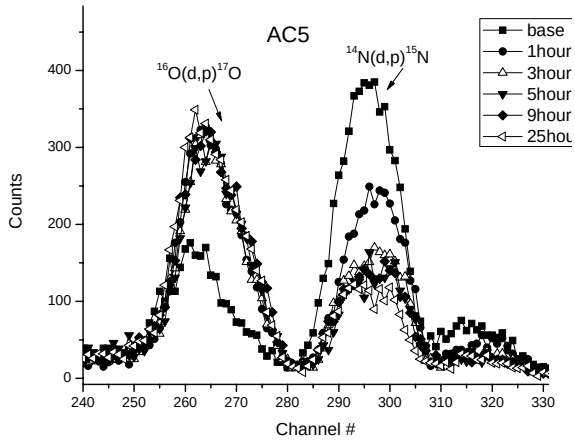

Figure 3 Overlapped spectra of sample AC5, taken after each oxidation period, with 1.1 MeV D+ beam at 170 degree scattering angle. Reactions shown are protons from the ^{16}O(d,p)17O and 14N(d,p)^{15}N.

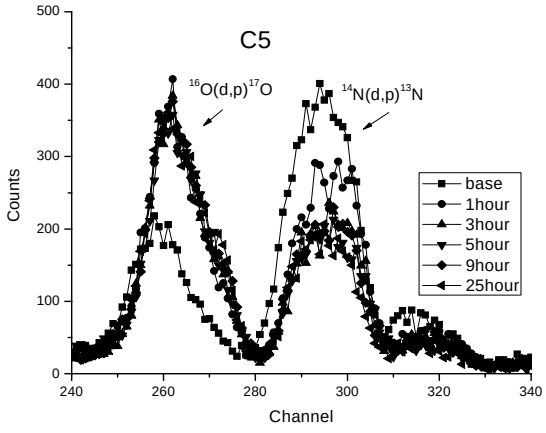

Figure 4 Overlapped spectra of sample C5, taken after each oxidation period, with 1.1 MeV D+ beam at 170 degree scattering angle. Reactions shown are protons from the ^{16}O(d,p)^{17}O and ^{14}N(d,p)^{15}N

samples, taken after each oxidation period. Oxygen and nitrogen have several nuclear reactions with the D^+ beam. The detected particles for these measurements shown in the figure 1, were protons from the $^{16}O(d,p)^{17}O$, $^{14}N(d,p)^{15}N$ and alpha from $^{16}O(d,\alpha)^{13}C$. The broader peak is from the nuclear reaction $^{16}O(d,\alpha)^{13}C$ because of energy straggling of the emitted α-particle in the coating.. This means that the coating has a higher stopping power for α - particle than for protons. The peaks shown are the most prominent nuclear reaction, but there are other small satellite peaks which are also reactions with nitrogen. Not shown in these figures is a nuclear reaction with carbon.

To determine oxygen and nitrogen concentrations, only $^{16}O(d,p)^{17}O$ reaction for oxygen concentration and $^{14}N(d,p)^{15}N$ reaction nitrogen concentration were modeled. As shown in the figures 1, 2, 3 and 4, notice the N loss and O gain in each of the samples as the oxidation of the samples were carried out. In some cases there is a rapid decrease in N content following the initial one-hour heat treatment, which is attributed to the transformation of CrN to Cr_2N [11,12]. Moreover, a more gradual loss of N during subsequent annealing is attributed to the transformation of Cr_2N to Cr_2O_3. Formation of Cr_2O_3 could have formed a barrier layer for the subsequent oxygen to defuse into the sample. The area specific resistivity (ASR) studies for uncoated and coated stainless steel samples for CrAl nitride coatings have shown that the values for both coated and uncoated samples reached a minimum of below 10 mohm-cm^2. However, the ASR value of the uncoated sample rose relatively fast compared to that for the coated sample, indicating reduced oxidation rate and increased electrical conductivity for the coated samples [13].

Nitrogen was lost with the gain of oxygen in the first 5 hours followed by relative stability. As shown in figure 1, the sample that performed the worst was A5. In first five hours of oxidation, A5 lost most of its nitrogen to oxygen. AC1, shown in figure 2, had a similar Cr/Al ratio as that of A5 and was also similar in performance. The performance of sample AC5, shown in figure 3, and sample C5, shown in figure 4, was almost the same and their Cr/Al ratios were similar as well. These two samples retained most of their nitrogen and therefore are better oxidation resistant samples. The low Cr/Al ratio samples performed poorly, while the high Cr/Al ratio samples were better. The sample that performed the best was C5 with a Cr/Al ratio of 0.9 which correlates with our earlier study [8].

References:

[1] B. C. H. Steele and A. Heinzel, Nature **414**, 345 (2001).
[2] Z. G. Yang, J. W. Stevenson, and P. Singh, Advanced Materials and Processes **161**, 34 (2003).
[3] Z. G. Yang, K. S. Weil, D. M. Paxton, and J. W. Stevenson, J. Electrochem. Soc. **150**, A1188 (2003).
[4] Z. G. Yang, G. Xia, and J. W. Stevenson, Electrochemical and Solid State Letters **8**, A168 (2005).
[5] T. Bjfrk, M. Berger, R. Westergard, S. Hogmark, and J. Bergstrfm, Surface and Coatings Technology **146**, 22-41, (2001).
[6] O. Knotek, M. Atzor, A. Barimani, and F. Jungblut, Surface and Coatings Technology **42**, 21-28 (1989).
[7] F.-H. Lu, H.-Y. Chen, and C.-H. Hung, J. Vac. Sci. Technol. A **21**, 671 (2003).
[8] K. Huang, P. Y. Hou, and J. B. Goodenough, Materials Research Bulletin **36,** 81 (2001).
[9] J. R. Tesmer and M. Nastasi, Handbook of Modern Ion Beam Materials Analysis, Materials Research Society,Pittsburgh, PA, 1995.
[10] M. Mayer, SIMNRA User's Guide, Technical Report IPP 9/113, Max-Planck-Institut fur Plasmaphysik, Garching, Germany, (1997).

[11] K. Huang, P. Y. Hou, and J. B. Goodenough, Materials Research Bulletin **36**, 81-95 (2001).
[12] H.-Y. Chen and F.-H. Lu, J. Vac. Sci. Technol. A **21**, 695 (2003).
[13] P. E. Gannon, C. T. Tripp, A. K. Knospe, C.V. Ramana, M. Deibert, R. J. Smith, and V. I Gorokhovsky, Surface and Coatings Technology **55**, 188-189 (2004).

5.3 Ion Beam Analysis of the Thermal Stability of Hydrogenated Diamond-Like Carbon Thin Films on Si Substrate

M. I. Nandasiri,[1] **K. J. Wickey**,[1] **A. Moore**,[1] **E. Garratt**,[1] **A. Kayani**,[1] and D. Ingram[2]

[1]Western Michigan University, Kalamazoo, MI 49008
[2]Ohio University, Athens, OH 45701

Diamond-like carbon (DLC) films have attracted a great deal of attraction because their properties are closely related to diamond. The properties of diamond like carbon films depend upon the growth conditions i.e. ion energy and substrate temperature. Ion beam deposition of diamond like carbon was first carried out by Aisenberg and Chabot [1]. They were able to produce films exhibiting the many of the properties of diamond and called them diamond like. Incorporation of hydrogen in the carbon films deposited by PECVD or sputtering system appears to be generally required in order to modify their optical and electrical properties.

An accessible and generally used method to determine the total hydrogen content in a thin film is elastic recoil detection Analysis (ERDA) [2]. In DLC, total hydrogen content critically determines film structure at the atomic level, and therefore the physical properties of the films. Hydrogen content is also a key to obtaining a wide optical gap and high electrical resistivity [3]. Raman studies on these films show that heating DLC in ambient air at temperatures above 300°C, significant conversion of DLC to nano-crystalline graphite takes place. This conversion is complete at 600°C [4]. The loss of hydrogen through annealing at high temperatures generally causes a collapse of the structure to a graphite-like phase dominated by sp^2 bonds [5].

DLC films are typically transparent in the infrared, with the exception of the CH_x bonds, which are weakly absorbing in the visible spectrum, and are increasingly absorbing with decreasing wave length in the UV. The hydrogen content is critical in controlling the optical properties, and removal of hydrogen from DLC films causes the loss of IR transparency [6]. A wide range of optical gap values (E_{opt}), spanning the range from 0.38 to 2.7 [7] were reported for DLC films prepared under presumably similar conditions, indicating the dependence of the property on the deposition conditions. For otherwise similar deposition conditions, E_{opt} was found to decrease strongly for DLC films deposited above 250°C [8]. This behavior reflects the role of hydrogen in stabilizing the structure of DLC layers.

Films deposited at lower temperatures (in the range 25-250°C) contain significant concentrations of hydrogen; most of the sp^3 coordinated carbon atoms, as well as a substantial fraction of the sp^2 coordinated carbons are bound to at least one hydrogen atom. The index of refraction is also affected by the hydrogen concentration in the DLC films. It generally increases with decreasing hydrogen content [9]. A higher index of refraction usually indicates DLC with higher hardness, and better wear resistance. The most substantial structural and property changes occurred at temperatures higher than 400°C [10].

Characterization of the samples is carried out using ion beam analysis (IBA) techniques, which include Rutherford backscattering spectroscopy (RBS), Forward Elastic Recoil detection analysis (ERDA) and Nuclear reaction analysis (NRA). Ion beam analysis of these samples was performed using a 6 MV tandem Van de Graaff accelerator at the department of physics, Western Michigan University, Kalamazoo, MI. Rutherford backscattering spectra (RBS) and Nuclear reaction analysis (NRA) were recorded using 2.5 MeV beam of H^+ ions, incident at 67.5° from the normal to the sample surface. Proton beam was used mainly to determine the C and O concentration in the film. The non-Rutherford enhancement in the cross section of C and O at this energy of protons is useful to precisely measure the concentration of the two elements, especially when these elements are sitting on heavier background like Si. Recoil spectra of the samples was obtained using 16 MeV O^{5+} beam, incident at 67.5° from the normal to the sample surface.

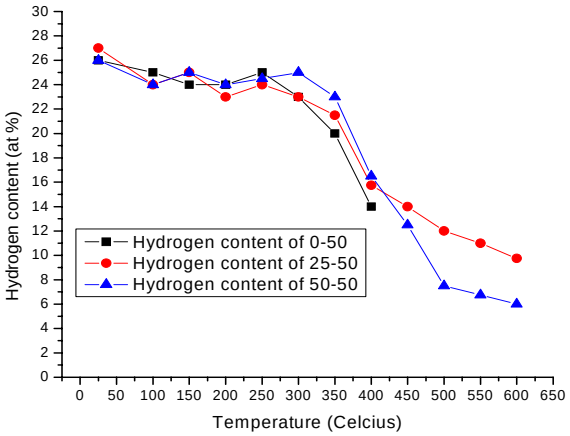

Figure 1 Hydrogen content (at %) with the annealing temperature for the samples 0-50, 25-50 and 50-50.

The onset temperature for hydrogen release for all of the samples was found to be around 400° C, as shown in the figure 1. We have shown a qualitative means of comparing the thermal stability of thin films of DLC, deposited on silicon substrates using ion beam analysis techniques. The results from ion beam analysis are both qualitative and quantitative and do not depend on the stoichiometry. From our results, we conclude that hydrogen evolution from DLC films takes place around 400° C. No significant bias effect on the deposited sample was observed. Future measurements will extend the annealing time to better simulate the samples. Also element diffusion process will be investigated quantitatively using He^+ beam.

References:

[1] S. Aisenberg, R. Chabot, J. Appl. Phys. **42,** 2953 (1971).
[2] A. Grill, V. Patel, and B. S. Meyerson, in Diamond and Diamondlike Films and Coatings, NATO-ASI Series B: Physics, R. E. Clausing, L. L. Horton, J. C. Angus, and P. Koidl, Eds., Plenum Publishing Co., New York **417**, (1991).
[3] H.-C. Tsai and D. B. Bogy, J. Vac. Sci. Technol. A **5**, 3287 (1987).
[4] D. R. Tallant, J. E. Parmeter, M. P. Siegal, R. L. Simpson, in Diamond Related Materials **4**, 191-199 (1995).
[5] A. Grill, V. Patel, and B. S. Meyerson, J. Mater. Res. **5**, 2531 (1990).
[6] H.-C. Tsai and D. B. Bogy, J. Vac. Sci. Technol. A **5**, 3287 (1987).
[7] P. Koidl, C. Wild, R. Locher, and R. E. Sah, in Diamond and Diamondlike Films and Coatings, NATO-ASI Series B: Physics, R. E. Clausing, L. L. Horton, J. C. Angus, and P. Koidl, Eds., Plenum Publishing Co., New York, **243** (1991).
[8] A. Grill and B. Meyerson, in Synthetic Diamond: Emerging CVD Science and Technology, K. E. Spear and J. P. Dismukes, Eds., John Wiley and Sons, Inc., New York **91**, (1994).
[9] A. Grill and V. Patel, Diamond & Related Mater. **4**, 62 (1994).
[10] T. M Wang, W. J. Wang, B. L. Chen, and S. H. Zhang, Phys. Rev. B **50**, 5587 (1994).

5.4 Shifts in the Melting Temperature of the Vortex Lattice in 9 MeV Proton Irradiated YBCO

L. M. Paulius,[1] L. Undreiu,[2] A. M. Troncalli,[3] and W.-K. Kwok[4]

[1]Western Michigan University, Kalamazoo, MI 49008
[2] University of Virginia's College at Wise, Wise VA 24293
[3]Austin College, Sherman, TX 75090,
[4]Materials Science Division, Argonne National Laboratory, Argonne, IL 60439

We compare the effects of low doses of 9 MeV proton irradiation on the first order melting transition temperature with theoretical predictions [1]. Three different single crystals were studied in this investigation. All were characterized before irradiation and after successive 9 MeV proton irradiations ranging from 0.25 x 10^{15} p/cm^2 to 2x10^{15} p/cm^2. The superconducting transition temperature was determined from the peak in the temperature derivative of the electrical resistivity curve, dρ/dT. The width of the transition was defined as the difference between T_c and the temperature where the resistance dropped to zero. The first crystal YBA285 had dimensions of 440 μm x 880 μm and a thickness of 40 μm along the crystallographic c-axis. The zero field superconducting transition temperature T_{co} before irradiation was 92.8K and ΔT_{co} = 0.4 K. The second crystal, YBA256, had dimensions of 680 μm x 630 μm (ab-plane) x 150 μm (c-axis) with a T_{co} = 93.0 K and ΔT_{co} = 0.44 K. The final crystal WYB005 had dimensions of 750 μm x 660 μm (ab-plane) x 80 μm (c-axis) with a pre-irradiation T_{co} = 93.4 K and ΔT_{co} = 0.4 K.

The 9 MeV proton irradiations were performed at Western Michigan University's tandem van de Graff accelerator at room temperature with the beam directed parallel to the crystallographic c-axis. A low flux of 6.25 x 10^{10} p/cm^{2}sec was used in order to minimize heating during irradiation. This resulted in a temperature increase less than 20°C above ambient temperature during irradiation. Calculations using TRIM [2] simulations give the range of 9 MeV protons in YBCO as 280μm, which is much larger than the thickness of the crystals used in this investigation. Simulations using the SRIM program with the default lattice energies of 3 eV for all the ions yield vacancy- displacement defect pairs with the following relative concentrations: 7.7% Y:15.4% Ba: 23.1% Cu: 53.8% O.

Figure 1 shows the normalized first order melting temperature as a function of dose in an applied magnetic field of H = 6T applied parallel to the crystallographic c-axis. For all three crystals investigated, the normalized melting temperature decreases roughly linearly with dose at a rate of 6.3 x10^{-3} per 10^{15} p/cm^2. This corresponds to a downward shift of 0.58 K for each 1 x 10^{15} p/cm^2 dose. This downward shift is of the same order of magnitude as predicted by Nonomura and Hu [3] who performed simulations based on a three dimensional frustrated XY model.

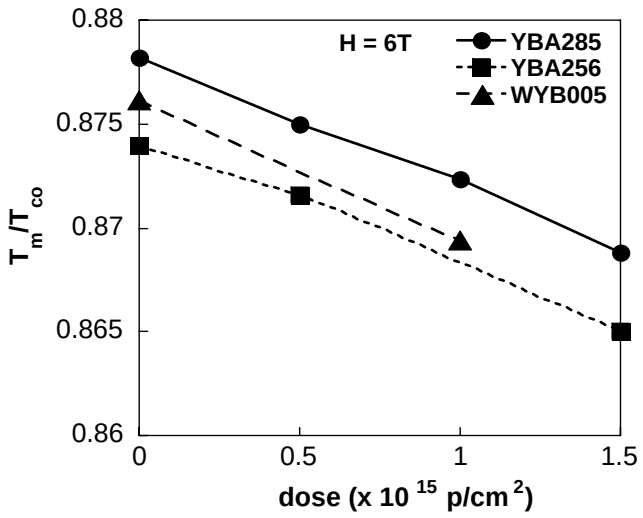

Figure 1 Normalized first order vortex melting transition temperature as a function of irradiation dose with 9 MeV protons. Results are shown for three different single crystals measure in an applied field of 6 T || c.

Dasgupta and Valls [1] used a numerical minimization of the Ramakrishnan-Yussouff [4] free energy to study the effects of strong random point pinning on the melting transition. They perform their calculations for a concentration of 1.36×10^{-4} defects per 100 units cells of the crystal lattice. This corresponds to 1 defect out of every 7.35×10^5 unit cells. In comparison, Transmission Electron Microscopy and SRIM calculations [5] show that the doses used in our experiments correspond to approximately one defect in 2.9×10^4 (for the 0.25×10^{15} p/cm^2) to 3.6×10^3 (for 2.0×10^{15} p/cm^2) unit cells of the crystal.

The results of Dasgupta and Valls [1] predict that the transition should cross over to a first order transition between a liquid and a vortex slush at intermediate concentrations of defects. The slush would consist of well defined crystalline domains separated by domain boundaries. However, our previous results have shown that the melting transition does not broaden with increasing defect density. Imry and Wortis argue that this lack of broadening indicates that the energy of creating domain walls in this systems is not energetically favourable [6].

References:

[1] C. Daspupta and O. Valls, Phys. Rev. B **76**, 184509 (2007).
[2] J. P. Biersack and L. G. Haggmark, Nucl. Instrum. Methods **174**, 257 (1980).
[3] Y. Nonomura and X. Hu Physica C **341**, 1307 (2000).
[4] T. V. Ramakrishnan and M. Yussouff, Phys. Rev. B **19**, 2775 (1979).
[5] L. M. Paulius et al, Phys. Rev. B **61**, R11911 (2000).
[6] Y. Imry and M. Wortis, Phys. Rev. B **19**, 3580 (1979).

6 NUCLEAR PHYSICS

6.1 Effects of β-Decays of Excited State Nuclei on the Astrophysical r-Process[1]

M. A. Famiano[1], R. N. Boyd[2], T. Kajino[3], K. Otsuki[4], M. Terasawa[5], and G. J. Mathews[6]

[1]Western Michigan University, Kalamazoo, MI 49008
[2]Lawrence Livermore National Laboratory, Livermore, CA 94550
[3]University of Tokyo, Tokyo, Japan 113-0033
[4]University of Chicago, Chicago, IL 60637
[5]Center of Nuclear Study, Wako, Japan 351-0198
[6]University of Notre Dame, Notre Dame, IN 46556

The solar system r-process abundances act as the canonical constraint to r-process theories as well as the prime indicator of the success of r-process models. Several r-process sites have been proposed; the hot-bubble region of a type II supernova (SNII) has been modeled fairly successfully. The composition of the environment in which the r-process occurs might be expected to have a profound effect on the final abundance distribution. Observations indicate that the r-process site is primary [1] and further evidence may suggest that the r-process is also unique [2], it may occur in a single site or event. The uniqueness of the r-process site, however, remains a subject of study [3].

Nuclear properties also constrain the r-process, and the purpose of this work is the examination of one particular characteristic - ß-decay - as it relates to the r-process. The ß-decay inputs, and other nuclear physics inputs, have been shown [4,5] to have important effects on the success or failure of r-process models. This is somewhat unfortunate, as properties of only a few nuclei on the neutron closed shells closer to stability have been experimentally determined, while data for the rest are relegated to calculation. Of paramount importance is the determination of nuclear masses and ß-decay rates. Nuclear mass formulae based on the microscopic properties of nuclei are slowly replacing the empirical droplet models, and these can change resulting reaction rates by factors as large as 10^8 [6]. As well, the r-process path is affected by the choice of mass formula, since the path roughly follows a line of constant S_n [6].

For the purposes of this study, the most recent semi-gross theory of ß-decay [7] has been adapted to neutron-rich nuclei relevant to the r-process. The ability of this model to determine decay properties of an extremely wide range of nuclei with reasonable accuracy and speed makes it ideal for this preliminary calculation. In particular, the semi-gross theory has good agreement for very neutron-rich nuclei [8,9]. It has also been used to improve the accuracy of decay rates for astrophysical calculations by incorporating first-forbidden transition strengths [10]. In its original form, the gross theory of β-decay assumed that the energy states of a nucleus consist of a smoothed distribution with transition strengths that peak at or near the

energy of the isobaric analog state[11]. Subsequent evolutions of the gross theory incorporated strength functions allowing for transitions of higher forbiddenness[12], as well as improvements over the original theory to include odd-odd effects[13], sum rules[14], even-odd mass differences[15], and improvements on the strength functions[16].

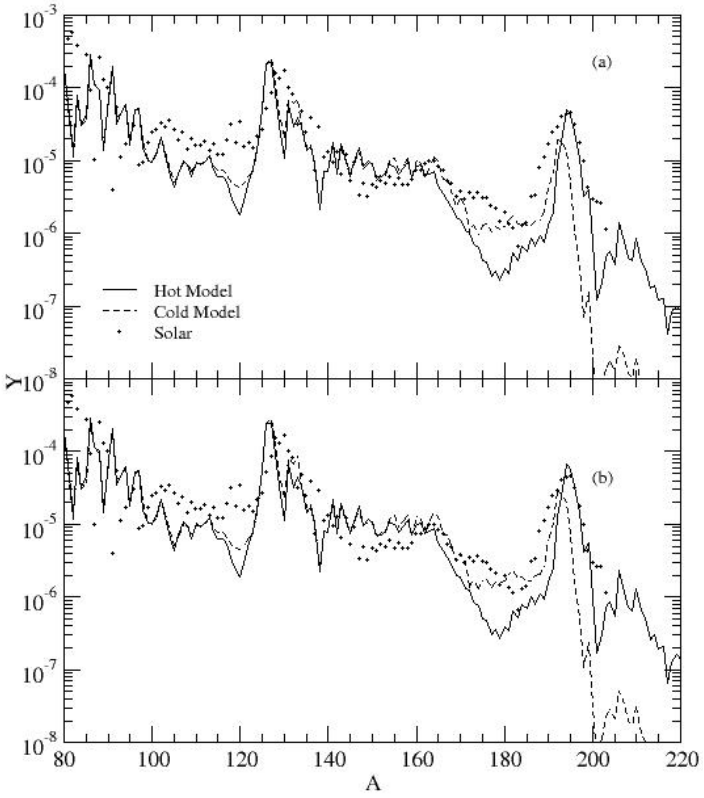

Figure 1 Comparison of r-process freezeout abundance distributions for two models (a) and (b) [19]. The dots correspond to the solar abundance distribution. The dashed line corresponds to a freezeout distribution assuming excited-state ß-decays, and the solid line corresponds to a model using only ground-state decays.

The results from several hydrodynamic parameter sets, as well as electron fraction parameter values Y_e, were examined. For each parameter set, the core mass in solar masses, core radius, neutrino luminosity, initial electron fraction, and whether or not ß - delayed neutron emission is included are listed. Using these parameters and the calculations of reference [17] the dynamic timescale and the entropy in the expansion are constrained. Though still in agreement with current predictions, the dynamic timescales in these calculations are shorter than average. However, the entropy is lower, and no artificial increase in the entropy (as is often assumed) was required [3].

Each simulation is run until several seconds beyond freezeout. While this time is sufficient to gauge the gross features of the r-process abundance distribution, a longer simulation may have resulted in more post-processing, allowing for smoother abundance distributions. One notes some residual even-odd effects in the calculated distribution as the effects of smoothing may not be complete, though the gross features of the distribution are noted.

Results from two representative models are displayed in Figure 1 for both the hot (i.e., including excited-state decays, solid line) and cold (i.e., not including excited state decays, dotted line) models[18]. The A~195 peak is most profoundly affected, along with the nuclei just below this mass region. From the relationship between the decay rates and temperature, it can be seen that decay rates of the nuclei in the region just below the A~195 peak (and - to a lesser extent - the region just below the A~130 peak) are quite sensitive to changes in temperature even at low temperatures. This is expected due to the high level densities of these nuclei (lying just below the N=126 and N=82 closed shells). Shell quenching has not been

included in this calculation, though the effect is noted, and no conclusions can be drawn from this study to evaluate the effects of quenched closed shells far from stability. Other rates, however, are not as sensitive to temperature changes at low temperatures and, as the r-process progresses, these rates would drop to their ground-state values before those of the nuclei in the regions below the abundance peaks. The decay rates of nuclei in this region would increase relative to those of nuclei in other regions of the path, selectively depleting the abundances of nuclei in this region.

References:

[1] C. Sneden, et al., ApJ **496**, 235 (1998).
[2] J. J. Cowan, B. Pfeiffer, K.-L. Kratz, F.-K. Theilemann, C. Sneden, S. Burles, D. Tytler, and D. Beers, ApJ **521**, 194 (1999).
[3] Y. Z. Qian, P. Vogel, and G. J. Wasserburg, ApJ **494**, 285 (1998).
[4] S. E. Woosley and et al., ApJ **433**, 229 (1994).
[5] B. S. Meyer, ApJ **449**, L55 (1995).
[6] J .J. Cowan, F.-K. Thielemann, and J. W. Truran, Phys. Rep. **208**, 267 (1990).
[7] H. Nakata, T. Tachibana, and M. Yamada, Nucl. Phys. A **625**, 521 (1997).
[8] S. Ichikawa, et al., Phys. Rev. C **71**, 067302 (2005).
[10] M. Asai, et al. Phys. Rev. C **59**, 3060 (1999).
[12] P. M. Moller, B. Pfeiffer, and K.-L. Kratz, Phys. Rev. C **67**, 055802 (2003).
[13] K. Takahashi, Prog. Theor. Phys. **47**, 1500 (1972).
[14] K. Takahashi, and M. Yamada, Prog. Theor. Phys. **41**, 1470 (1969).
[15] K. Takahashi, Prog. Theor. Phys. **45**, 1466 (1971).
[16] H. Nakata, T. Tachibana, and M. Yamada, Nucl. Phys. A **95**, 27 (1995).
[17] T. Tachibana, M. Yamada, and K. Yoshida, Prog. Theor. Phys. **84**, 641 (1990).
[18] S.Koyama, K. Takahashi, and M. Yamada, Prog. Theor. Phys. **44**, 663 (1970).
[19] T. Kondoh, T. Tachibana, and M. Yamada, Prog. Theor. Phys. **72**, 708 (1985).
[20] K. Otsuki, et al., ApJ **533**, 424 (2000).

6.2 Mass Measurements of Astrophysically Interesting Nuclei: Commissioning of the Zero Degree Spectrometer

M. A. Famiano,[1] T. Kubo,[2] T. Onishi,[2] N. Fukuda,[2] D. Bazin[3]

[1] Western Michigan University, Kalamazoo, MI 49008
[2] RIKEN Nishina Center for Accelerator Based Science, Wako, Saitama, Japan
[3] National Superconducting Cyclotron Laboratory, East Lansing, MI 48824

The rapid proton capture process, or rp-process, has seen a great deal of attention as the source of heat and light in X-ray bursts [1]. The rp-process is thought to occur in hot ($T\sim10^9$) environments in which the nuclei involved are far from stability. In the case of the rp-process, many of these nuclei lie close to the proton drip line [2]. Theoretical descriptions of the rp-process rely on nuclear reaction network calculations involving hundreds of nuclei and thousands of reactions for the simplest networks. While progress continues in studying important reaction rates and nuclei involved, there is still much to be learned.

A successful model of the rp-process site depends heavily on knowledge of nuclear masses, decay rates, and proton capture rates. These nuclear properties dictate the environment necessary for a successful rp-process. However, because of the expected low level densities of the nuclei involved in the rp-process, statistical rate calculations such as those based on the Hauser-Feshbach formalism are not as accurate as in the cases of the neutron-rich nuclei. For many cases, theoretical predictions of Q-values vary by amounts greater than the temperature of the rp-process environment [3-5], and – though progress is being made - experimental masses of several of the rp-process nuclei are still unknown, and many experimentally determined masses still have large uncertainties. (See, for example, references [6-8].) Likewise, mass models, such as the FRDM and the HF(+BCS), which are used to predict masses of the exotic nuclei, disagree in many cases by several hundred keV near the drip line [9,10]. Experimental validation of the rp-process nuclei is necessitated by these uncertainties [11].

Nuclear reactions from the rp-process are thought to drive the explosive hydrogen burning in X-ray bursts from accreting neutron stars, and the interdependency of the nuclear properties of rp-process nuclei and conditions on the surface of the accreting neutron star has been explored [2]. The light curve of the associated X-ray burst is directly determined by heating from the nuclear reactions within the burst. The burst luminosity and it ensuing evolution are both dictated by the initial amount of hydrogen accreted onto the neutron star and the rate at which it is consumed. Calculations predict that processing to A~100 may be responsible for bursts with timescales of several hundred seconds. Additionally, the shape of the light curve is determined by the rate of processing. Processing dominated by β-decay due to low (p, γ) rates along the rp-process path will cause a "bottleneck" or "waiting point" in the processing, directly affecting the X-ray burst luminosity and lengthening the burst in time. Understanding the luminosity of the burst and the nuclear physics involved will permit a better understanding of the dynamics of the neutron star crust, its composition, rotation, and magnetic field [2,12]. The composition of material produced in the burst is also important, as it has been recently

shown that at least 1% of the p-nuclei in the solar system may have been produced in X-ray bursts [13].

For reasonable analyses of the rp-process environment, Q-values and masses should be known to within roughly kT~100 keV. Widely used mass formulae may suffer disagreements greater than this value. Mass measurements of rp-process nuclei, especially those near the waiting points and out to the proton drip line are extremely useful for not only constraining the rp-process path and pace, but also in constraining mass parametrizations of exotic nuclei. Recent experimentation has been conducted by the spokesperson at the National Superconducting Cyclotron Laboratory to explore the (p, γ) Q-values of the nucleus ^{69}Br – a possible rp-process waiting point nucleus, and analysis is underway [14]. Other recent measurements have either measured for the first time or reduced the uncertainty in masses of some of the nuclei in the ^{65}As/^{70}Br region using TOF techniques [15]. A reduction in the uncertainties of the previous mass measurements along with the measurements of new masses will help to further constrain uncertainties in the mass models used while providing experimental data for current network calculations. Nuclei around this waiting point may include $^{60\text{-}64}$Ga, $^{62\text{-}65}$Ge, $^{64\text{-}67}$As, $^{66\text{-}69}$Se, and $^{70\text{-}72}$Br, as the rp-process path is thought to pass through these nuclei. The accuracy of current mass models at the proton-drip line would also be tested in a study of these nuclei. Finally, measurements of these nuclei would present new experimental challenges as good statistics can now be obtained for mass measurements using TOF techniques with the RIBF facility, pushing the limits of studied masses towards the proton drip line.

The masses of several nuclei near the ^{68}Se waiting point will be measured directly using the TOF-Bρ technique [1,15]. The nuclei studied include, but are not necessarily limited to, ^{60}Ga, ^{62,63}Ge, $^{64\text{-}66}$As, ^{66,67}Se, ^{70,71}Br. Some of these nuclei have been studied before using the TOF-Bρ or other techniques, and the current experiment seeks to verify the previous measurements with high statistics provided by the RIBF. The masses of most of these nuclei have never been measured, and will represent a first measurement. The accelerator settings used to produce the studied nuclei will also produce nuclei for which masses are already well known. These nuclei will be used as reference masses to calibrate the TOF experiment.

Using this technique, the time-of-flight (TOF) of a nucleus between two points in the accelerator is related to its mass:

$$\gamma \frac{m}{Q} = \frac{B\rho}{L} t$$

where a nucleus of mass m, charge Q, Lorentz factor γ, and rigidity Bρ takes a time t to travel a distance L along the beamline. The travel time for two nuclei, one of well-known mass, can be compared using this technique. It is expected that masses of individual beam particles can be measured to an accuracy of ~10^{-4} with average mass measured to an accuracy of about 2×10^{-6}. The expected lifetime limit for nuclei studied in this experiment is about 445 ns.

In addition to an accurate mass measurement of new proton-rich nuclei, the accuracy of mass formulae in this region can be gauged [1-3].

Phase I of an experimental program to measure the masses of exotic nuclei is now in progress with the completion of the commissioning of the RIBF zero-degree spectrometer. This

commissioning includes the operation and testing of the spectrometers in various optics modes. Of particular interest is the rigidity resolution of the spectrometer (A/Q) in these modes. Preliminary particle identification is shown in Figure 1 for a ^{238}U primary beam, and the resulting A/Q resolution has been measured to be as low as 0.1% for the full acceptance mode of operation. For modes with a much tighter acceptance, this resolution can be improved dramatically.

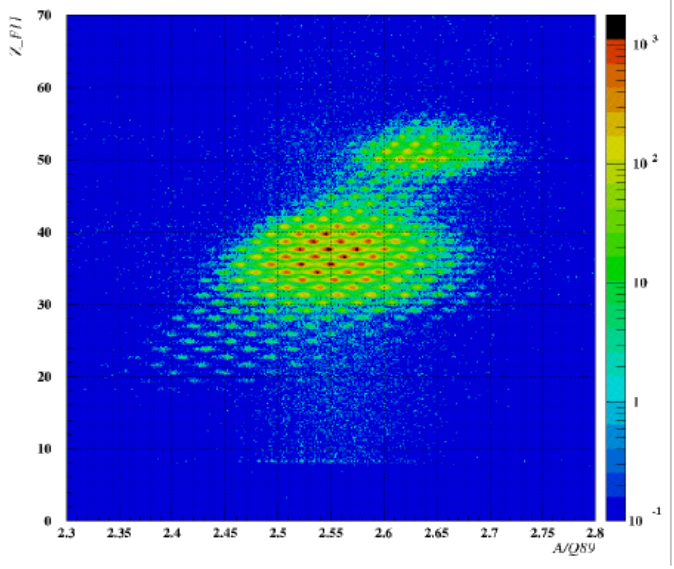

Figure 1 Preliminary PID plot for the ZDS commissioning corresponding to the full acceptance optics mode of the ZDS.

References:

[1] G. Wallerstein, et al., Rev. Mod. Phys. **69**, 995 (1997).
[2] H. Schatz, et al., Phys. Rep. **294**, 167 (1998).
[3] C. Iliadis, et al, ApJ **524**, 434 (1999).
[4] J. Jose, A.. Coc, and M. Hernanz, ApJ **560**, 897 (2001).
[5] P. Descouvemont, ApJ **543** 425 (2000).
[6] G. Audi, A. H. Wapstra, and C. Thibault, Nuc. Phys. A **729**, 337 (2003).
[7] D. Rodriguez, et al., Phys. Rev. Lett. **93**, 161104 (2004).
[8] J. A.. Clark, et al., Phys. Rev. C **92**, 192501 (2004).
[9] S. Goreily, et al., Phys. Rev. C **66**, 0243246 (2002).
[10] P. Moller, et al., At. Dat. Nuc. Dat. Tab. **59**, 185 (1995).
[11] H. Schatz, astro-ph/0607625 and references therein.
[12] F., Rembges, et al., ApJ **484**, 412 (1997).
[13] N. N. Weinberg, L. Bildsten, and H. Schatz, ApJ **639**, 1018 (2006).
[14] M. Famiano, et al. http://groups.nscl.msu.edu/hira/02023/index.htm. Analysis pending.
[15] G. Lima, et al., Phys. Rev. C 65, 044618 (2002).

6.3 Constraining the Nuclear Equation-of-State

M.B. Tsang,[1] Y. Zhang,[1,2] P. Danielewicz,[1] **M. Famiano**,[3] Z. Li,[3] W.G. Lynch,[1] & A. Steiner[4f]

[1]National Superconducting Cyclotron Laboratory, East Lansing, MI 48824
[2]China Institute of Atomic Energy, Beijing, P.R. China 102413
[3]Western Michigan University, Kalamazoo, MI 49008
[4]Michigan State University, East Lansing, MI 48824

Collisions involving ^{112}Sn and ^{124}Sn nuclei have been calculated with the Improved Quantum Molecular Dynamics transport model. The results of the calculations reproduce the data from two isospin diffusion measurements and the ratios of neutron and proton spectra. By comparing these data to calculations performed over a range of symmetry energies at saturation density and different representations of the density dependence of the symmetry energy, constraints on the density dependence of the symmetry energy at sub-normal density are obtained. These constraints are compared to existing constraints from other recent analyses.

The nuclear symmetry energy, which describes the difference between the binding energy of symmetric matter, with equal proton (Z) and neutron (N) numbers, and that of neutron rich matter, governs important properties of nuclei and neutron stars [1,2]. In nuclei, the symmetry energy and the Coulomb energy define the binding energy minimum where nuclei are stable against beta decay [3,4]. In neutron stars, the symmetry energy and its density dependence influence strongly the nature and stability of the phases within the star [5], the feasibility of direct URCA cooling processes within its interior [6], the composition [5] and the thickness of its inner crust, the frequencies of its crustal vibrations [7], as well as its radius, and mass [7].

The sum of the symmetry energy and the energy per nucleon of symmetric matter, $E(\rho,\delta) = E0(\rho,\delta=0) + E_{sym}$, provides the total energy per nucleon (i.e. the Equation of State (EoS)) of cold matter. The average symmetry energy per nucleon in uniform matter can be written as $E_{sym}=S(\rho)\delta^{22}$, where the asymmetry $\delta=(\rho_n-\rho_p)/\rho/$ ρ where ρ_n, ρ_p, and ρ are the neutron, proton and nucleon number densities, and $S(\rho)$ describes the density dependence of E_{sym}. Both symmetry and total binding energy terms in the nuclear semi-empirical binding energy formulae reflect averages of E_{sym} over the densities of nuclei [3]. The values of surface and volume symmetry energy terms obtained over fits of such formula to measured masses provide some sensitivity to the density dependence of $S(\rho)$ near saturation density [3,4]. Giant resonances, low-lying electric dipole excitations and the difference between neutron and proton matter radii may also provide sensitivity to the density dependence of $S(\rho)$ near saturation density [8-11].

We have preformed a series of ImQMD calculations at b=6 fm with different values of γ_i with S_0 between 25 to 40 MeV to locate the approximate boundaries in the S_0 and L plane that satisfy the 2σ criterion in the χ2 analysis of the isospin diffusion data where the slope parameter $L=3\rho_0 dS(\rho)/d\rho|_{\rho 0}=[3/\rho_0]p_0$. Even though the sensitivity of constraints on S_0 and L to differences between m_n^* and m_p^* and to the in-medium cross-sections have not been fully

explored, BUU calculations indicate that their sensitivities to these are weaker than their sensitivities to S_0 and L.

Initially, neutron/proton double ratio data have been calculated using the ImQMD model [12]. This observable derives its sensitivity to the symmetry energy from the opposite sign of the symmetry force for neutrons as compared to protons [13]. First experimental comparisons of neutron to proton spectra in ref. [14] used a double ratio to reduce sensitivity to uncertainties in the neutron detection efficiencies and to relative uncertainties in energy calibrations of neutrons and protons. This double ratio

$$DR(Y(n)/Y(p)) = \frac{R_{n/p}(A)}{R_{n/p}(B)} = \frac{dM_n(A)/dE_{CM}}{dM_p(A)/dE_{CM}} \bullet \frac{dM_n(B)/dE_{CM}}{dM_p(B)/dE_{CM}}$$

is constructed from the ratios of energy spectra, dM/dEC.M, of neutrons and protons for two systems A and B characterized by different isospin asymmetries. The star symbols in the left panel of Figure 1 show the neutron-proton double ratios measured at $70° \le \theta_{CM} \le 110°$ as a function of center-of-mass (C.M.) energy for nucleons for central collisions of ^{124}Sn+^{124}Sn and ^{112}Sn+^{112}Sn [14].

We have performed calculations for two systems: A=^{124}Sn+^{124}Sn and B=^{112}Sn+^{112}Sn. About 60,000 events are simulated for each impact parameter. Within the statistical uncertainties, the double ratio observable, DR(Y(n)/Y(p)), is nearly independent of impact parameter over a range of $0 \le b \le 5$ fm. The lines in the left panel of Figure 1 show double ratios vs. the C.M. energy of nucleons emitted at $70° \le \theta_{C.M.} \le 110°$ for γ_i=0.35, 0.5, 0.75, 1 and 2. The computation uncertainties in Figure 1 are statistical. To increase the statistics for high energy nucleons, the double ratios are averaged over b=1, 2, 3 fm.

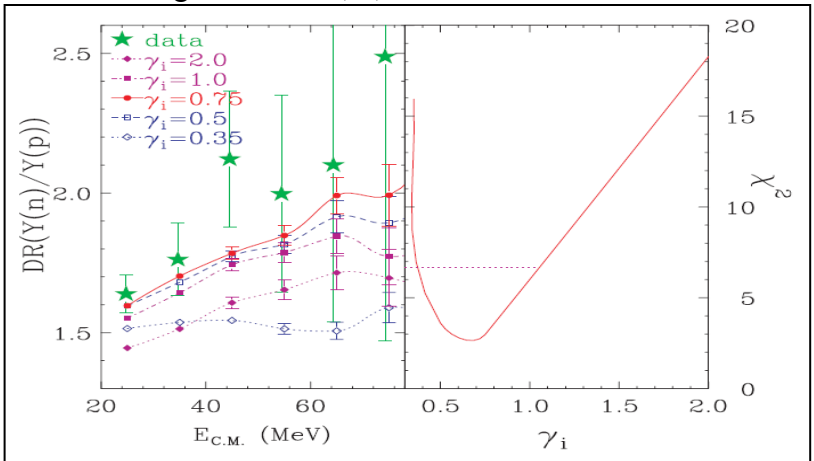

Figure 1 (Left) Comparison of neutron-proton double ratios for the as a function of CM energy compared to the ImQMD calculations for different density dependences. (Right) Variation of the density parameter γ as a function of the fit parameter χ^2.

Despite the large experimental uncertainties for higher energy data, these comparisons definitely rule out both very soft (γ_i=0.35, dotted line with closed diamond points) and very

stiff (γ_i=2, dotted line with open diamond symbols) density-dependent symmetry terms. The right panel shows the dependence on γ_i of the *total* χ^2 computed from the difference between predicted and measured double ratios. We determine to within a 2σ uncertainty, $0.4 \leq \gamma_i \leq 1.05$ corresponding to an increase in χ^2 by 4 above its minimum of near $\gamma_i \sim 0.7$.

In summary, the ability of QMD models to reproduce both isospin diffusion and double ratio of neutron and proton spectra data is an important step forward in obtaining information about the symmetry energy in heavy-ion collisions. All three observables examined here provide consistent constraints on the density dependence of the symmetry energy. Some shifts in the boundaries of the constraints can be expected with improvements in the precision of the experimental data and in the understanding of transport calculations. Nevertheless, the consistency between the different probes of the symmetry energy suggests that increasingly stringent constraints on the symmetry energy at sub-saturation density can be expected.

References:

[1] Bao-An Li, Lie-Wen Chen, and Che Ming Ko, Phys. Rep. **464**, 113 (2008), and references therein.
[2] A. W. Steiner, M. Prakash, J. M. Lattimer, and P. J. Ellis, Phys. Rep. **411,** 325 (2005), and references therein.
[3] P. Danielewicz, Nucl. Phys. A **727,** 233 (2003), and references therein.
[4] Pawel Danielewicz and Jenny Lee, arXiv:0807.3743, and references therein.
[5] A. W. Steiner, Phys. Rev. C **77**, 035805 (2008).
[6] B. G. Todd-Rutel and J. Piekarewicz, Phys. Rev. Lett. **95,** 122501 (2005).
[7] J. M. Lattimer and M. Prakash, Science **304**, 536 (2004).
[8] T. Li, et al., Phys. Rev. Lett. **99,** 162503 (2007).
[9] A. Klimkiewicz et. al., Phys. Rev. C **76**, 051603(R) (2007).
[10] C. J. Horowitz and J. Piekarewicz, Phys. Rev. Lett. **86**, 5647 (2001).
[11] J. Piekarewicz, Phys. Rev. C **69,** 041301 (2004).
[12] Y. Zhang, P. Danielewicz, M. Famiano, Z. Li, W. G. Lynch, and M. B. Tsang, Phys. Lett. B **664,** 145 (2008), and references therein.
[13] B. A. Li, C. M. Ko, and Z. Z. Ren, Phys. Rev. Lett. **78,** 1644 (1997).
[14] M. A. Famiano, et al., Phys. Rev. Lett. **97**, 052701 (2006).

6.4 The *p*-Shell Λ-Hypernuclci with the Nijmegen ESC04 Baryon-Baryon Potential

Dean Halderson

Western Michigan University, Kalamazoo, MI 49008

Beginning in 1998 a series of experiments using the Hyperball detector [1] attempted to measure gamma rays from *p*-shell Λ-hypernuclei. The experiments ended in 2005 with KEK 566. Data from this last experiment are still under analysis, but the energy and yield of the measured gamma rays from all experiments have provided valuable information on the structure of seven nuclei. These experiments were motivated by the work of Refs. [2] and [3]. It was shown in Ref. [2] that the five $p_N s_\Lambda$ two-body matrix elements depend on the radial integrals associated with each component of the standard interaction, $V_{\Lambda N}(r) = V_0(r) + V_\sigma(r)\boldsymbol{s}_N\cdot\boldsymbol{s}_\Lambda + V_\Lambda(r)\boldsymbol{l}_{N\Lambda}\cdot\boldsymbol{s}_\Lambda + V_N(r)\boldsymbol{l}_{N\Lambda}\cdot\boldsymbol{s}_N + V_T(r)S_{12}$. The radial integrals are conventionally denoted by the parameters $\bar{V}, \Delta, S_\Lambda, S_N$, and T. The energy splitting of spin partners can be related to these parameters and, therefore, to the spin-dependent components of the Λ*N* interaction. Hence, calculations for the *p*-shell nuclei provide a test of these components. This test is applied to the new Nijmegen ESC04 potentials [4].

Effective interactions were generated via the Brueckner-Hartree procedure with ^{4}He and ^{16}O cores for the four ESC04 potentials. Structure calculations were then performed for the seven nuclei in the RCCSM formalism and with the Cohen and Kurath (6-16) [5] *NN* interaction. This formalism allows expansion of the Λ wave function in a series of oscillators as measured from the center of mass of the core. It also allows use of the Λ mass, and yet still allows no spurious components. The results for $^{7}_{\Lambda}$Li with the ^{4}He core interaction are shown in Fig. 1. From the results of Ref. [6], one expects to see overbinding from the ESC04 potentials. However, one sees that ESC04B gives excellent values for the two splittings. The $1/2^+$ - $3/2^+$ splitting depends almost entirely on the spin-spin parameter Δ. One cannot calculate a value of Δ for realistic interactions like those from ESC04 because they have different even and odd components. However, one can extract an effective Δ by turning off all components of the interaction except the triplet and singlet central terms and then compare the calculated splitting with the formula in Ref. [7], $1/2^+ - 3/2^+ = 1.461\Delta$. With the ^{4}He core interaction one extracts a effective Δ value of 0.428. This compares favorable with that obtained from fits with the standard interaction, Δ = 0.430. The standard interaction requires a smaller Δ from the middle to the end of the *p*-shell [7]. Figure 2 demonstrates that this requirement arises very naturally as the Pauli operator changes from the ^{4}He core to the ^{16}O core and weakens the spin- spin interaction. The ESC04B interaction continues to do very well on the structure throughout the *p*-shell. ESC04A also does well until $^{16}_{\Lambda}$O. ESC04C and ESC04D do miserably. The refit NSC89 is slightly worse than ESC04A. The primary difference between the pair A,B and the pair C,D is the spin-spin interaction. This can be seen in the ratio of the

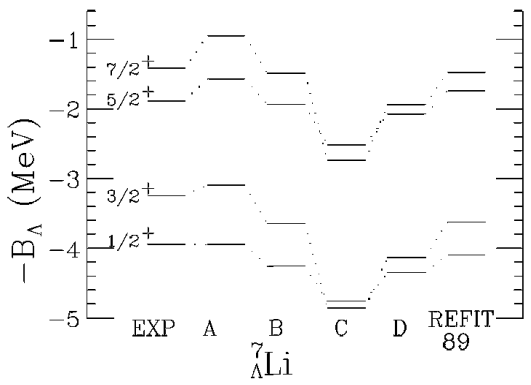

Figure 1

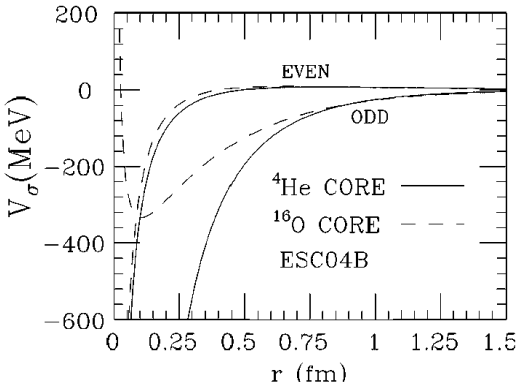

Figure 2

relative *g*-matrix elements $^1S_0/^3S_1$ for n=0. For A, B, C, D, and the refit 89, this value with the ^{4}He core is 1.65, 1.48, 1.06, 1.18, and 1.50, respectively.

Clearly, any new *YN* interaction must have a value close to those of A and B.

References:

[1] O. Hashimoto and H. Tamura, Prog. Part. Nucl. Phys. **57**, 564 (2006).
[2] A. Gal, J. M. Soper, and R. H. Dalitz, Ann. Phys. (N. Y.) **63**, 53 (1971); **72**, 445 (1972); **113**, 79 (1978).
[3] D. J. Millener, A. Gal, C. B. Dover, and R. H. Dalitz, Phys. Rev. C **31**, 499 (1985).
[4] T. A. Rijken and Y. Yamamoto, Phys. Rev. C **73**, 44008 (2006).
[5] D. Kurath and S. Cohen, Nucl. Phys. **73**, 1 (1965).
[6] D. Halderson, Phys. Rev. C **76**, 047301 (2007).
[7] D. J. Millener, Proc. Int. Conf. on Hypernuclear and Strange Particle Physics, HYP2006, to be published by Società Italiana di Fisica and Springer-Verlag.

6.5 The Structure of ^{7}He

A. H. Wuosmaa,[1] K. E. Rehm,[2] J. P. Greene,[2] D. J. Henderson,[2] R. V. F. Janssens,[2] C. L. Jiang,[2] L. Jisonna,[3] **J. P. Lighthall**,[1] **S. T. Marley**,[1] E. F. Moore,[2] R. C. Pardo,[2] Steven C. Pieper,[2] J. P. Schiffer,[2] R. E. Segel,[3] X. Tang,[2] and R. B. Wiringa[2]

[1]Western Michigan University, Kalamazoo, MI 49008
[2]Argonne National Laboratory, Argonne, IL 60439
[3]Northwestern Universtiy, Evanston, IL 60208

Although the resonance corresponding to the ground state of ^{7}He has been known for over three decades, the properties of excited states of this exotic, very neutron-rich system have remained uncertain. With only seven nucleons, this system is one in which modern theories of nuclear structure such as the Quantum Monte Carlo (QMC) approach can be readily applied. This technique can predict not only the spins, parities, and excitation energies of states in light nuclei with A<12, but also can be used to calculate the spectroscopic factors for nucleon transfer reactions. In ^{7}He, the low-lying excited states are predicted to be populated very selectively by neutron stripping (adding one neutron to ^{6}He) or proton pickup (removing one proton from ^{8}Li) reactions. Previously, we have studied the neutron-stripping reaction ^{6}He(d,p)^{7}He, and identified a likely candidate for the $J^{\pi}=1/2^{-}$ first-excited state. More recently, we have used the proton-removal reaction ^{8}Li(d,^{3}He)^{7}He to produce ^{7}He in a complementary fashion, using a radioactive ^{8}Li beam produced with the in-flight facility at the ATLAS accelerator at Argonne National Laboratory. The ^{3}He ejectiles, and the ^{6}He and ^{4}He residual nuclei left from the decay of ^{7}He, were detected using a set of silicon detectors. Theory predicts that this second reaction should populate the ground and second-excited $5/2^{-}$ of ^{7}He. Figure 1 shows excitation-energy spectra from these two reactions, where the excited states in ^{7}He are identified by their decay properties. The first excited state decays by single-neutron emission (Fig. 1b) and experimentally is produced only in neutron transfer. The second-excited state populated in the (d,^{3}He) reaction decays by 3-neutron emission (Fig. 1f).

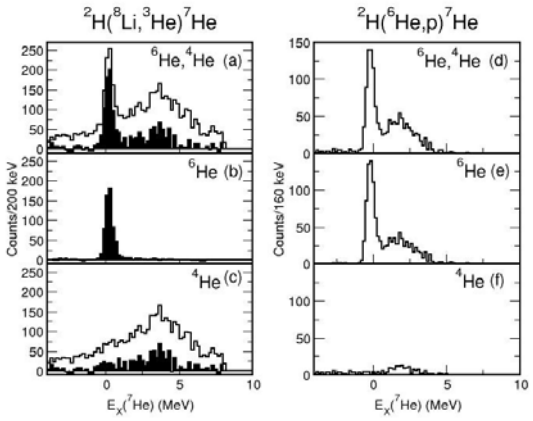

Figure 1 Excitation-energy spectra for the ^{2}H(^{8}Li,^{3}He)^{7}He and ^{2}H(^{6}He,*p*)^{7}He reactions. The ^{3}He particles in (a-c) and protons in (d-f) are detected in coincidence with ^{6}He and ^{4}He, ^{6}He, and ^{4}He ions, respectively.

The QMC calculations, combined with a distorted-wave Born approximation (DWBA) of the scattering reaction can predict the cross sections for the ^{8}Li(d,^{3}He)^{7}He reaction. Figure 2 shows angular distributions for this reaction (Fig. 2d, Fig. 2e) as well as for (d,t) and (d,^{3}He) reactions with a stable ^{7}Li beam as a calibration reaction. The theoretical results are in quite reasonable agreement with the data, giving confidence in the predictions from the modern nuclear-structure calculations even for the exotic, unbound neutron-rich ^{7}He.

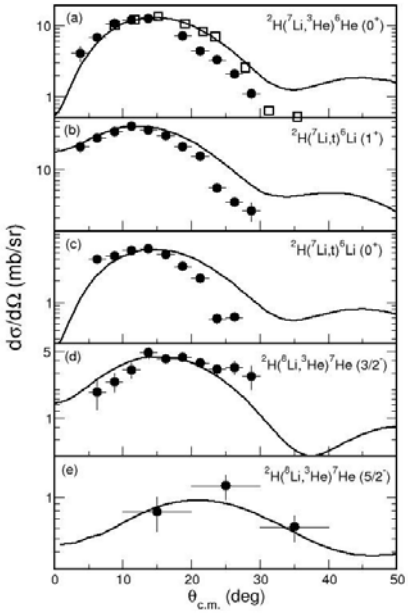

Figure 2 Angular distributions for various transitions in ^{7}Li+*d* and ^{8}Li+*d* interactions. The curves are described in the text.

6.6 The ^{2}H(^{11,12}B,*p*)^{12,13}B Reactions and the Influence of ^{11,12}B(n, γ) on the r-Process Abundance of Light Elements

H. Y. Lee,[2] **A. H. Wuosmaa**,[1] K. E. Rehm,[2] **N. J. Goodman**,[1], J. P. Greene,[2] D. J. Henderson,[2] R. V. F. Janssens,[2] C. L. Jiang,[2] L. Jisonna,[3] **J. P. Lighthall**,[1] **S. T. Marley**,[1] E. F. Moore,[2] M. Notani,[2] R. C. Pardo,[2] N. Patel,[4] J. P. Schiffer,[2] R. E. Segel,[3] X. Tang[2]

[1]Western Michigan University, Kalamazoo, MI 49008
[2]Argonne National Laboratory, Argonne, IL 60439
[3]Northwestern Universtiy, Evanston, IL 60208
[4]Colorado School of Mines, Golden, CO 80401

The rapid neutron capture process, or r-process, is a set of neutron-capture and beta-decay reactions thought to occur in violent, explosive astrophysical environments such as Type II supernovae, neutron-star mergers, or gamma-ray bursts. The r-process is responsible for the production of many heavy elements, but recently the success of the neutrino-driven wind model for core-collapse supernova have suggested that light, neutron-rich nuclei should also be considered. To determine the possible reaction paths and predict the abundance of nuclei produced in this particular r-process, it is important to understand the properties of the nuclei involved. Two reactions that could influence the r-process are the neutron-capture reactions on ^{11,12}B. The ^{12}B(n, γ) neutron-capture reaction cannot be performed in the laboratory, however it is possible to study some of the relevant aspects of the residual nucleus ^{13}B using the neutron-transfer reaction ^{12}B(d,p)^{13}B. We have studied this reaction using a radioactive ^{12}B beam produced at the In-Flight facility at the ATLAS accelerator laboratory at Argonne National Laboratory. In the same experiment, the ^{11}B(d,p)^{12}B reaction was also studied with a stable ^{11}B beam that was used as calibration. The protons from the (d,p) reactions were detected using an array of segmented silicon detectors, and the ^{13}B and ^{12}B (^{12}B and ^{11}B) fragments from bound and unbound states in ^{13}B (^{12}B**)** were detected in a set of silicon ΔE-E telescopes to provide particle identification.

The most important state in ^{11}B for the r-process is the 3.389 MeV state that lies just above the neutron-decay threshold in ^{12}B. For this level, we have determined the neutron-decay branching ratio Γ_n/Γ_γ to be 94±5 compared to a previous estimate of 124 from Raucher et al [1]. This result increases the resonance strength ωγ by approximately 50% over previous estimates, and the reaction rate of ^{11}B(n, γ)^{12}B increases by approximately the same amount. For ^{13}B, the important states above the neutron-decay threshold in the vicinity of 5 MeV excitation energy were previously thought to have negative parity; the present results suggest positive parity instead and the influence of resonant neutron capture through these levels is currently being assessed.

Reference

[1] T. Rauscher et al, ApJ **429**, 499 (1994).

6.7 HELIOS: The HELIcal Orbit Spectrometer

A. H. Wuosmaa,[1] B. B. Back,[2] **J. P. Lighthall**,[1] C. J. Lister,[2] **S. T. Marley**,[1] R. C. Pardo,[2] K. E. Rehm,[2] J. P. Schiffe,r[2] **J. Winkelbauer**[1]

[1]Western Michigan University, Kalamazoo, MI 49008
[2]Argonne National Laboratory, Argonne, IL 60439

The HELIOS device is a novel new spectrometer, based on a large-volume high-field magnetic solenoid, designed to study nucleon transfer and other reactions in inverse kinematics. A detailed technical description of the device and its expected capabilities are contained in Ref. [1]. HELIOS plays a prominent role in the future Strategic Plan for the ATLAS facility, as it is well matched to the ongoing CARIBU radioactive beam source development project.

Over the past year, major progress has been made in the HELIOS project, and the spectrometer is complete in its prototype form. The magnetic solenoid, obtained from Siemens, is installed at the ATLAS facility at Argonne National Laboratory, and the mechanical elements that transform the bore of the magnet into an evacuated reaction chamber are complete and installed. The HELIOS beam line has also been constructed and is now ready to accept both stable, and unstable beams from the ATLAS accelerator. Commissioning experiments that will demonstrate the functionality of the device are scheduled for 2008 and 2009, using stable, and unstable beams, respectively. Figure 1 shows the upstream end of the spectrometer with detector electronics installed.

The heart of the spectrometer is an array of position-sensitive silicon detectors constructed at WMU (Fig. 2). The energy and position resolutions of the detectors used in the array were previously evaluated using proton beams from the WMU tandem accelerator. The silicon array is now installed in the magnet (See Fig. 3), and the performance of the device has been evaluated using alpha particles from a radioactive source. The performance of the silicon array was excellent, and should provide the resolution necessary to identify closely spaced excited states populated in inverse-kinematic transfer reactions that will make up a significant fraction of the physics program that will utilize the unstable beams from the CARIBU source.

Reference:

[1] A. H. Wuosmaa *et al.*, Nucl. Instr. and Meth. in Phys. Res. A **580**, 1290 (2007).

Figure 1 Completed HELIOS spectrometer at the ATLAS facility at Argonne National Laboratory.

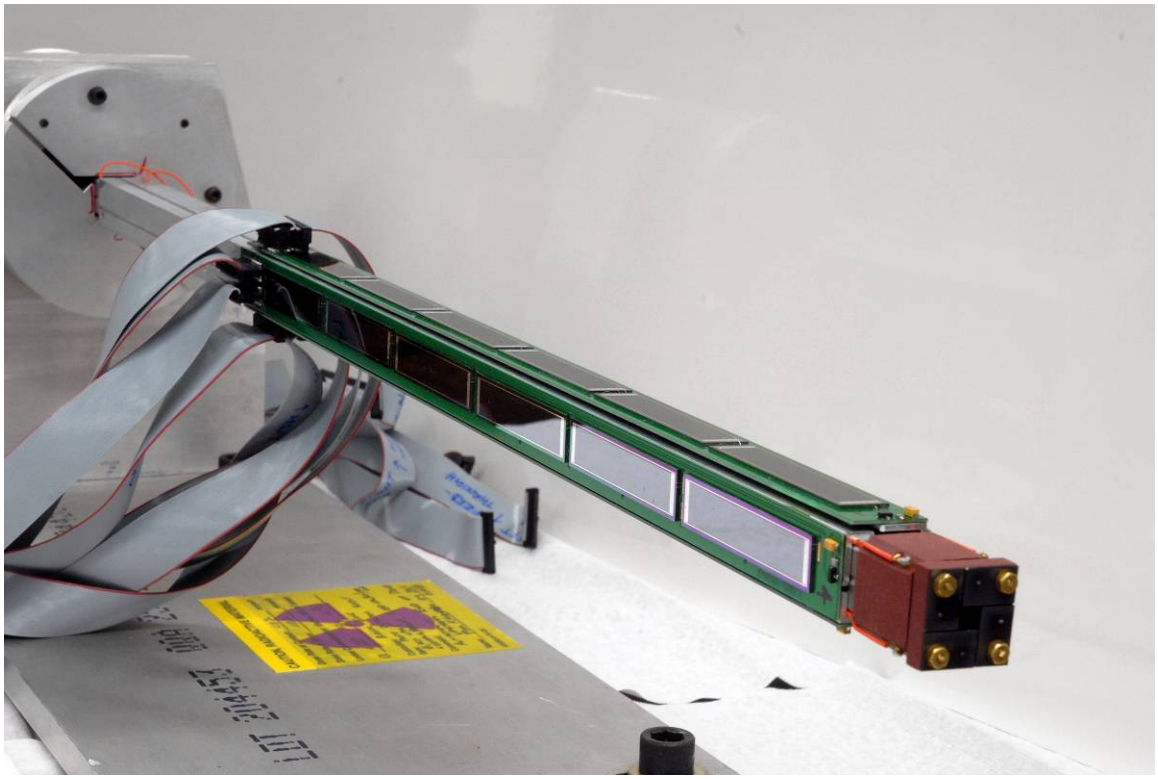

Figure 2 Assembled HELIOS silicon-detector array ready for installation in the HELIOS chamber.

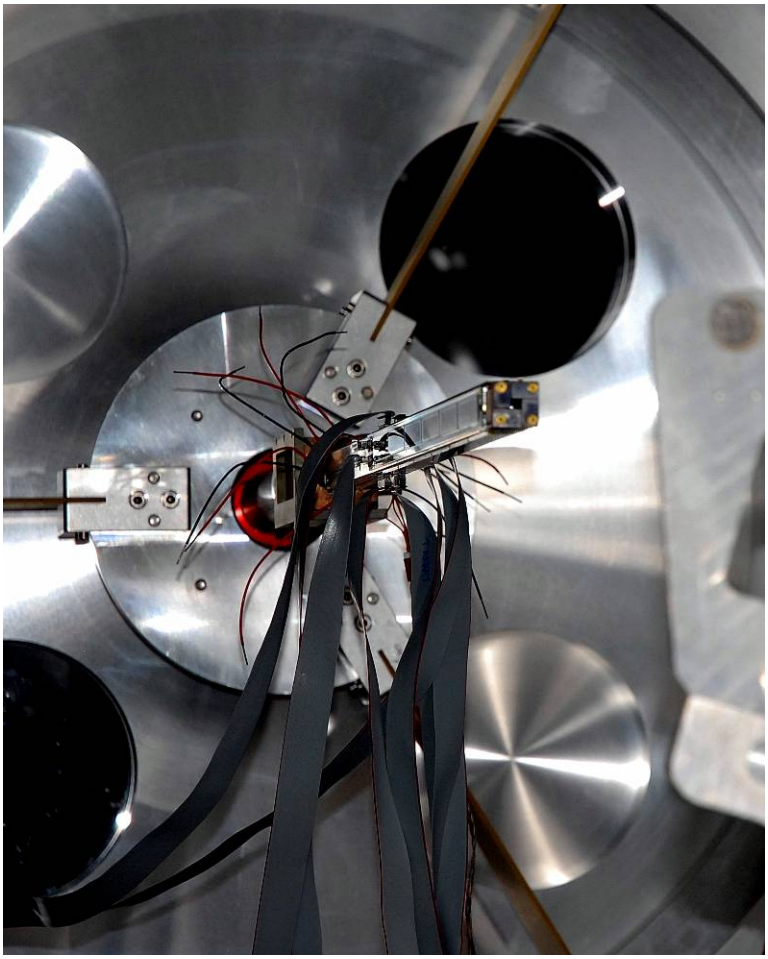

Figure 3 Silicon-detector array installed in HELIOS chamber.

7 PHYSICS EDUCATION

7.1 Facilitating Change in Undergraduate STEM: Initial Results from an Interdisciplinary Literature Review

Charles Henderson,[1] Andrea Beach,[2] Noah Finkelstein,[3] R. Sam Larson[4]

[1]Department of Physics, Western Michigan University, Kalamazoo, MI 49008
[2]Department of Educational Leadership, Western Michigan University, Kalamazoo, MI 49008
[3]University of Colorado at Boulder, Boulder, CO 80309
[4]Integrated Quality Systems and Tools, Kaiser Permanente Colorado, Denver, CO 80237

Introduction

Recent decades have seen increasing calls for fundamental change in the teaching of Science, Technology, Engineering, and Mathematics (STEM) based, in part, on the concern that the United States will lose its role as a leader in science and technology fields due to outdated and inappropriate instructional practices [1]. The resulting significant expenditures of time and money focused on improving teaching and learning have met with only modest success [2].

We see three distinct research communities involved in this endeavor to improve undergraduate instruction in STEM disciplines. Disciplinary-based STEM Education Researchers (SER) are particularly interested in studying student learning within their discipline and developing discipline-specific curricular materials to improve this learning. Faculty Development Researchers (FDR) often focus on providing faculty with more general pedagogical skills or motivation and tools for self-improvement. Higher Education Researchers (HER) often study how cultural norms, organizational structures, and state and national environments and policy influence higher education practices.

We see a need for interdisciplinary research on STEM instructional improvement that draws from the knowledge and experiences of all of these research communities. The initial analysis of the peer-reviewed literature presented here is one of the early steps in this agenda. The research questions are:

1) What strategies do change agents use to promote change in undergraduate STEM teaching practices?

2) How do change strategies described by authors relate to the disciplinary background of the authors?
3) What evidence is available to support the effectiveness of these strategies?

4) How do authors connect their work with other change literature (e.g., individual and organizational change theories)?

Methods

We identified journal articles that describe efforts by change agents to improve instructional practices used in undergraduate STEM education. For this initial review, we examined 130 randomly chosen articles from the set of 295 articles identified. An inductive analysis process led to the emergence of four categories of change strategies. In a second analysis round, we selected 10 articles from each of the four categories for further qualitative examination. Additional details about the methodology and results can be found in Ref. [3].

Analysis and Results

The four proposed categories of change strategies are based on the answers to two fundamental questions. The first question was, "What is the primary aspect of the system that the change strategy seeks to directly impact: individuals or environments and structures?" The second question was, "To what extent is the intended outcome for the individual or environment known in advance: prescribed or emergent?"

Four Categories of Change Strategies

Based on the possible combinations of responses to the two guiding questions, we developed a four-square typology of change strategies (Figure 1). Of the 130 articles, 15 were not relevant to our analysis and were removed. Four articles could not be classified in a single category. The remaining 111 articles fit into one of the four core categories.

	Aspect changed: Individuals		
Intended Outcome: Prescribed	I. Disseminating: CURRICULA & PEDAGOGY Tell/Teach individuals about new teaching conceptions and/or practices and encourage use.	II. Developing: REFLECTIVE TEACHERS Encourage/Support individuals to develop new teaching conceptions and/or practices.	Intended Outcome: Emergent
	III. Developing: POLICY Develop new environmental features that Require/Encourage new teaching conceptions and/or practices.	IV. Developing: SHARED VISION Empower/Support stakeholders to collectively develop environmental features that support new teaching conceptions and/or practices.	
	Aspect changed: Environments and Structures		

Figure 1 Four-Square Typology of Change Categories

<u>Individual/Prescribed: Focus on Disseminating Curriculum and Pedagogy</u>. (39 articles, 30%).

The emphasis of this type of intervention is on communicating the change agent's vision of good teaching to individual instructors. The prominent aspects of the interventions typically include curricular materials, instructional strategies, and/or associated instructor knowledge/conceptions.

<u>Individual/Emergent: Focus on Developing Reflective Teachers</u>. (40 articles, 31%). The emphasis of this type of intervention is on encouraging teachers to use their own knowledge, experience, or skill to improve their instructional practices. Information about various instructional strategies and materials may be provided, but this is not the main focus.

<u>Environments/Prescribed: Focus on Developing Policy</u>. (18 articles, 14%). The emphasis is on developing appropriate environments (e.g., rules, reward systems, reporting requirements, investments in support structures) to facilitate instructors' engaging in specific or desired activities.

Environments/Emergent: Focus on Developing Shared Vision. (6 articles, 5%). The emphasis is on developing a new collective vision for the department, institutional unit, or institution that supports new modes of instruction. The change agent uses stakeholders to develop a shared vision and design new environments that are consistent with this vision.

Conclusions

1. Change Strategies Used. Change strategies described in the articles were much more likely to focus on changing individual faculty (61% of all 130 articles) than on changing environments or structures (19%). The articles were more evenly divided between working towards prescribed outcomes (44%) and emergent outcomes (36%). We conclude that change agents frequently work at the individual level, rather than at extra-individual levels.

2. Use of Different Change Strategies by Different Disciplines. We proposed that the three different disciplines (SER, FDR, and HER) each operate more or less independently of one-another and that each has their own distinct perspectives and strategies about change. The literature classification supports this proposition.

3. Evidence of Effectiveness of Change Strategies. Of the 43 articles analyzed, 13 did not present a specific change strategy warranting evidence of success. Of the 30 remaining, we judged 12 (40%) to have at least moderate evidence supporting their assertions of success (or lack thereof) of a change strategy. Five articles were judged to offer weak support, and 11 offered little or no support. No articles offered strong evidence supporting the success of a change intervention.

4. Connections with Other Change Literature. Fewer than half (20/43) of the articles cited literature that we could label "change literature." Those that did not fit within our assessment of using change literature typically not only failed to ground their selected change strategy in the change literature, but also failed to justify their choice of change strategy. This trend was consistent across the four change categories.

Discussion

We plan to continue with the analysis. An important trend thus far is that it appears to be possible to use two relatively simple criteria to usefully categorize articles about STEM instructional change into a small number of meaningful categories In addition, the categories presented here support our supposition that the three disciplines operate independently and use largely different strategies for promoting change. This finding supports our expectation that interdisciplinary work involving researchers from SER, FDR, and HER might be productive since each group can bring different sets of knowledge. There is no evidence that we have missed an important disciplinary community. Finally, an important trend is the presence of common weaknesses across all four change categories and all three research communities. Many of the articles did not present convincing evidence to support the conclusions drawn and many articles did not build arguments and change strategies from the

research literature. This finding suggests that there is substantial need for synthesis work such as the work represented by this project.

Acknowledgements:

We wish to thank the National Science Foundation for their support of this project (SES-0623009, DRL-0723699) as well as participants at the June 2008 Facilitating Change symposium for their valuable feedback on this work.

References:

[1] Center for Science, Math, and Engineering Education, Transforming Undergraduate Education in Science, Mathematics, Engineering, and Technology, Washington, D.C.:National Academy Press, 1999.

[2] D. Bok, Our Underachieving Colleges: A Candid Look at How Much Students Learn and Why They Should Be Learning More, Princeton, NJ: Princeton University Press, 2006.; Boyer Commission on Undergraduates in the Research Universities, Reinventing Undergraduate Education: A Blueprint for America's Research Universities, Menlo Park, CA: Carnegie Foundation for the Advancement of Teaching, 1998.; J. Handelsman et al., "EDUCATION: Scientific Teaching," Science 304 (5670), 521-522 (2004).

[3] C. Henderson, A. Beach, N. Finkelstein, and R. S. Larson, “Preliminary Categorization of Literature on Promoting Change in Undergraduate STEM,” paper presented at the Facilitating Change in Undergraduate STEM symposium, Augusta, MI, (2008). <http://www.wmich.edu/science/facilitating-change/PreliminaryCategorization.pdf.

8 PUBLICATIONS

8.1 Papers Published

J. L. Baran, **S. Das**, F. Járai-Szabó, K. Póra, L. Nagy, and **J. A. Tanis**, *Suppression of Primary Electron Interferences in the Ionization of N_2 by 1-5 MeV/u Protons,* Phys. Rev. A **78**, 012710 (2008).

N. Berrah, **R. C. Bilodeau**, **I. Dumitriu**, J. D. Bozek, G. D. Ackerman, **O. Zatsarinny**, and **T. W. Gorczyca**, *Shape Resonances in Absolute K-Shell Photodetachment of B^-*, Phys. Rev. A **76**, 032713 (2007).

N. Berrah, **R. C. Bilodeau,** J. D. Bozek, **I. Dumitriu,** D. Toffoli, and R. R. Lucchese, *Inner-Shell Photodetachment and Fragmentation of Small Clusters B_2^-, B_3^-*, Phys. Rev. A **76**, 042709 (2007).

C. A. Burns, *Is Lithium Ammonia Suitable for a Liquid Lunar Telescope*?, Pub. Astron. Soci. Pac. **864**, 188 (2008).

C. N. Kodituwakku, **C. A. Burns**, A. H. Said, H. Sinn, X. Wang, T. Gog, D. M. Casa, and M. Tuel, *Resonant Inelastic X-ray Scattering Studies of the Organic Semiconductor Copper Phthalocyanine*, Phys. Rev. B **77**, 125205 (2008).

S. G. Chung and K. Ueda, *Entanglement Perturbation Theory for the Quantum Ground States in Two Dimensions*, Physics Letters A **372**, 4845 (2008).

S. Das, **B. S. Dassanayake**, **M. Winkworth**, **J. L. Baran**, N. Stolterfoht, and **J. A. Tanis**, *Inelastic Guiding of Electrons in Polymer Nanocapillaries,* Phys. Rev. A **76**, 042716 (2007).

Michael A. Famiano, **Ravin S. Kodikara**, **Brenna M. Giacherio**, **V. G. Subramanian**, and **Asghar Kayani**, *Measurement of the (p,γ) Cross Sections of ^{46}Ti, ^{64}Zn, ^{114}Sn, and ^{116}Sn at Astrophysically Relevant Energies,* Nuclear Physics A **802**, 26 (2008).

R. J. Charity, S. A. Komarov, and L. G. Sobotka,J. Clifford, D. Bazin, A. Gade, Jenny Lee, S. M. Lukyanov, W. G. Lynch, M. Mocko, S. P. Lobastov, A. M. Rogers, A. Sanetullaev, M. B. Tsang, and M. S. Wallace, S. Hudan and C. Metelko, **M. A. Famiano**, and **A. H. Wuosmaa**, and M. J. van Goethem, *Particle decay of ^{12}Be excited states* Physical Review C **76**, 064313 (2007).

J. Fu, **T. W. Gorczyca**, **D. Nikolic**, N. R. Badnell, D. W. Savin, and M. F. Gu, *Orbital Sensitivity in Mg^{2+} Dielectronic Recombination Calculations*, Phys. Rev. A **77**, 032713 (2008).

D. W. Savin, N. R. Badnell, P. Beirsdorfer, B. R. Beck, G. V. Brown, P. Bryans, **T. W. Gorczyca**, M. F. Gu, S. M. Kahn, J. M. Laming, D. A. Liedahl, W. Mitthumsiri, J. H. Scofield, and K. L. Wong, *Analog and Digital Simulations of Maxwellian Plasmas for Astrophysics*, Can. J. Phys**. 86**, 209 (2008).

J. Grineviciute and **D. Halderson**, *Proton Capture by ^{14}N at Astrophysical Energies*, J. Phys. G: Nucl. Part. Phys. **35**, 055201 (2008).

D. Halderson, *Λ-Hypernulcear Single-Particle Energies with the Nijmegen ESC04 Baryon-Baryon Potential*, Phys. Rev. C **76**, 047301 (2007).

D. Halderson, *The p-Shell Λ-Hypernulcear with the Nijmegen ESC04 Baryon-Baryon Potential*, Phys. Rev. C **77**, 034304 (2008).

E. Yerushalmi, **C. Henderson**, K. Heller, P. Heller, and V. Kuo, *Physics Faculty Beliefs and Values about the Teaching and Learning of Problem Solving Part I: Mapping the Common Core*, Physical Review Special Topics: Physics Education Research **3** (2), 020109 (2007).

C. Henderson, E. Yerushalmi, K. Heller, P. Heller, and V. Kuo, *Physics Faculty Beliefs and Values about the Teaching and Learning of Problem Solving Part II: Procedures for Measurement and Analysis*, Physical Review Special Topics: Physics Education Research **3** (2), 020110 (2007).

C. Henderson and M. Dancy, *Physics Faculty and Educational Researchers: Divergent Expectations as Barriers to the Diffusion of Innovations*, American Journal of Physics (Physics Education Research Section) **76** (1), 79-91 (2008).

C. Henderson, *Promoting Instructional Change in New Faculty: An Evaluation of the Physics and Astronomy New Faculty Workshop*, American Journal of Physics **76** (2), 179-187 (2008).

C. Henderson, *Promoting Instructional Change in New Faculty: An Evaluation of the Physics and Astronomy New Faculty Workshop*, Proceedings of the 2007 Physics Education Research Conference (2007).

M. Dancy, E. Brewe, and **C. Henderson,** *Modeling Success: Building Community for Reform*, Proceedings of the 2007 Physics Education Research Conference (2007).

C. Henderson, *External Evaluator Report,* New Physics and Astronomy Faculty Workshop (2007).

E. Y. Kamber, O. Abu-Haija, and **J. A. Wardwell**, *State-Selective Electron Capture by O^{3+} Ions from Atomic and Molecular Targets*, Physical Review A **77**, 012701 (2008).

W. Priyantha, H. Chen, M. Kopczyk, R. J. Smith, **A. Kayani**, A. Comouth, M. Finsterbusch, P. Nachimuthu, and D. McCready, *Interface Mixing of Al/Fe and Fe/Al Bilayer Systems and the Role of Ti as a Stabilizing Interlayer using Rutherford Backscattering Spectrometry and X-ray Reflectometry*, Appl. Phys. **103**, 014508 (2008).

Adam McClure, **A. Kayani**, Y. U. Idzerda, E. Arenholz, and E. Cruz, *Characteristics of $Co_xTi_{1-x}O_2$ Thin Films Deposited by MOCVD*, Journal of Applied Physics **104**, 084911 (2008).

P. E. Gannon, V. I. Gorokhovsky, M. C. Deibert, R. J. Smith, **A. Kayani**, P. T. White, S. Sofie, Zhenguo Yang, D. McCready, S. Visco, C. Jacobson, and H. Kurokawa, *Enabling Inexpensive Metallic Alloys as SOFC Interconnects: An Investigation into Hybrid Coating Technologies to Deposit Nanocomposite Functional Coatings on Ferritic Stainless Steels*, International Journal of Hydrogen Energy **32**, 3672 (2007).

A. R. McGurn, *Transmission through Nonlinear Junction of Photonic Crystal Waveguides*, Journal of Physics: Condensed Matter **20**, 025202 (2008).

A. R. McGurn, *Nonlinear Optical Media in Photonic Crystal Circuits: Device Applications*, an invited chapter in the book "Nonlinear Phenomena Research Perspectives," Edited by C. W. Wang, Nova Science Publishers Inc., NY (2007).

A. R. McGurn, *Transmission through Nonlinear Barriers*, Physical Review B **77**, 115105 (2008).

D. Nikolic, **T. W. Gorczyca**, **J. Fu**, D. W. Savin, and N. R. Badnell, *Steps Toward Dielectronic Recombination of Argon-Like Ions: A Revisited Theoretical Investigation of Sc^{3+} and Ti^{4+}*, Nucl. Inst. Meth. Phys. Research B **261**, 145 (2007).

David Schuster, William W. Cobern, Brooks Applegate, Renee' Schwartz, Paul Vellom, Adriana Undreiu, and Betty Adams, *Assessing Pedagogical Content Knowledge of Inquiry Science Teaching,* Proceedings of the 2006 National STEM Assessment Conference, Washington DC. (2007)

David Schuster, William W. Cobern, Brooks Applegate, Renee' Schwartz, Paul Vellom, Adriana Undreiu, and **Betty Adams**, *Design and Development of an Instrument to Assess Pedagogical Content Knowledge of Inquiry Science Teaching,* Proceedings of the National Association for Research in Science Teaching Annual International Conference (2008).

David Schuster, Adriana Undreiu, and **Betty Adams**, *Multiple Modes of Reasoning in Physics Problem Solving, with Implications for Instruction*, Proceedings of the 2007 Physics Education Research Conference, American Institute of Physics AIP Conference Proceedings Vol.951, 184-187 (2007).

D. Strohschein, D. Röhrbein, T. Kirchner, S. Fritzsche, **J. Baran**, and **J. A. Tanis**, Nonstatistical Enhancement of the 1s2s2p ^{4}P State in Electron Transfer in 0.5 – 1.0 MeV/u $C^{4,5+}$ + He and Ne Collisions, Phys. Rev. A **77**, 022706 (2008).

L. Wang and **S. G. Chung**, *Precise Implementation of the Cluster Transfer Matrix Method in the Single Electron Box*, Phys. Lett. A **372**, 2925 (2008).

M. Wiedenhoeft, **S. E. Canton**, **A. A. Wills**, **T. W. Gorczyca**, J. Viefhaus, U. Becker, and **N. Berrah**, *Coincident Energy and Angular Distributions in Xenon $4d_{5/2}$ Inner-Shell Double Photoionization*, J. Phys. B **41**, 095202 (2008).

X. D. Tang, K. E. Rehm, I. Ahmad, C. R. Brune, A. Champagne, J. P. Greene, A. A. Hecht, D. Henderson, R.V. F. Janssens, C. L. Jiang, L. Jisonna, D. Kahl, E. F. Moore, M. Notani, R. C. Pardo, N. Patel, M. Paul, G. Savard, J. P. Schiffer, R. E. Segel, S. Sinha, B. Shumard, and **A. H. Wuosmaa,** *New Determination of the Astrophysical S Factor SE1 of the $^{12}C(\alpha,\gamma)^{16}O$ Reaction,* Physical Review Letters **99,** 052502 (2007).

A. H. Wuosmaa, K. E. Rehm, J. P. Greene, D. J. Henderson, R. V. F. Janssens, C. L. Jiang, L. Jisonna, **J. C. Lighthall**, **S. T. Marley**, E. F. Moore, R. C. Pardo, N. Patel, M. Paul, D. Peterson, S. C. Pieper, G. Savard, J. P. Schiffer, R. E. Segal, R. H. Siemssen, S. Sinha, X. Tang, and R. B. Wiringa, *Nucleon Transfer Reactions with Exotic Beams at ATLAS,* European Physics Journal Special Topics **150**, 79–82 (2007).

A. H. Wuosmaa, J. P. Schiffer, B. B. Back, C. J. Lister, and K. E. Rehm, *A Solenoidal Spectrometer for Reactions in Inverse Kinematics,* Nuclear Instruments and Methods in Physics Research A **580**, 1290–1300 (2007).

C. Tur, **A. H. Wuosmaa**, S. M. Austin , K. Starosta, J. Yurkon, A. Estrade, **N. Goodman**, **J. C. Lighthall**, G. Lorusso, **S. T. Marley,** and **J. Snyder**, *A High Efficiency, Low Background Detector for Measuring Pair-decay Branches in Nuclear Decay*, Nuclear Instruments and Methods in Physics Research A **594**, 66 (2008).

8.2 Papers in Press

N. Mulders, J. West, M. H. W. Chan, **C. N. Koddituwakku**, **C. A. Burns**, and L. B. Lurio, *Torsional Oscillator and Synchrotron X-ray Experiments on Solid Helium in Aerogel*, Phys. Rev. Lett.

C. A. Burns, N. Mulders, L. Lurio, M. H. W. Chan, **A. Said**, **C. N. Kodituwakku**, and P. M. Platzman, *X-ray Studies of Structure and Defects in Solid ^{4}He from 50 mK to Melting*, Phys. Rev. B.

S. Das, **B. S. Dassanayake**, N. Stolterfoht, and **J. A. Tanis**, *Inelastic Processes Associated with Electron Guiding through Insulating PET Nanocapillaries,* Revista Mexicana de Física (2008).

B. S. Dassanayake, **S. Das**, N. Stolterfoht, and **J. A. Tanis**, *Guiding of Electrons through Insulating PET Nanocapillaries*, Revista Mexicana de Física (2008).

J. Froyd, A. Beach, **C. Henderson,** and N. Finkelstein, *Improving Educational Change Agents' Efficacy in Science, Engineering, and Mathematics Education*, *in Exporting Sociology to STEM Fields*, edited by Harriet Hartman. [part of the Elsevier series on Research in Social Problems and Public Policy]

J. A. Tanis, *Interferences in Coherent Electron Emission from Diatomic Molecules*, Nucl. Instrum. Meth. Phys. Res. B (2008).

M. Winkworth, P. D. Fainstein, M. E. Galassi, **J. Baran**, **B. S. Dassanayake**, **S. Das**, **A. Kayani** and **J. A. Tanis**, *Interferences in Electron Emission from O2 by 30 MeV O5,8+ Impact*, Nucl. Instrum. Meth. Phys. Res. B (2008).

8.3 Papers Submitted

C. Henderson and K. Harper, *Quiz Corrections: Improving Learning by Encouraging Students to Reflect on Their Mistakes*, The Physics Teacher, June 2008.

H. Fynewever, **C. Henderson**, S. Barry, S. Erwin, S. Hanson, M. Huber, M. Lindow, and K. Mirakovits, *Honing Teachers' Behind the Scenes Work: Pragmatic Ideas from Best Practices*, Science Teacher, July 2007.

D. Nikolic, **T. W. Gorczyca**, and N. R. Badnell, *Resonance Asymmetry and External Field Effects in the Photorecombination of Ti4+*, Phys. Rev. A (2008).

Z. Pešić, D. Rolles, R. C. Bilodeau, I. Dimitriu, and **N. Berrah**, *Three-Body Fragmentation of* CO_2^{2+} *Upon K-Shell Photoionization,* Phys. Rev. A (R).

D. Rolles, G. Prumper, H. Fukuzawa, X.-J. Liu, **Z. D. Pesic**, R. F. Fink, A. N. Grum-Grzhimailo, **I. Dumitriu**, **N. Berrah**, and K. Ueda, *Molecular-Frame Angular Distributions of Resonant CO:C(1s) Auger Electrons*, Phys. Rev. Lett.

D. Rolles, H. Zhang, Z. D. Pešić, J. D. Bozek, and **N. Berrah**, *Emergence of Band Structure in Valence Photoemission from Rare Gas Clusters*, Phys. Rev. Lett.

G. Prumper, **D. Rolles**, H. Fukuzawa, X. J. Liu, **Z. Pešić**, **I. Dumitriu**, R. R. Lucchese, K. Ueda, and **N. Berrah**, *Measurements of Auger Electron Angular Distributions in the C 1s¡12¼* Resonance with High Energy Resolution,* J. Phys. B.

G. Prumper, H. Fukuzawa, **D. Rolles**, K. Sakai, K. Prince, J. Harries, Y. Tamenori, **N. Berrah,** and K. Ueda, *Is CO C 1s Auger Electron Emission Affected by the Photoelectron?*, Phys. Rev. Lett.

J. A. Tanis, *Coincidence Techniques in Atomic Collisions*, Techniques for Highly Charged Ion Spectroscop*y*, edited by R. Hutton and Y. Zou, (Taylor and Francis Group, Boca Raton, 2009), submitted.

H. Zhang, D. Rolles, J. D. Bozek, B. Rude, **R. C. Bilodeau**, and **N. Berrah**, *Angle-Resolved Photoelectron Spectroscopy of Kr Van der Waals Clusters*, Phys. Rev. A.

8.4 Books Published

David Schuster, *Light: Inquiry and Insights.* Second Edition, Kendall/Hunt Publishing Company, Dubuque, Iowa, ISBN 0-7575-5783-5 (2007).

9 DISSERTATIONS

9.1 Ph.D

Talal Ghannam, *Quantum Properties of Light Emitted from Dipole Nano-Laser*, December 2007. Advised by **Alvin Rosenthal**.

Xue Wang, *Structure and Excitations in Metal Ammonia Compounds*, December 2007. Advised by **Clement Burns.**

9.2 Masters

Yingfa Zhang, *The Effect of a Skyrme Interaction an Nucleon Induced Reactions*, December 2007. Advised by **Dean Halderson.**

10 PRESENTATIONS

10.1 Research Talks at Professional Meetings and Other Institutions

10.1.1 Invited

N. Berrah, *Future Light Sources*, Workshop on 4th Generation Light Sources, Berkeley, CA, October 2007.

N. Berrah, *Atomic, Molecular, and Cluster Physics using Future Light Sources*, Workshop on 4th Generation Light Sources, Baton Rouge, Louisiana, January 28, 2008.

N. Berrah, *Resonances in Atoms*, Atomic Physics Symposium at Notre Dame University, April 4-5, 2008.

N. Berrah, *Gender Equity in Physics*, 2008 APS April Meeting, St Louis, MO, April 14, 2008.

N. Berrah, *Probing Cluster from Within with the ALS*, International Conference in X-Ray Processes, Paris, France, June 22-27, 2008.

N. Berrah, *Gender Equity: Strengthening the Physics Enterprise in Physics Department and National Laboratories*, Graduate College, WMU, November 9, 2007.

N. Berrah, *Cluster Physics using Light Sources*, Colloquium, Michigan State University, November 2007.

N. Berrah, *Probing Matter from Within*, Colloquium, Temple University, Philadelphia, PA, April 7, 2008.

C. A. Burns, *Next Generation Science with Inelastic X-ray Scattering*, NSLS-II Workshop, Brookhaven National Laboratory, Brookhaven, NY, July 18, 2007.

C. A. Burns, *Introduction to Inelastic X-ray Scattering*, National School for X-ray and Neutron Physics, Argonne National Laboratory, Argonne, IL, August 20, 2007.

C. A. Burns, *Electronic Interactions in a Highly Correlated Liquid Metal*, The University of Chicago Science Review Committee Meeting for the Advanced Photon Source at Argonne National Laboratory, Advanced Photon Source, Argonne National Laboratory, September 18, 2007.

C. A. Burns, *X-ray Studies of Electronic Interactions in Expanded Metals*, Physics Colloquium, Oakland University, Rochester MI, October 4, 2007.

C. A. Burns, *Electronic Interactions in the Strongly Correlated Liquid Metal Li-NH_3*, IXS Workshop, APS Users Meeting, Argonne, IL May 6, 2008.

C. A. Burns, *An Extremely High Resolution Beamline for NSLS-II – The Scientific Case,* NSLS-II EFAC Presentation, Brookhaven National Laboratory, Brookhaven New York, May 7, 2008.

S. G. Chung, *Novel Many-Body Method for Strongly Correlated Condensed Matter Systems*, at ISSP, The University of Tokyo, Tokyo, January 18, 2008.

S. G. Chung, *Novel Many-Body Method for Strongly Correlated Condensed Matter Systems*, Group Seminar of Professors, Ueda, February 5, 6, and 12, 2008.

S. G. Chung, *Novel Many-Body Method for Strongly Correlated Condensed Matter Systems,* The Yukawa Institute of Theoretical Physics, The University of Kyoto, Kyoto, February 20-21, 2008.

S. G. Chung, *Novel Many-Body Method for Strongly Correlated Condensed Matter Systems*, The Ryukyu University, Okinawa, March 5-8, 2008.

M. A. Famiano, *Current Results and Plans for Isotopic Observables of the Asymmetry Term of the Nuclear EOS,* Argonne National Laboratory, Argonne, IL, October 8, 2007.

M. A. Famiano, *Radiative Capture Cross Sections With a Tandem Accelerator*, DUSEL Town Meeting, Washington, D.C., November 2, 2007.

M. A. Famiano, *Constraining Isotopic Observables of the Asymmetry Term of the Nuclear EOS*, Gordon Research Conference on Nuclear Chemistry, June 16, 2008.

T. W. Gorczyca, *The Role of Theoretical Atomic Physics in Astrophysical Plasma Modeling,* 212th American Astronomical Society Meeting, June 2, St. Louis, MO (2008).

C. Henderson, *Problem Solving in Science: Instructional Considerations for Improving Student Learning*, Cookbook to Inquiry: Best Practices in Science and Mathematics Grades 7-12 Mini-Conference, Kalamazoo Area Mathematics and Science Center, Kalamazoo, MI, September 28, 2007.

C. **Henderson** and B. Ambrose (joint presentation), *How Can Physics Education Research Help Me Teach More Effectively?*, NSTA Physics Strand Day, Detroit, MI, October 18, 2007.

C. Henderson, *Models of Educational Change: Where are We Now and Where do We Need to go?*, Discipline-Based Educational Research Collaborative Colloquium, University of Colorado, Boulder, March 13, 2008.

C. Henderson, *Physics Education Research and Research-Based Instructional Strategies*, Action Research and Professional Development in Math, Science and Technology Education Conference, Lissgarden, Sweden, April 2, 2008.

C. Henderson, *Barriers to Instructional Change*, Action Research and Professional Development in Math, Science and Technology Education Conference, Lissgarden, Sweden, April 3, 2008.

C. Henderson, *Putting Values into Practice,* Physics Colloquium, Göteborg University, Göteborg, Sweden, April 4, 2008.

C. Henderson, A. Beach, N. Finkelstein, and R. S. Larson, *Preliminary Categorization of Literature on Promoting Change in Undergraduate STEM*, Facilitating Change in Undergraduate STEM Symposium, Augusta, MI, June 17, 2008.

A. R. McGurn, *Cavities of Crystal Light: Electronically Injected Photonic Crystal Microcavity Light Source May Realized High-Efficiency Single-Mode LED' S*, 8th Understanding Complex Symposium, University of Illinois, Urban-Champagne, May 12-15, 2008.

D. Rolles, *Size Effects in Van-der-Waals Clusters: Spin, Angle-Resolved and Imaging Studies,* International Conference on Photonic, Electronic and Atomic Collisions, ICPEAC 07, Freiburg, July 25-31, Germany.

J. A. Tanis, *Nonstatistical Enhancement of (1s2s2p) ^4P and (2p^5 3s3p) ^4D Metastable States in Electron Transfer*, Symposium at the Institute of Modern Physics, Fudan University, Shanghai, China, November 21, 2007.

J. A. Tanis, *Interferences in Coherent Electron Emission from Diatomic Molecules,* 4th Conference on Elementary Processes in Atomic Systems (CEPAS), Cluj, Romania, June 18, 2008.

A. H. Wuosmaa, *Invited Lectures on Nuclear Reactions*, at the 6th Summer School on Nuclear Physics with Exotic Beams, National Superconducting Cyclotron Laboratory, Michigan State University, E. Lansing MI, August 2007.

A. H. Wuosmaa, *Properties of ^7He from Single-nucleon Transfer Reactions* Nuclear Chemistry Symposium, American Chemical Society National Meeting, Boston MA, August 2007.

A. H. Wuosmaa, *The Structure of ^7He*, Second International Conference on the Frontiers of Nuclear Structure and Astrophysics (FINUSTAR2) Crete, Greece, September 2007.

A. H. Wuosmaa, *Nucleon Transfer Reactions with Exotic Light Nuclei*, American Chemical Society National Meeting, New Orleans LA, March 2008.

A. H. Wuosmaa, *Transfer Reactions with Exotic Beams at ATLAS*, International Workshop on Halo Nuclei HALO08, Tri-University Meson Facility (TRIUMF), Vancouver, CA, March 2008.

A. H. Wuosmaa, *Nucleon Transfer Reactions with Exotic Light Beams at ATLAS*, Nuclear Structure 2008, Michigan State University, E. Lansing MI, June 2008.

A. H. Wuosmaa, *HELIOS at ATLAS – A New Tool for Inverse-kinematic Reactions*, Nuclear Chemistry Department, Washington University at St. Louis, March 2008.

A. H. Wuosmaa, *Insights into the Structure of ^{7}He*, Heavy-Ion Discussion Group, Physics Division Argonne National Laboratory, March 2008.

10.1.2 Contributed

Sh. A. Abdel-Naby, **D. Nikolic**, **T. W. Gorczyca**, N. R. Badnell, and D. W. Savin, *Dielectronic Recombination of Al-Like Ions*, American Physical Society, 39th Annual Meeting of the Division of Atomic, Molecular, and Optical Physics, May 27-31, State College, PA, abstract #L2.00064 (2008).

Sh. A. Abdel-Naby, **M. F. Hasoglu**, **D. Nikolic**, **T. W. Gorczyca**, B. M. McLaughlin, and S. T. Manson, *X-ray Absorption in Carbon Ions Near the K-edge*, Abstracts of the 25th International Conference on Photonic, Electronic, and Atomic Collisions, Freiburg, Germany, July 25-31, 2007, abstract#Fr031.

R. Sacks, **O. Abu-Haija, G. Olmez**, and **E. Y. Kamber**, *State-Selective Single-Electron Capture in Slow Collisions of Ne^{q+} (q = 4 – 6) Ions with Molecules*, 25th International Conference on Photonic, Electronic and Atomic Collisions, Freiburg, Germany, July 25 - 31, 2007, Conference Program. Edited by Josef Anton, Robert Moshammer, Claus Dieter Schroter, and Joachim, Mo119.

L. Nagy, F. Járai-Szabó, K. Póra, **J. Baran**, and **J. A. Tanis**, *First-order Calculations for Interference Effects in the Ionization of N_2 by Fast Charged Projectiles,* XXV International Conference on Photonic, Electronic, and Atomic Collisions (ICPEAC), Freiburg, Germany, July 25-31, 2007, Conference Program, Abstracts, edited by J. Anton *et al*., Th124.

J. L. Baran, **S. Das**, F. Járai-Szabó, L. Nagy, and **J. A. Tanis**, *Secondary Interferences in Electron Emission from N_2 by Fast H^+ Impact,* XXV International Conference on Photonic, Electronic, and Atomic Collisions (ICPEAC), Freiburg, Germany, July 25-31, 2007, Conference Program, Abstracts, edited by J. Anton *et al*., Mo118.

L. F. DiMauro, J. Arthur, **N. Berrah**, J. Bozek, J. N. Galayda, and J. Hastings, *Progress Report on the LCLS XFEL at SLAC***,** J. Phys.: Conf. Ser. **88**, 012058 (2007).

D. Cubaynes, J-M. Bizau, S. Diehl, F. J. Wuilleumier, H. L. Zhou, S. T. Manson, A. Hibbert, **N. Berrah**, **S. Canton**, J. D. Bozek, E. T. Kennedy, L. Voky, and X. Y. Han, *Inner-Shell Photoionization of Sodium: A Combined Experimental and Theoretical Study*, XXV International Conference on Photonic, Electronic and Atomic Collision, Freiburg, Germany, July 25-31, 2007 (Fr016).

N. Berrah, **R. C. Bilodeau,** C. W. Walter, **I. Dumitriu**, N. D. Gibson, G. D. Ackerman, J. D. Bozek, B. S. Rude, R. Santra, and L. S. Cederbaum, *Novel Inner-Valence Mediated Electronic Decay in Molecular Anions*, 15th International Conference on Vacuum Ultraviolet Radiation Physics, p. 107, Berlin, Germany, pg. 111, (July-August 2007).

N. Berrah, *Probing Complexity Using the ALS*, 2007 AMOS DOE Workshop, Airlie Center, Warrenton VA, September 2007.

N. Berrah, *Report of the Gender Equity Workshop*, Bulletin of the American Physical Society, April meeting 2008, St Louis, MO, Volume 53, No. 5, p. 179.

R. C. Bilodeau, C. W. Walter, **I. Dumitriu,** N. D. Gibson, G. Ackerman, J. D. Bozek, B. S. Rude, R. Santra, L. S. Cederbaum, and **N. Berrah**, *Novel Inner-Valence Mediated Electronic Decay in Molecular Anions*, XXV International Conference on Photonic, Electronic and Atomic Collision, Freiburg, Germany, July 25-31, 2007 (Tu031).

R. C. Bilodeau, **N. Berrah**, **I. Dumitriu**, **O. Zatsarinny**, **T. W. Gorczyca**, J. D. Bozek, N. D. Gibson, C. W. Walter, D. Toffoli, and R. R. Lucchese, *K-shell Photodetachment of Small Size-Selected Negative Ion Clusters: Experiment and Theory*, American Physical Society, 39th Annual Meeting of the Division of Atomic, Molecular, and Optical Physics, May 27-31, State College, PA, abstract #L2.00027 (2008).

R. Bilodeau, **I. Dumitriu**, D. Gibson**,** W. Walter**, T. Gorczyca**, **O. Zatzirini**, and **N. Berrah**, *K-Shell Photodetachment of Small Size-Selected Negative Ion Clusters: Experiment and Theory*, 39th Annual Meeting of the APS Division of Atomic, Molecular, and Optical Physics, May 27–31, 2008; State College, Pennsylvania.

C. A. Burns, C. N. Kodituwakku, A. Said, P. M. Platzman, A. C. Clark, J. T. West, M. H. W. Chan, L. B. Lurio, and N. Mulders, in Abstracts of the QFS'07 Symposium, Kazan, 1–6 August (2007), p. 82.

J. West, M. H. W. Chan, N. Mulders, C. N. Kodituwakku, **C. A. Burns**, and L. B. Lurio, *Torsional Oscillator and Synchrotron X-ray Experiments on Solid Helium in Aerogel*, APS March Meeting, New Orleans, LA, March 11, 2008.

S. Das, **B. S. Dassanayake**, **M. Winkworth**, **J. L. Baran**, N. Stolterfoht, and **J.A. Tanis**, *Inelastic Electron Guiding through Insulating Nanocapillaries,* XXV International Conference on Photonic, Electronic, and Atomic Collisions (ICPEAC), Freiburg, Germany, July 25-31, 2007, Conference Program, Abstracts, edited by J. Anton *et al*., We163.

S. Das, **B. S. Dassanayake**, N. Stolterfoht, and **J. A. Tanis**, *Inelastic Processes Associated with Electron Guiding through Insulating PET Nanocapillaries,* Pan American Advanced Studies Institute (PASI): Ultrafast and Ultrasmall; New Frontiers in AMO Physics, Buzios, Brazil, April 2008.

B. S. Dassanayake, **S. Das**, **M. Winkworth**, **J. L. Baran**, N. Stolterfoht, and **J. A. Tanis**, *Electron Guiding in Insulating Polymer Nanocapillaries,* XXV International Conference on Photonic, Electronic, and Atomic Collisions (ICPEAC), Freiburg, Germany, July 25-31, 2007, Conference Program, Abstracts, edited by J. Anton *et al*., We162.

B. S. Dassanayake, **S. Das**, N. Stolterfoht, and **J. A. Tanis**, *Guiding of Electrons through Insulating PET Nanocapillaries,* Pan American Advanced Studies Institute (PASI): Ultrafast and Ultrasmall; New Frontiers in AMO Physics, Buzios, Brazil, April 2008.

I. Dumitriu, **R. C. Bilodeau**, **T. W. Gorczyca**, C. W. Walter, N. D. Gibson, A. Aguilar, **Z. Pešić**, **D. Rolles**, **N. Berrah**, *Inner-Shell Photodetachment of Iron and Ruthenium Negative Ions*, American Physical Society, 39th Annual Meeting of the Division of Atomic, Molecular, and Optical Physics, May 27-31, State College, PA, abstract #I6.00004 (2008).

I. Dumitriu, **R. Bilodeau**, D. Gibson, W. Walter, and **N. Berrah**, I*nner-Shell Photodetachment of Iron and Ruthenium Negative Ions*, 39th Annual Meeting of the APS Division of Atomic, Molecular, and Optical Physics, State College, Pennsylvania, May 27–31, 2008.

M. A. Famiano, *Reactions Experiments at the NSCL*, NSCL User Workshop, August 16, 2007.

M. A. Famiano, *Current Results and Plans for Isotopic Observables of the Asymmetry Term of the Nuclear EOS*, 234th ACS National Meeting, Boston, MA, August 19, 2007.

M. A. Famiano, *Isotopic Observables of the High Density EOS*, TPC Workshop at the NSCL, East Lansing, MI , December 6-7, 2007.

N. J. Goodman, **J. Bos**, **J. C. Lighthall**, **S. T. Marley**, **J. Snyder**, **A. H. Wuosmaa**, C. Tur, Sam M. Austin, E. Estrada, and G. Lorusso, *New Measurement of $\Gamma_{\pi\Gamma}$ for the 0^+_2 (7.65 MeV) State in ^{12}C*, 2007 Division of Nuclear Physics Meeting of the American Physical Society, Newport News, VA, October 2007.

Hye Young Lee, M. Notani, K. E. Rehm, J. P. Greene, D. Henderson, R. V. F. Janssens, C.-L. Jiang, R. C. Pardo, J. P. Schiffer, **N. J. Goodman**, **J. C. Lighthall**, **S. T. Marley**, A**. Wuosmaa**, L. J. Jisonna , R. E. Segel, N. Patel, M. Paul, and X. D. Tang, *Rp-Process and r-Process Studies with Radioactive Beams at ATLAS*, 2007 Division of Nuclear Physics Meeting of the American Physical Society, Newport News, VA, October 2007

T. W. Gorczyca, **M. F. Hasoglu**, **D. Nikolic**, B. M. McLaughlin, M. H. Chen, S. T. Manson, and N. R. Badnell, *Production and Decay of Atomic K-shell Vacancy States*, 212th American Astronomical Society Meeting, June 1-5, St. Louis, MO, abstract #03.09 (2008).

M. F. Hasoglu, **D. Nikolic**, **T. W. Gorczyca**, S. T. Manson, N. R. Badnell, and D. W. Savin, *K-Shell Fluorescence Yields of Li- to F-like Ions*, Abstracts of the 25th International Conference on Photonic, Electronic, and Atomic Collisions, Freiburg, Germany, July 25-31, 2007, abstract#Fr130.

M. F. Hasoglu, **D. Nikolic**, **T. W. Gorczyca**, B. M. McLaughlin, M. H. Chen, S. T. Manson, and N. R. Badnell, *Production and Decay of K-shell Vacancy States*, Southeast Laboratory Astrophysics Community Workshop, February 25-30, Auburn, AL, abstract #P11 (2008).

M. F. Hasoglu, **D. Nikolic**, **T. W. Gorczyca**, M. H. Chen, and N. R. Badnell, *Anomalous Behavior of Auger and Radiative Rates and Fluorescence Yields Along the $1s2s^22p^3$ K-Shell Isoelectronic Sequence*, American Physical Society, 39th Annual Meeting of the Division of Atomic, Molecular, and Optical Physics, May 27-31, State College, PA, abstract #R1.00016 (2008).

C. Henderson, Evaluation of the Physics and Astronomy New Faculty Workshop, AAPT 2007 Summer Meeting, Greensboro, NC, July 30, 2007.

E. Brewe, M. Dancy, and **C. Henderson**, *Toward More Effective Dissemination: Lessons From the Modeling Physics Project*, AAPT 2007 Summer Meeting, Greensboro, NC, July 31, 2007.

N. Finkelstein, **C. Henderson**, A. Beach, and R. S. Larson, *Facilitating Change in STEM Education: A Research-Based Perspective on Initiating and Sustaining Change*, AAPT 2008 Winter Meeting, Baltimore, MD, January 22, 2008.

N. Finkelstein, **C. Henderson**, A. Beach, and R. S. Larson, *Considering Change in STEM Education: A Research-Based Perspective on Initiating and Sustaining Change*, Physics Teachers Education Coalition National Meeting, Austin, TX, February 29, 2008.

H. Fynewever, **C. Henderson**, S. Barry, S. Erwin, S. Hanson, M. Huber, M. Lindow, and K. Mirakovits, *Evaluating What Teachers Do Outside the Classroom*, National Science Teachers Association National Conference, Boston, MA, March 28, 2008.

A. Beach and **C. Henderson**, *Identifying Connections within the Literature on STEM Instructional Change Using a Historiographic Approach,* Facilitating Change in Undergraduate STEM Symposium, Augusta, MI, June 17, 2008.

M. Dancy and **C. Henderson**, *Barriers to the use of Research-Based Instructional Strategies: The Influence of Both Individual and Situational Characteristics*, Facilitating Change in Undergraduate STEM Symposium, Augusta, MI, June 17, 2008.

C. Henderson and M. Dancy, *Science Faculty and Educational Researchers: Divergent Expectations as Barriers to Instructional Change*, Facilitating Change in Undergraduate STEM symposium, Augusta, MI, June 17, 2008.

J. Froyd, **C. Henderson**, J. Layne, N. Finkelstein, A. Beach, and R. S. Larson, *More Than Good Curricula: A Guide For Curricular Change Agents*, American Society for Engineering Education Annual Conference, Pittsburg, PA, June 23, 2008.

E. Y. Kamber, *Non-Dissociative Single-Electron Capture in Slow Collisions of O_2^{2+} Ions with O_2, Ar, and Ne,* 25th International Conference on Photonic, Electronic and Atomic Collisions (ICPEAC), Freiburg, Germany, July 25 - 31, 2007, Conference Program, edited by Josef Anton, Robert Moshammer, Claus Dieter Schroter, and Joachim, Th130.

W. Priyantha, H. Chen, M. Kopczyk, A. Comouth, M. Finsterbusch, **A. Kayani**, D. Tonn, R. J. Smith, D. McCready, and P. Nachimuthu, *Ti as an Interface Stabilizer for Fe-Al Interfaces,* American Vacuum Society, Seattle, WA, October 15, 2007.

Scott Marley, **N. J. Goodman**, **J. C. Lighthall**, **A .H. Wuosmaa**, C. L. Jiang M. Notani R.C. Pardo K. E. Rehm J. P. Schiffer X. D. Tang, and L. Jisonna, *Study of the $^3He(^{14}O, \alpha)^{13}O$ Reaction,* 2007 Division of Nuclear Physics Meeting of the American Physical Society, Newport News, VA, October 2007.

D. Nikolic, **Sh. A. Abdel-Naby**, **T. W. Gorczyca**, N. R. Badnell, and D. W. Savin, *Dielectronic Recombination of Al- and Ar-Like Ions*, Abstracts of the 25th International Conference on Photonic, Electronic, and Atomic Collisions, Freiburg, Germany, July 25-31, 2007, abstract#We109.

Wai-Kwong Kwok, Ulrich Welp, John Schlueter, Ruobing Xie, Jiong Hua, Zhili Xiao, **L. M. Paulius**, and Morten R. Eskildsen, *Competition of Point and Correlated Vortex Pinning in Irradiated YBCO*, Bulletin of the American Physical Society 53, J10.00005 (2008).

R. Xie, A. Rydh, U. Welp, W.-K. Kwok, M. R. Eskildsen, and **L. M. Paulius**, *Evolution of Vortex Phase Diagram in Heavy Ion Irradiated YBCO*, Bulletin of the American Physical Society 53, J10.00003 (2008).

Andra Petrean-Troncalli, **Lisa Paulius**, Heather Quantz, Valentina Tobos, and Wai -K Kwok, *Investigation of Vortex Pinning Anisotropy in the High Temperature Superconductor $YBa_2Cu_3O_{7-\delta}$*, Bulletin of the American Physical Society 53, D11.00012 (2008).

Z. Pešić,, D. Rolles, R. C. Bilodeau, I Dumitriu, A. L. D. Kilcoyne, and **N. Berrah,** *Photofragmentation of Molecules Studied by Multi-Coincidence Imaging*, XXV International Conference on Photonic, Electronic and Atomic Collision, Freiburg, Germany, July 25-31, 2007 (We039).

D. Rolles, H. Zhang, Z. D. Pešić, **R. C. Bilodeau, A. A. Wills**, E. Kukk, B. Rude, J. D. Bozek, R. Diez Muino, F. G. Garcia de Abajo and **N. Berrah,** *Angle-Resolved Photoelectron Spectroscopy of Free Rare Gas Clusters*, XXV International Conference on Photonic, Electronic and Atomic Collision, Freiburg, Germany, July 25-31, 2007 (We055).

D. Rolles, Z. Pešić,, H. Zhang, R. C. Bilodeau, J. D. Bozek, and **N. Berrah**, *Fragmentation of Rare Gas Clusters Subsequent to Vuv-Photoionization*, XXV International Conference on Photonic, Electronic and Atomic Collision, Freiburg, Germany, July 25-31, 2007 (We057).

E. Kukk, **D. Rolles, H. Zhang, A. Wills, R. Bilodeau**, B. Rude, G. Ackerman, J. Bozek R. Diez Muino, F. J. Garcia, and **N. Berrah**, *Size Effects in Angle Resolved Photoelectron Spectroscopy of Rare Gas Clusters*, 15th International Conference on Vacuum Ultraviolet Radiation Physics, p. 78, Berlin, Germany, (July 2007).

D. Rolles, Z. D. Pešić, M. Perri, R. Bilodeau, G. Ackerman, B. Rude, D. Kilcoyne, J. D. Bozek, and **N. Berrah,** *Photofragmentation of Rare Gas Clusters Studied by Multi-Coincidence Imaging*, 15th International Conference on Vacuum Ultraviolet Radiation Physics, p. 107, Berlin, Germany, pg. 112, (July-August 2007).

D. Rolles, Z. Pešić, H. Zhang, R. Bilodeau, M. Hoener, J. Bozek and **N. Berrah**, *Probing Rare Gas Clusters from Within*, p. 54., 21st International Conference on X-ray and Inner-shell Processes, June 22-27, 2008, Paris, France.

Adriana Undreiu, **David Schuster**, and **Betty Adams**, *Multiple Modes of Reasoning in Physics Problem Solving,* American Association of Physics Teachers meeting, Greensboro, NC, July 28-Aug 1, 2007.

David Schuster, Adriana Undreiu, **Betty Adams**, and Eric Arsznov, *From Motion Diagrams to Motion Graphs,* Michigan Section of the American Association of Physics Teachers, April 12, 2008.

David Schuster, *Stump the Professor: Wondering about Wheelchairs,* Michigan Section of the American Association of Physics Teachers, April 12, 2008.

Adriana Undreiu, **David Schuster, Betty Adams,** and **Philip Kaldon**, *Motion Matching: A Challenge Game to Generate Motion Descriptor Concepts,* Michigan Section of the American Association of Physics Teachers, April 12, 2008.

D. Strohschein-Lovett, **J. Baran**, and **J. A. Tanis**, *Enhancement of the 1s2s2p ^4P State in Electron Transfer to $C^{4,5+}$ Ions,* XXV International Conference on Photonic, Electronic, and Atomic Collisions (ICPEAC), Freiburg, Germany, 25-31 July 2007, Conference Program, Abstracts, edited by J. Anton *et al*., We145.

J. A. Tanis, *Interferences in Coherent Electron Emission from Diatomic Molecules,* 4th Conference on Elementary Processes in Atomic Systems (CEPAS), Cluj, Romania, June 2008, Book of Abstracts, edited by K. Póra, V. Chiş, and L. Nagy, p. 30.

F. Frémont, A. Hajaji, A. Naja, C. Leclercq, J. Soret, **J. A. Tanis**, B. Sulik and J.-Y. Chesnel, *Fast Oscillating Structures in Electron Spectra Following Slow He^{q+} + He Collisions: Search for Electron Interferences,* 4th Conference on Elementary Processes in Atomic Systems (CEPAS), Cluj, Romania, June 2008, Book of Abstracts, edited by K. Póra, V. Chiş, and L. Nagy, p. 31.

G. Turri, B. Lohmann, B. Langer, G. Snell, U. Becker and **N. Berrah,** *Spin Polarization of the Ar^* $2p^{-1}_{1/2}4s$, and $2p^{-1}_{1/2}3d$ Auger Decay,* 15th International Conference on Vacuum Ultraviolet Radiation Physics, p. 107, Berlin, Germany, July-August (2007).

E. Sokell, **A. A. Wills, M. Wiedenhoeft, X. Feng, D. Rolles**, and **N. Berrah**, *Inner-Shell Photoionization of Molecules using a Two-Dimensional Imaging Technique*, XXV International Conference on Photonic, Electronic and Atomic Collision, Freiburg, Germany, July 25-31, 2007 (We027).

M. Winkworth, P. D. Fainstein, M. E. Galassi, **J. Baran**, **B. S. Dassanayakea**, **S. Das**, **T. Elkafrawy**, **D. Cassidy**, **A. Kayani**, and **J. A. Tanis**, *Interfererces in Electron Emission from O_2 by 30 MeV O^{q+} Impact*, 4th Conference on Elementary Processes in Atomic Systems, Cluj-Napoca, Romania, June 18, 2008**.**

M. Winkworth, **J. L. Baran**, **B. S. Dassanayake**, **S. Das**, and **J. A. Tanis**, *Interference Effects in Electron Emission from 30 MeV O^{8+} + O_2 Collisions,* XXV International Conference on Photonic, Electronic, and Atomic Collisions (ICPEAC), Freiburg, Germany, 25-31 July 2007, Conference Program, Abstracts, edited by J. Anton *et al*., Mo117.

M. Winkworth, P. D. Fainstein, M. E. Galassi, **J. Baran**, **B. S. Dassanayake**, **S. Das**, **T. Elkafrawy**, **D. Cassidy**, **A. Kayani** and **J. A. Tanis**, *Interferences in Electron Emission from O_2 by 30 MeV O^{q+} Impact,* 4th Conference on Elementary Processes in Atomic Systems (CEPAS), Cluj, Romania, June 2008, Book of Abstracts, edited by K. Póra, V. Chiş, and L. Nagy, p. 136.

K. E. Rehm, X. D. Tang, M. Carpenter, J. P. Greene, R. V. F. Janssens, L. Jisonna, C. L. Jiang, C. J. Lister, M. Notani, N. Patel, R. C. Pardo, G. Savard, J. P. Schiffer, R. E. Segel, **A. Wuosmaa**, and S. Zhu, *The Branching Ratio of the Sub-Threshold 1^- State in the Beta-Decay of ^{16}N*, 2007 Division of Nuclear Physics Meeting of the American Physical Society, Newport News, VA, October 2007.

A. H. Wuosmaa, **J. C. Lighthall**, **S. T. Marley**, J. P. Schiffer, C. L. Jiang, H. Y. Lee, M. Notani, R. C. Pardo, K. E. Rehm, I. Tanihata, X. D. Tang, and N. Patel, *Identifying Spins and Configurations of States in ^{13}B*, 2007 Division of Nuclear Physics Meeting of the American Physical Society, Newport News, VA, October 2007.

H. Zhang, D. Rolles, Z. D. Pešić, J. D. Bozek, and **N. Berrah**, *Study of Photoionization of Rare Gas Clusters*, AAPT, American Association of Physics Teachers, March 2008, Kalamazoo, MI.

H. Zhang, **D. Rolles**, **Z. Pesic**, J. Bozek and **N. Berrah**, *Photoionization of Variable-Size Rare Gas Clusters*, 39th Annual Meeting of the APS Division of Atomic, Molecular, and Optical Physics**,** May 27–31, 2008, State College, Pennsylvania.

10.2 Research and Public Lectures at WMU

The Department of Physics sponsors lectures on physics research intended mainly for graduate students and faculty. These talks inform faculty and students at Western of research efforts here and at other institutions as well as acquaint visiting speakers with our research and academic programs at Western. The Department of Physics also sponsors public lectures on physics topics of general interest. These talks are intended for faculty, physics graduate students, physics undergraduate students, and non-physicists. The research and public lectures are listed below.

Novel Many-Body Method in Statistical Mechanics and Strongly Correlated Condensed Matter Systems, **Sung G. Chung**, Department of Physics, Western Michigan University, September 10, 2007.

The Precise Implementation of Cluster Transfer Matrix Method in Single Electron Box, **Lihua Wang**, Department of Physics, Western Michigan University, September 17, 2007.

Applications of Ion Beam Analysis to Materials Characterization for Solid Oxide Fuel Cells, R. J. Smith, Physics Department, Montana State University, Bozeman, MT, September 19, 2007.

Superconducting Vortices in Cecoin5: Beyond the Abrikosov-Ginzburg-Landau Paradigm, Morten Ring Eskildsen, University of Notre Dame, September 24, 2007.

Smashed Atoms Tamed - Thermalized Rare Isotope Beams from Projectile Fragmentation for Mass Measurements and Other Precision Experiments, Georg Bollen, National Superconducting Cyclotron Laboratory, Michigan State University, October 1, 2007.

Shell Evolution and Structure of Exotic Nuclei in the sd-pf Shell Region, Utsuno Yutaka, Japan Atomic Energy Research Institute, October 8, 2007.

Educational Outreach in Physics, Elizabeth Simmons, Michigan State University, October 15, 2007.

Solar UV-B Radiation: Measurements, Models and Effects, James R. Slusser, IUVB Radiation Monitoring and Research Program, Natural Resource Ecology Laboratory, Colorado State University, October 19, 2007.

Big-Bang and Stellar Nucleosynthesis Studied in the Laboratory, Fred Becchetti, University of Michigan, October 22, 2007.

Simple Atoms, Extreme Nuclei – From Precision Atomic Physics to Exotic Nuclear Structure, Peter Mueller, Argonne National Laboratory, October 29, 2007.

Strong Isotope Effects on Charge Transfer in Slow Collisions of He^{2+} with Atomic Hydrogen, Deuterium, and Tritium, N. Stolterfoht, Hahn-Meitner-Institut Berlin, Germany, October 30, 2007.

Probing Magnetism using Synchrotron Radiation, Jonathan Lang, Argonne National Laboratory, November 5, 2007.

Network-Based Manipulation of Complex Systems, Adilson E. Motter, Northwestern University, November 12, 2007.

Thermal Lens Shaping: A New Modality for Diode-Pumped Solid-State Lasers, W. Andreas Schroeder, Department of Physics, University of Illinois at Chicago, November 19, 2007.

Experimental Tests of Extra Dimensions and String Theory, Rolf Schimmrigk, Indiana University South Bend, November 26, 2007.

Acoustic Birefringence in Superfluid ^3He, William P. Halperin, Department of Physics, Northwestern University, December 3, 2007.

Quasars and the Birth and Evolution of Galaxies, **Kirk Korista**, Department of Physics, Western Michigan University, January14, 2008.

The Geek Group: Like Willy Wonka with High Voltage, Chris Boden, The Geek Group, January 28, 2008.

Gas Phase Physics and the Evolution of Galaxies, J. Christopher Howk, Department of Physics, University of Notre Dame, February 4, 2008.

The Mars Exploration Rover Mission, Ray Arvidson, Washington University in St. Louis, February 11, 2008.

The Fascinating World of Exotic Nuclei, Werner Richter, University of the Western Cape, South Africa, February 13, 2008.

Predicting the Properties of Atomic Clusters when Every Atom Counts, Koblar Alan Jackson, Department of Physics, Central Michigan University, February 18, 2008.

The Tevatron and the CDF Experiment – A Year in Review, Robert Roser, Fermi National Accelerator Laboratory, February 25, 2008.

Spartan Infrared Camera, High Resolution Imaging for the Soar Telescope, Ed Loh, Department of Physics and Astronomy, Michigan State University, March 10, 2008.

Magnetic Measurements of Electrodeposited Thin Films and Multilayers, Jennifer Hampton, Hope College, March 17, 2008.

Reflections of AGN Outbursts in the Hot Gas in Galaxies and Clusters, Christine Jones, Center for Astrophysics, Harvard University, March 24, 2008.

Reflections from Outbursts of Supermassive Black Holes at the Centers of Galaxies, Christine Jones, Center for Astrophysics, Harvard University, March 25, 2008.

Using X-rays to Probe Biomolecular Interfaces, Andrew Richter, Valparaiso University, March 31, 2008.

The Role of Language in Learning Physics, David Brookes, Postdoctoral Research Associate, Illinois Physics Education Research Group, University of Illinois at Urbana-Champaign, April 7, 2008.

Hans Bethe – Master Calculator and Gentleman of Science, Robert Manweiler, Valparaiso University, April 14, 2008.

11 PROPOSALS AND GRANTS

N. Berrah (PI)**,** Department of Energy, Office of Science, BES, Division of Chemical Sciences, Geosciences and Biosciences grant. Project title: *Probing Complexity using the ALS and the LCLS*, funded $590,000 for period March 2008-2011.

N. Berrah, Advanced Light Source Support toward a postdoctoral fellow Rene Bilodeau, awarded $12,000 for 2007-2008.

N. Berrah (Co-PI), and Subra Mural (Co-PI), WMU Chemistry Department, Presidential Innovation Fund, WMU to establish a Center for Nano-Enabled Instrumentation and Nanofabrication (CNIN), awarded $383,000, for the period 03/06-02/08.

N. Berrah (PI), Artie Bienenstock, Stanford University and Judy Franz, APS (Co-PIs), *Gender Equity: Strengthening the Physics Enterprise in Physics Departments and National Laboratories*, NSF, awarded $90,000 for the period 2006-2008.

N. Berrah (PI), Artie Bienenstock, Stanford University and Judy Franz, APS (Co-PIs), *Gender Equity: Strengthening the Physics Enterprise in Physics Departments and National Laboratories*, DOE, Office of Science, awarded $90,000 for the period 2006-2008.

N. Berrah (PI), *Gender Equity: Strengthening the Physics Enterprise in Physics Departments and National Laboratories*, NSF and DOE funded, supplement, $10,000 for Fall 2007.

N. Berrah (PI), applied for 12% of beamtime, every six months, for three years on undulator beamline 10.0.1 of the Advanced Light Source, Lawrence Berkeley National Laboratory, CA, beamtime to carry out research experiments was granted for 2008-2011.

N. Berrah (PI), applied for beamtime at a higher energy undulator beamline, (8.0.1) at the Advanced Light Source, beamtime granted for 3 weeks (2007-2008).

N. Berrah (PI), NSF, Project title: *PROMISE: Providing Resources, Opportunities, and Mentoring In Science and Engineering for Women Faculty at Western Michigan University*, $3,912,516 requested, not funded.

S. Chung, National Science Foundation, *Entanglement Perturbation Theory for Strongly Correlated Condensed Matter Systems*, requested $499,502, not awarded.

S. Chung, National Science Foundation SU of Teragrid Cobalt Supercomputer at the University of Illinois at Urbana-Champaign, *A Novel, Many-Body Method in Condensed Matter Physics*, awarded $10,000 to February 28, 2009.

M. A. Famiano, *Characterization of the Density Dependence of the Asymmetry Term of the Nuclear EOS*, submitted to NSF Program 06-632, NSF Physical Sciences, awarded $119,365, for period of May 2008 - April 2011.

M. A. Famiano, *U.S. -Japan Cooperative Agreements: Mass Measurements of rp-Process Nuclei Near the Proton Drip Line*, award $18,056, for period of 9/1/2007–8/31/2009.

T. W. Gorczyca (PI), NASA Solar and Heliospheric Research and Technology Program, for project entitled *Calculations of High Temperature Dielectronic Recombination Rate Coefficients in Support of NASA's Sun-Earth Connection Program*, funded $461,693 for period 2/1/2005-1/31/2008.

T. W. Gorczyca (PI), NASA Solar and Heliospheric Research and Technology Program, for project entitled *Calculations of High Temperature Dielectronic Recombination Rate Coefficients in Support of NASA's Sun-Earth Connection Program*, awarded an additional $20,000 in close-out funds for period 3/1/2008-2/28/2009.

T. W. Gorczyca (PI) and K. T. Korista, NASA Astrophysics Research and Analysis Program, for project entitled *Improved Simulations of Astrophysical Plasmas: Computation of New Atomic Data*, funded $369,999 for period 4/1/2007-3/31/2010.

H. Fynewever (PI), **C. Henderson** and H. Petcovic**, (**Co-P Is), *Alignment of Secondary Science Teacher Practice and Materials in the Battle Creek Region*, Michigan Department of Education, awarded $215,287 for the period 9/1/07 to 6/30/09.

C. Henderson (PI) and M. Dancy, (Co-PI), *Understanding Instructor Practices and Attitudes Towards the Use of Research-Based Instructional Strategies In Introductory College Physics*, National Science Foundation, $331,143 awarded for the period 1/1/08 to 12/31/10.

A. Beach (PI), **C. Henderson** and N. Finkelstein, (Co-PIs), *STEM Educational Change Efforts in Higher Education: A Meta-Synthesis of Activities, Strategies, Concepts, and Theories across Disciplines*, National Science Foundation, $198,379 awarded for the period 9/15/07 to 9/14/09.

C. Henderson (PI), H. Fynewever, S. Lentz, and H. Petcovic, (Co-PIs), *Rethinking the Science Ph.D. as Preparation for a Community College Science Teaching Career: An Empirical Research and Evaluation Project*, National Science Foundation, submitted 1/29/07 $787,377, not funded.

A. N. Kayani (PI), **M. A. Famiano** (co-PI), **E. Y. Kamber** (co-PI), **J. A. Tanis** (co-PI), and **A. H. Wuosmaa** (co-PI), *MRI: Equipment Acquisition for WMU Accelerator Lab Upgrade*, National Science Foundation – Major Research Instrumentation program, requested $284,101, declined.

D. Schuster (PI), W. Cobern, R. Schwartz, P. Vellom, *Assessing Pedagogical Content Knowledge of Inquiry Science Teaching,* National Science Foundation, awarded $440,000 for the period 2006-2010.

David Schuster (PI), Paul Vellom and **Charles Henderson**, *Integrated Apprenticeship in the Teaching of Elementary Science (IATES),* National Science Foundation, awarded $200,000 for the period 2006-2009.

W. Cobern (PI), **D. Schuster**, B. Applegate, R. Schwartz. *An Experimental Efficacy Study of Science Achievement and Attitude Development amongst 8th grade students Using an Inquiry, Integrated Science-mathematics-engineering Model of Instruction,* National Science Foundation, awarded $1,900,000 for the period 2005-2009.

J. A. Tanis (PI), *Travel Grant for US-Based Student and Postdoctoral Participants to Attend ICPEAC XXV*, National Science Foundation – Atomic and Molecular Dynamics Program, awarded $7500 for the period 06/15/07-05/31/08.

J. A. Tanis, *Visiting Lecturer/Researcher*, Institute of Modern Physics, Applied Ion Beam Physics Laboratory, Fudan University, Shanghai (China), awarded $7,500 for two visits of one month duration each during the period 11/01/07-12/30/08.

J. A. Tanis (PI), *Guiding of Fast Electrons and Positive Ions in Nanocapillaries*, Research Corporation, awarded $50,000 (sponsor) + $25,000 (required matching) for the period 6/30/07-06/29/09.

J. A. Tanis (PI), *Transmission and Scattering of Electrons and Ions in Nanocapillaries*, U.S. Department of Energy, BES-Materials Science and Engineering, requested: $640,282 for the period 06/01/08-05/31/11, declined.

J. A. Tanis (PI) and C. Whelan (co-PI), *Collaborative Research: Atomic Collision Physics at Extreme Velocities and Field Strengths*, National Science Foundation – Atomic and Molecular Physics program, requested $544,815 for the period 06/01/08-05/31/011.

A. H. Wuosmaa (PI), Department of Energy Office of Nuclear Physics, *Study of Exotic Light Nuclei with Few Nucleon Transfer Reactions*, awarded $440,000 over three-year period 5/15/07-5/14/10.

A. H. Wuosmaa (PI), Argonne National Laboratory, *Research in Nuclear Physics*, awarded $8,000 for the period 7/1/07-12/31/07.

A. H. Wuosmaa (PI), Argonne National Laboratory, *Research in Nuclear Physics*, awarded $14,841 for the period 9/1/07-12/31/07.

12 SCHOLARLY ACTIVITY

N. Berrah, member, Basic Energy Science Advisory Committee (BESAC) for the Office of Science, U. S. Department of Energy, 2002-2011.

N. Berrah, member, ALS, LBNL, UC, Berkeley, Science Advisory Committee (SAC), 2007-2010.

N. Berrah, member, SSRL, SLAC, Stanford University, Science Advisory Committee (SAC), 2006-2009.

N. Berrah, co-team leader (with Lou Dimauro), for Atomic and Molecular Science at the femtosecond Linac Coherent Light Source (LCLS) at SLAC, Stanford, CA, 2004-present.

N. Berrah, chair, Local Committee, International Conference on Photonic, Electronic, and Atomic Collisions, ICPEAC09.

N. Berrah, member, Executive Committee, International Conference on Photonic, Electronic, and Atomic Collisions, 2005-2009.

N. Berrah, chair, Committee of the Status of Women in Physics, CSWP, 2007-2008.

N. Berrah, chair, Davisson-Germer Prize, American Physical Society, 2007.

N. Berrah, member, APS, DAMOP, Nominating Committee, 2008-2010.

N. Berrah, member, Executive Committee of the Division of Atomic, Molecular, and Optical Physics (DAMOP) of the American Physical Society, 2005-2008.

N. Berrah, member, Executive Committee of the APS Topical Group on Few-Body Physics (GFB).

N. Berrah, member, committee of the International Conference in X-Ray and Inner-Shell Processes, 2005-2008.

N. Berrah, member, review committee of the FOCUS NSF Laser Center, University of Michigan, 2007-2009.

C. Burns, reviewed 2 papers for Physical Review B (2008).

C. Burns, member of Executive Board for Inelastic X-ray Scattering Collaborative Development Team (IXS-CDT).

C. Burns, member of Beamline Advisory Committee for Sector 30, Advanced Photon Source, Argonne National Laboratory.

C. Burns, chair of the Beamline Advisory Team (BAT) for the Ultra-high Resolution Inelastic X-ray Scattering Beamline under construction at NSLS-II, Brookhaven, NY.

C. Burns, co-organizer of the Workshop on Inelastic X-ray Scattering at NSLS-II, Feb. 7-8, 2008, Brookhaven National Laboratory, Upton, NY.

C. Burns, book reviewer for the American Association for the Advancement of Science.

S. Chung, refereed 3 papers for Nanotechnology, 3 papers for Journal of Physics Condensed Matter, 1 paper for Physics Letters A, and 1 National Science Foundation proposal.

M. A. Famiano, reviewed 2 DOE grant proposals.

M. A. Famiano, refereed for Proceedings of Science.

M. A. Famiano, member of the Michitoshi Soga Japan Center Faculty Advisory Committee, May 2007 - Present.

T. W. Gorczyca, reviewed two manuscripts for Physical Review Letters and one manuscript for Journal of Physics B.

T. W. Gorczyca, served on a 2-day panel review for the NASA Solar and Heliospheric Research and Technology Program (4/08 in Washington, D. C.).

T. W. Gorczyca, member Executive Committee for the International Conference on Photonic, Electronic, and Atomic Collisions (ICPEAC), July 2007-2009.

T. W. Gorczyca, co-chair, Local Committee, International Conference on Photonic, Electronics and Atomic Collisions, ICPEAC 2009.

C. Henderson, refereed 7 papers for i) Proceedings, Physics Education Research Conference; ii) The Physics Teacher; iii) Journal of Science Teacher Education; iv) Journal of Engineering Education; v) American Physical Review - Special Topics: Physics Education Research.

C. Henderson, reviewed 22 grant proposals for i) National Science Foundation; ii) US Department of Education, Fund for the Improvement of Post Secondary Education (FIPSE); iii) National Research Foundation, International Science Cooperation Grants (Swedish Research Collaboration Programme)

C. Henderson, chair, American Association of Physics Teachers Committee on Research in Physics Education.

C. Henderson, president, Michigan Chapter of the American Association of Physics Teachers.

C. Henderson, member, Physics Education Research Leadership and Organizing Council.

C. Henderson, co-editor, Proceedings of the Annual Physics Education Research Conference.

C. Henderson, external evaluator, Physics and Astronomy New Faculty Workshop.

E. Y. Kamber, reviewed two papers for Physical Review A.

E. Y. Kamber, member, Executive Committee for the International Conference on Photonic, Electronic, and Atomic Collisions (ICPEAC), July 2007-2009.

E. Y. Kamber, co-chair, Local Committee, International Conference on Photonic, Electronics and Atomic Collisions, ICPEAC 2009.

A. R. McGurn, elected a Fellow of the Optical Society of America.

A. R. McGurn, citied by the American Physical Society as an Outstanding Referee of the American Phyical Society.

A. R. McGurn, awarded the distinguished Faculty Scholar Award at Western Michigan University.

L. M. Paulius, refereed 4 proposals for the National Science Foundation and 1 proposal for the Research Corporation.

D. Schuster, Referee for Physics Education Research Conference proposals and papers.

D. Schuster, Referee for the National Association for Research in Science Teaching proposals and papers.

D. Schuster, Physics textbook reviewer for John Wiley & Sons.

J. A. Tanis, selected as one of the inaugural group of 534 Outstanding Referees by the American Physical Society.

J. A. Tanis, refereed 2 papers for Physical Review Letters, 2 papers for Physical Review A, and 2 papers for Nuclear Instruments and Methods in Physics Research.

J. A. Tanis, served as *ad hoc* Divisional Associate Editor for Physical Review Letters.

J. A. Tanis, chair, Local Committee, XXVI International Conference on Photonic, Electronic, and Atomic Collisions (ICPEAC) to be held in Kalamazoo, July 22-28, 2009.

J. A. Tanis, member, Executive Committee, International Conference on Photonic, Electronic, and Atomic Collisions (ICPEAC), 2003-11.

J. A. Tanis, member, International Scientific Committee, International Conference on X-ray and Inner Shell Processes, 2002-08.

J. A. Tanis, member, International Advisory Committee, 20th International Symposium on Ion-Atom Collisions (XX ISIAC), Crete, Greece, 2005-07.

A. H. Wuosmaa, reviewed 4 articles for *Physical Review C*, 2 articles for *Physics Letters B*, 1 article for *Physical Review Letters*.

A. H. Wuosmaa reviewed 2 DOE Phase I SBIR/STTR grant proposals, 1 DOE Phase II SBIR/STTR grant proposal, 2 proposals for the UK Science and Technologies Facilities Council, 1 proposal for the South African National Research Foundation.

A. H. Wuosmaa, served on Review Panel of DOE visiting committee for the Texas A&M University Cyclotron upgrade project.

A. H. Wuosmaa, served on Review Panel of DOE visiting committee for the Holifield Rare Isotope Beam Facility (HRIBF) Scientific and Technical Review.

A. H. Wuosmaa WMU representative to Central States Universities Incorporated, Secretary and Board Member.

13 PERSONNEL

Faculty
Berrah, Nora
Burns, Clement
Chung, Sung
Dobbin, Donya (Part Time)
Famiano, Michael
Gorczyca, Thomas
Halderson, Dean
Hardie, Gerald (Assistant Chair)
Henderson, Charles
Kaldon, Philip (Part Time)
Kamber, Emanuel
Kayani, Asghar
Korista, Kirk
McGurn, Arthur
Miller, Mark (Part Time)
Pancella, Paul (Chair)
Paulius, Lisa
Rosenthal, Alvin
Schuster, David
Tanis, John
Wuosmaa, Alan

Faculty Emeriti
Bernstein, Eugene
Kaul, Dean
Soga, Michitoshi
Poel, Robert
Shamu, Robert

Adjunct Faculty
Stolterfoht, Nikolaus

Staff
Cochran, Kerry
Gaudio, Benjamin
Kern, Allan
Krum, Lori
Scherzer, Bob
Welch, Rick

Post-Docs
Bilodeau, René
Hoener, Matthias
Nikolić, Dragan
Pesic, Zoran
Rolles, Daniel
Said, Ayman

Graduate Students
Abdel Naby, Shahin
Adams, Betty
Adams, Dan
Al-Amar, Mohammad
Al Faify, Salem
Ayyad, Asmá
Baran, Jamie
Bedoor, Shadi
Cassidy, David
Das, Susanta
Dassanayake, Buddhika
Dumitriu, Ileana
Durren, Michael
El Kafrawy, Tamer
Ganapathy, Subramanian
Gao, Xuan
Garratt, Elias
Ghannam, Talal
Giacherio, Brenna

Graduate Students (cont.)
Goodman, Nicholas
Grineviciute, Janina
Hamam, Khalil
Hasoglu, Muhammet Fatih
Ihrig, Caleb
Kodikara, Ravin
Lagha, Rahmah
Li, Chengyang
Li, Shujun
Lighthall, Jonathan
Marley, Scott
Moore, Andrew
Nandasiri, Manjula
Rai, Buddhi
Stefanick, Trevor
Vyas, Anjali
Wang, Lihua
Wang, Xue
Winkworth, Melike
Zhang, Huaizhen
Zhang, Yingfa